2013

Discovery and Characterization of Methylation of Arginine 42 on Histone H3: A Novel Histone Modification with Positive Transcriptional Effects

Fabio Casadio

DISCOVERY AND CHARACTERIZATION OF METHYLATION OF ARGININE 42 ON HISTONE H3: A NOVEL HISTONE MODIFICATION WITH POSITIVE TRANSCRIPTIONAL EFFECTS

A Thesis Presented to the Faculty of

The Rockefeller University

in Partial Fulfillment of the Requirements for

the degree of Doctor of Philosophy

by

Fabio Casadio

June 2013

DISCOVERY AND CHARACTERIZATION OF METHYLATION OF ARGININE 42 ON HISTONE H3: A NOVEL HISTONE MODIFICATION WITH POSITIVE TRANSCRIPTIONAL EFFECTS

Fabio Casadio, Ph.D.

The Rockefeller University 2013

Eukaryotic genomic DNA is packaged in the form of chromatin, which contains repeating nucleosomal units consisting of roughly two super-helical turns of DNA wrapped around an octamer of core histone proteins composed of four histone species: one histone H3/H4 tetramer and two histone H2A/H2B dimers. Histones are basic globular proteins rich in lysine and arginine residues, with unstructured N-terminal “tail” regions protruding outside the nucleosome structure, and structured “core” domains in the DNA-associated portion. Several core residues, and in particular arginines in H3 and H4, mediate key interactions between the histone octamer and DNA in forming the nucleosomal particle.

Histone post-translational modifications (PTMs) lead to downstream effects indirectly by allowing or preventing docking of effector molecules, or directly by changing the intrinsic biophysical properties of local chromatin. To date, little has been done to study PTMs that lie outside of the unstructured tail domains of histones. I describe here the identification by mass spectrometry of a novel methylation site on histone H3, the asymmetric dimethylation of arginine 42 (H3R42me2a). H3R42 is conserved through evolution and is at the DNA entry/

exit position within the nucleosome core, with likely interactions with the DNA backbone. I show that methyltransferases CARM1 and PRMT6 methylate this residue *in vitro* and *in vivo*. Using chemically-defined "designer" histones I also show that methylation of H3R42 stimulates transcription *in vitro* from chromatinized templates. Using peptide pull down experiments combined with enzymatic assays I demonstrate that H3R42me2a prevents the stimulation of the histone deacetylase activity of the N-CoR co-repressive complex by impeding its binding to H3.

Thus, H3R42 is a new histone methylation site with stimulating effects on transcription. I propose that methylation of basic histone residues at the DNA interface may be a general mechanism to disrupt histone:DNA interactions, with effects on downstream processes, including transcription.

Acknowledgements

First, I would like to thank my advisor, Dr. David Allis for his support and scientific guidance throughout my graduate career. Dave enthusiastically supported me during this technically challenging project, he encouraged me to establish key collaborations, and his enthusiasm has allowed me to surpass even the hardest of moments. I am particularly grateful to Dave for his full support of my future career choices.

I thank my faculty advisory committee, Dr. Fred Cross and Dr. Robert Roeder for their time and all the helpful suggestions. In particular, I thank Dr. Cross for serving as the chair of my committee and Dr. Mark Bedford for serving on my thesis committee as the external member.

I must also thank the many people that collaborated with me on this project: Dr. Gary LeRoy, Dr. Ben Garcia, Dr. Xiangdong Lu, Dr. Robert Roeder, Sam Pollock and Dr. Tom Muir for their work and thoughtful scientific discussions. My thesis work would have not been possible without their contribution.

I thank all my current and past Allis lab colleagues for their support and insightful discussions; in particular I thank Ben Sabari, Dr. Ronen Sadeh, Dr. Simon Elsaesser, Dr. Peter Lewis, Dr. Sonja Staedler, Dr. Alex Ruthenburg, Dr. Tom Milne and Dr. Christina Hughes for many coffees, many scientific

discussions and many (more) non-scientific ones. I also thank our lab assistant Marisa Cerio and our lab manager Jamie Winshell for everything they do every day to keep the lab running.

Many thanks to the members of the David Rockefeller Graduate Program Dean's Office for their help and support throughout the years. I am also thankful to have received financial support for this research through the David Rockefeller Graduate Program, the Anderson Cancer Center and the Boehringer Ingelheim Foundation.

I must thank my family for their constant support and encouragement, even from a distance. I thank my friends, my running buddies and the Ciccios for having been there for me when I needed to be distracted or encouraged. Last but not least, my girlfriend Melina deserves special thanks for her patience while I was working on this thesis and for her proofreading help, and for having been so caring and supportive throughout the past few years.

Table of Contents:

List of Figures:

List of Tables:

Chapter 1: Introduction

1.1 Chromatin is the physiological form of our genome

All organisms, prokaryotic or eukaryotic, must deal with the problem of packing a relatively long piece of DNA into a small space within the cell. In eukaryotic mammalian cells, around two meters of genomic DNA are compacted over 10,000-fold to be packaged into a nuclear structure called chromatin (Allis et al., 2007), which was first identified and named by Walther Flemming in 1882 because of its refractory nature and affinity for dyes that preferentially stain basic residues (Flemming, 1882). The primary proteins that mediate the folding of DNA into chromatin are the histones, a series of acid-soluble proteins that were first isolated and characterized by Albrecht Kossel in 1884 (Kossel, 1911).

Histones achieve DNA compaction through the assembly of repeating units called nucleosomes. In each nucleosome, 146 base pairs (bp) of DNA wrap 1.65 times around an octamer formed by the four core histone proteins: an H3-H4 tetramer and two H2A-H2B dimers (Kornberg, 1974; Kornberg and Thomas, 1974; Luger et al., 1997). This array of repeating units is further compacted into more complex fibers, a process regulated by modifications of the histones themselves, linker histone H1 association, and the recruitment of structural proteins (Hansen, 2002) (**Figure 1.1**).

All core histones within a given family are remarkably conserved in protein length and amino acid sequence through evolution (Allis et al., 2007; Van Holde, 1989), and contain relatively large amounts of lysine and arginine (over 20% of total number of amino acids). Histones H2A and H2B are lysine-rich (14 out of

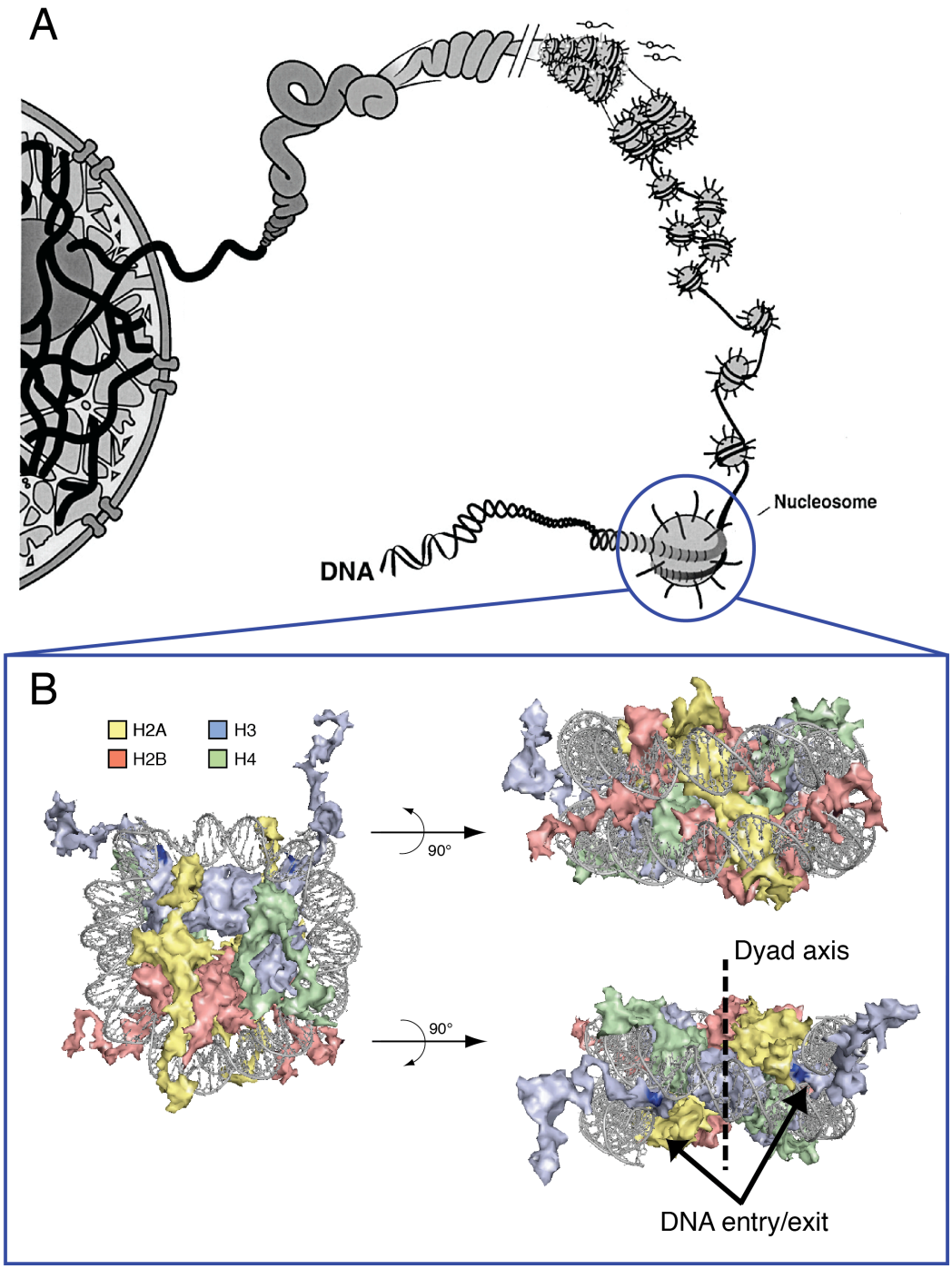

Figure 1.1: The organization of chromatin

A) Schematic illustration of chromatin fiber condensation. Adapted from (Hansen, 2002). B) Surface rendition of the nucleosome structure (PDB code 1KX5). DNA is colored in gray, H2A, H2B, H3 and H4 are colored in yellow, red, blue and green, respectively.

Table 1.1: Lysine and arginine content in human histones
Modified from (Van Holde, 1989).

	No. of residues	% Lys	% Arg
H1	224	29.5	1.3
H2A	129	10.9	9.3
H2B	126	16	6.4
H3	135	9.6	13.3
H4	102	10.8	13.7

129, and 20 out of 126 amino acids, respectively, in humans), while histones H3 and H4 contain more arginine (18 out of 135, and 14 out of 102 amino acids, respectively, in humans) (**Table 1.1**). All four histones contain a globular histone fold domain at the carboxyl (C-) terminal end that mediates histone-histone and histone-DNA interactions, and charged tails at the amino (N-) terminal end which contain the bulk of lysine residues (Arents et al., 1991; Luger et al., 1997) (**Figure 1.2**).

1.2 DNA-Histone interactions are key for nucleosome stability

Even when compacted in the form of chromatin, DNA must remain accessible to the molecular machineries that execute critical DNA-templated processes like replication, transcription or repair. As a consequence, chromatin is a very dynamic structure. The key to understanding this dynamic nature lies in the structure of the nucleosome core particle itself, and in particular in the interaction between DNA and histones.

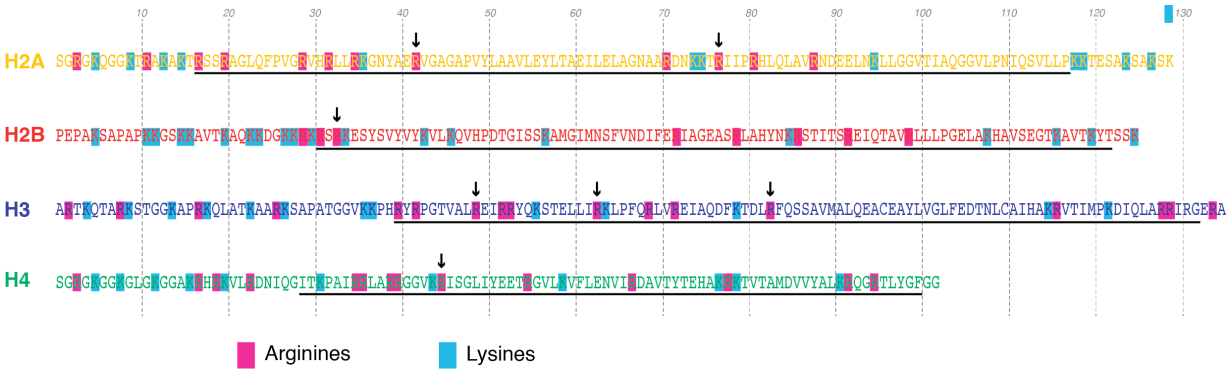

Figure 1.2: Core histone sequences

The amino acid sequences of the human core histones are shown. Arginines are highlighted in pink, and lysines are highlighted in light blue. Arrows designate arginine side-chains that are inserted into the DNA minor grove. Structured core regions are underlined. Modified from (Luger et al., 1997).

Histones are bound to the DNA by noncovalent forces: the majority of interactions appear to be electrostatic since histones can be removed from DNA by high salt concentrations (Van Holde, 1989). Histones H2A and H2B dissociate first as the salt concentration is raised, followed by arginine-rich histones H3 and H4 (Burton et al., 1978). Zama and colleagues showed that the electrostatic interactions between the phosphodiester backbone of DNA and arginine residues present in the histone octamer are the most important for organizing DNA in the nucleosome (Ichimura et al., 1982). This major role of arginines is due to their capacity to form both hydrogen bonds and electrostatic interactions with phosphate residues along the DNA backbone.

Following the seminal work of Karolin Luger, Tim Richmond and colleagues, who solved the crystal structure of recombinant nucleosomes (Luger et al., 1997)

(**Figure 1.1**), we now know in great detail how histones interact with each others and how the octamer they form interacts with DNA. Histone H2A forms a heterodimer with H2B, and H3 forms a heterodimer with H4. Two H3/H4 dimers join together to form a tetramer, which plays the central role in organizing the nucleosome. Two histone H2A/H2B dimers interact on either side of the tetramer and consequently with DNA towards the ends of the molecule as it wraps around the histone core. The conformation of histones in the nucleosome structure places several arginines so that their side-chains are inserted into the DNA minor groove at every turn of the double helix (Luger et al., 1997) (**Figure 1.2**) and creates a positively charged, arginine-rich grove on its surface that creates a ramp onto which DNA is wrapped (Arents and Moudrianakis, 1993; Luger et al., 1997) (**Figure 1.3**).

More recent biophysical studies provided a high-resolution quantitative map of histone-DNA interactions in a nucleosome (Hall et al., 2009). The interaction map revealed that histone-DNA interactions within a nucleosome are not uniform: the strongest region of interactions is located at the dyad axis (**Figure 1.1**) and another two regions of strong interactions lie approximately ±40 bp from the dyad. Mutations in these regions are known to greatly destabilize the nucleosome (Fry et al., 2006). Weaker interactions were measured in the regions where the DNA enters and exits (**Figure 1.1**). Despite the observed weakness, the interactions at the DNA entry and exit points have been shown to be fundamental in controlling nucleosomal DNA accessibility and overall nucleosome unwrapping (North et al., 2012; Somers and Owen-Hughes, 2009).

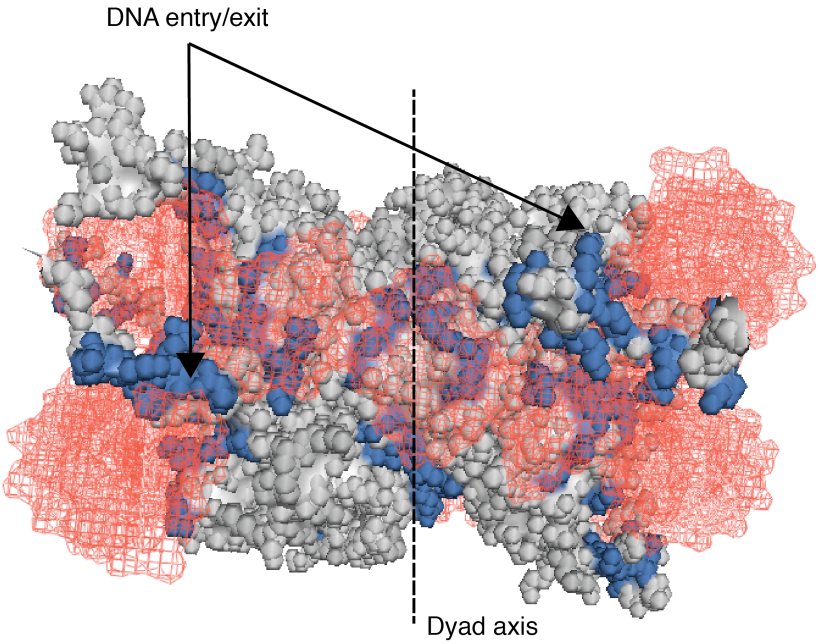

Figure 1.3: Coincidence of basic residues and DNA path.
Surface rendition of the nucleosome structure (PDB code 1KX5). DNA is colored in red, and the histone octamer is colored in grey. Basic residues are colored in blue. Modified from (Arents and Moudrianakis, 1993)

The work presented in this thesis was aimed at understanding how the post-translational modification of one particular arginine residue in histone H3 at the DNA entry/exit region might affect the process of transcription.

1.3 Histone post-translational modification

The study of histone modifications began when Murray reported the identification of lysine methylation in calf thymus histones (Murray, 1964). We now know that many different post-translational modifications (PTMs) can be affixed to histones, such as methylation, acetylation, phosphorylation,

ubiquitylation, citrullination, ADP-ribosylation, sumoylation, biotinylation and others (Kouzarides, 2007; Tan et al., 2011). The number of identified modifications and of enzymes responsible for installing or removing them continues to increase as more sensitive methods, such as mass spectrometry, are applied to histone proteins (Garcia et al., 2007b). These modifications are attached to specific residues and deposited at specific genomic locations, and it has been suggested that a given collection of PTMs on one or more histones can contribute to the creation of a "histone code" that modulates gene expression, regulates chromatin structure, and dictates cellular and epigenetic identities during development, therefore extending the information potential of the genetic code encoded in DNA alone (Jenuwein and Allis, 2001; Strahl and Allis, 2000; Turner, 2000).

Histone PTMs can function either through a direct, in *cis,* mechanism, or through an effector-mediated, in *trans*, mechanism (**Figure 1.4**) (Allis et al., 2007). Modifications that function in *cis* directly alter the biophysical properties of chromatin; those that function in *trans* influence the recruitment or activity of non-histone proteins on chromatin.

Histone lysine acetylation can be used as an example of histone PTM that can function in *cis.* Early work conducted by Vincent Allfrey at The Rockefeller University correlated for the first time histone acetylation and methylation with active transcription (Allfrey et al., 1964), although rigorous sites of modification had yet to be identified. Later work supported this notion, demonstrating that some transcriptional co-activators possess an acetyltransferase activity (Brownell

et al., 1996) and that some transcriptional co-repressors are histone deacetylases (Taunton et al., 1996). The DNA backbone is negatively charged and electrostatically interacts with histones that are enriched in positively charged side-groups. Addition of one acetyl group to the ε-amino group of lysine neutralizes its positive charge. It has been shown that histone tail acetylation antagonizes chromatin fiber compaction and results in a chromatin template that is more permissive to transcription (Tse et al., 1998). In addition, the positively

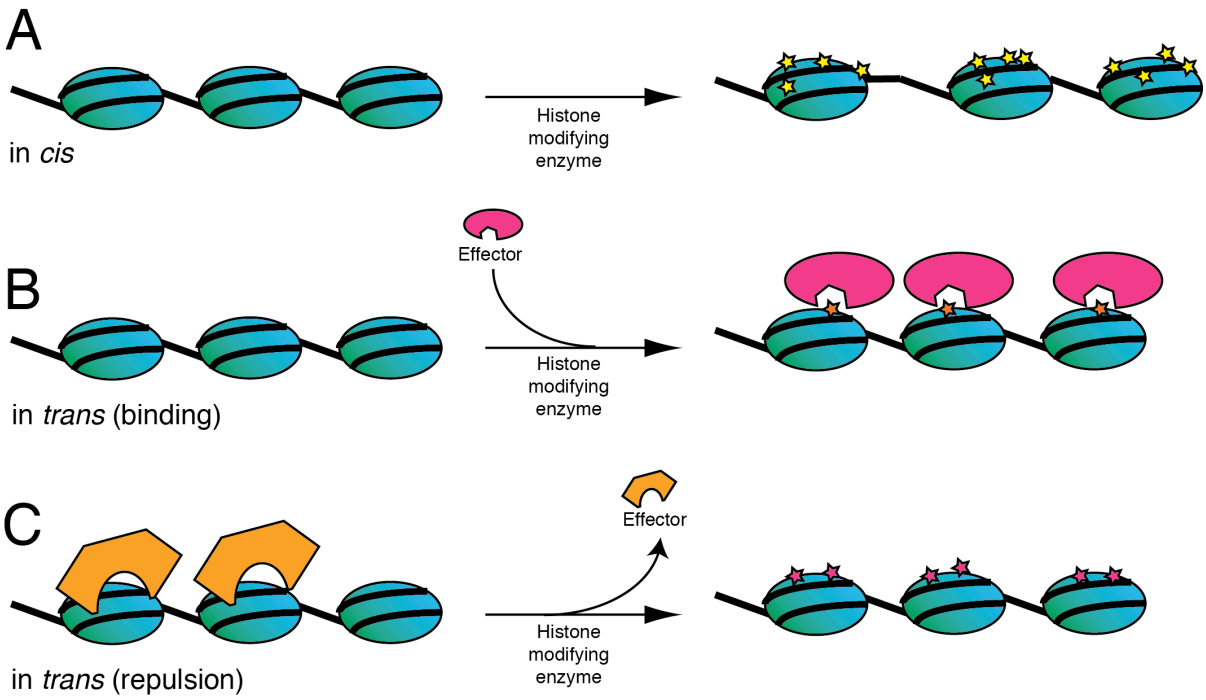

Figure 1.4: Mechanisms of histone PTM function.

A) Histone PTMs (colored stars) that result in chromatin with different physical properties function *in cis*. Covalent modifications that function *in trans* either stabilize (B) or inhibit (C) the binding of effector proteins on chromatin. (Adapted from Allis et al, 2007)

charged N-terminal of H4 interacts with an acidic patch on adjacent nucleosomes, and acetylation of a single lysine on the H4 tail (H4K16) is able to reduce chromatin compaction (Robinson et al., 2008; Shogren-Knaak et al., 2006).

Lysine methylation is one of the better-studied examples of histone PTM that can function in *trans*. Although methylation of lysine residues does not perturb their charge, specialized protein domains (also known as “reader” modules) exist that interpret particular methylation states (mono-, di- or trimethyl) and particular methylation sites in histone tails (Taverna et al., 2007). Chromodomains were the first class of protein domains shown to be specifically recruited by methylated lysines: in landmark papers, several groups showed that the chromodomain-mediated binding of Heterochromatin Protein 1 (HP1) to histone H3 methylated on lysine 9 (H3K9) was necessary for its proper localization and function (Bannister et al., 2001; Lachner et al., 2001). More recently, domains other than chromodomains capable of binding methyl marks on histone tails have been identified. They include WD40-repeats, PHD, Tudor, plant Agenet, PWWP, SWIRM, and MBT domains (Martin et al., 2006; Maurer-Stroh et al., 2003; Shi et al., 2006; Taverna et al., 2006; Wysocka et al., 2005; Wysocka et al., 2006).

PTMs can also prevent association with binding proteins (**Figure 1.4C**). For example, recent studies have demonstrated that asymmetric dimethylation of arginine 2 of histone H3 (H3R2me2a) is a repressive mark that is mutually exclusive with H3K4me2/me3 both in yeast and human cells (Guccione et al., 2007; Hyllus et al., 2007; Iberg et al., 2007; Kirmizis et al., 2007). While

H3K4me3 is enriched in the promoter of expressed genes and absent from downstream sequences, H3R2me2a is highest on inactive promoters, but also enriched inside and at the 3' end of genes regardless of expression levels (Guccione et al., 2007; Guccione et al., 2006). This distribution pattern is explained by the fact that H3 recognition by WDR5, a common subunit of the MLL family of H3K4 methyltransferase complexes, is abolished by the presence of H3R2me2a in *in vitro* binding assays (Couture et al., 2006; Guccione et al., 2007; Hyllus et al., 2007; Iberg et al., 2007).

Direct recruitment is not the only mode of action of histone methylation. Allostery is, in fact, another mechanism that extends the repertoire of *trans* effects of histone PTMs. Recent studies have shown that the H3K27 methyltransferase complex PRC2 specifically binds to histone tails carrying H3K27me3 through its subunit EED, and that this binding leads to the allosteric activation of the methyltransferase activity of the complex (Margueron et al., 2009).

1.4 Histone arginine methylation by PRMTs and its consequences

Arginines in histones can be mono- or di-methylated, the latter either in a symmetric (me2s) or asymmetric form (me2a) (Bedford and Clarke, 2009). The enzymes that mediate arginine methylation have been characterized and belong to the Protein aRginine MethylTransferase (PRMT) family. Nine enzymes within this family share conserved signature amino acid motifs, and are able to transfer

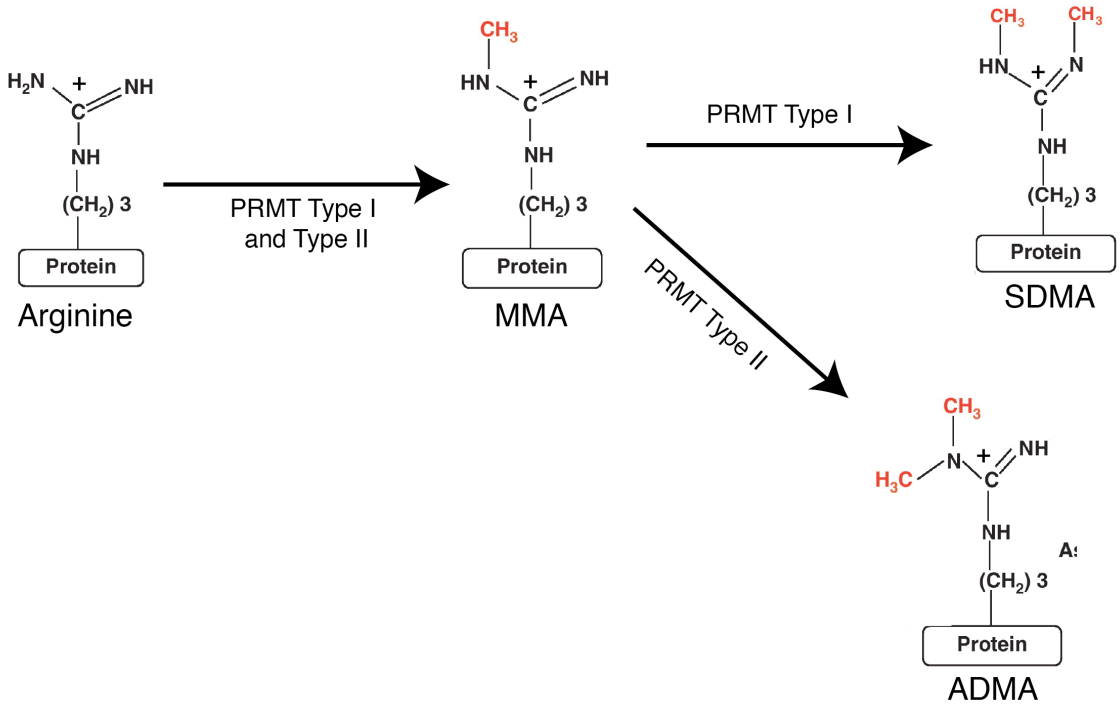

Figure 1.5: Arginine methylation

Addition of methyl groups (shown in red) to guanidine nitrogens of arginine forms monomethylarginine (MMA), dimethylarginine — symmetric (SDMA) and asymmetric (ADMA). Type-I and type-II protein arginine methyltransferase (PRMT) are the catalytic enzymes for arginine methylation. Modified from (Bedford and Clarke, 2009).

a methyl group from a donor S-adenosylmethionine (SAM) to a guanidino nitrogen of an arginine (**Figure 1.5**). Methylated arginines come in three possible forms in histones: monomethylarginine (MMA), asymmetric dimethylarginine (ADMA), and symmetric dimethylarginine (SDMA). PRMTs are classified on the basis of what modification they can catalyze: both type I and type II PRMTs can form an MMA intermediate; type I enzymes (PRMT1, 2, 3, 4, 6 and 8) catalyze the production of ADMA, while type II enzymes (PRMT5 and 7) catalyze the

formation of SDMA. (Bedford and Clarke, 2009; Krause et al., 2007). PRMTs methylate many cellular proteins, and most have histones among their substrates. The best-known arginine methylation sites on histones include arginine 3 on histone H4 (H4R3) and arginine 2, 17 and 26 on histone H3 (H3 R2, R17, R26) (Bernstein et al., 2007).

Since methylation of arginines changes their shape and removes a potential hydrogen bond donor, but does not affect their positive charge, it has been proposed that the main mode of action of histone arginine methylation is via recruitment of effector proteins, similarly to the mode of action of lysine methylation. In addition to preventing the binding of effector proteins described in Section 1.3, methylated arginines in histones have been recently shown to recruit the tudor domain protein TDRD3 (Yang et al., 2010). TDRD3 binds to both activating marks H3R17me2a and H4R3me2a, and this results in its recruitment to active promoters to exert its co-activator function (Yang et al., 2010).

Arginine residues can also be converted to citrulline by deimination catalyzed by enzymes called Peptidyl-Arginine Deiminases (PADs). Enzyme PAD4 targets several arginine residues on H3 and H4 including H3R17 and H4R3 (Cuthbert et al., 2004; Wang et al., 2004), and recruitment of PAD4 to promoters results in loss of H3R17me2a (Denis et al., 2009). Given the lack, to this day, of a confirmed arginine demethylase enzyme (Chang et al., 2007; Webby et al., 2009), deimination is the only known mechanism to counteract arginine methylation.

The experiments presented in this thesis demonstrate that methylation of H3R42 is carried out *in vitro* and *in vivo* by methyltransferases CARM1 and PRMT6, which I will now cover in greater detail:

1) CARM1

PRMT4, also referred to as CARM1, was identified by Stallcup and colleagues as a steroid receptor-interacting protein capable of enhancing transcriptional activation, and was the first *histone* methyltransferase to be reported (Chen et al., 1999). The same group also demonstrated functional synergy between histone acetylation and CARM1 activity (Koh et al., 2001). These findings were the first piece of evidence that arginine methylation affects transcription. CARM1 methylates histone H3 at R17 and R26 (Schurter et al., 2001), as well as several transcriptional regulators (Lee and Stallcup, 2009). Work from the Roeder laboratory at The Rockefeller University showed that methylation of specific H3 arginines by CARM1, in cooperation with methyltransferase activity by PRMT1 and acetyltransferase activity by p300, is critical in bringing about robust p53-dependent transcription from chromatin templates (An et al., 2004). The critical role of CARM1 in transcriptional activation is reflected in its requirement during development: CARM1 knock-out mice die quickly after birth (Yadav et al., 2003) as a result of improper development or proliferation of T cells, adipocytes, chondrocytes and pulmonary epithelial cells (Ito et al., 2009; Kim et al., 2004; O'Brien et al., 2010; Yadav et al., 2008).

2) PRMT6

PRMT6 was first characterized by Mark Bedford and colleagues as an arginine methyltransferase with automethylation activity and distinct substrate specificity from PRMT1 and CARM1 (Frankel et al., 2002). PRMT6 is the main methyltransferase for H3R2 and H2AR29 in mammalian cells (Guccione et al., 2007; Hyllus et al., 2007; Iberg et al., 2007; Waldmann et al., 2011). As mentioned in the Section 1.3, H3R2me2a prevents the MLL1 complex from methylating H3K4, making it a repressive histone modification. Moreover, H3R2me2a also prevents binding of many effectors that recognize H3K4me3 marks (Iberg et al., 2007; Vermeulen et al., 2007). Despite its initial identification as transcriptional repressor, it has been recently reported that PRMT6 might have a positive role in regulating the transcription of a subset of nuclear receptor target genes (Harrison et al., 2010). Consistently with its role in transcriptional regulation, PRMT6 activity has been reported to influence embryonic stem cell identity (Lee et al., 2012) as well as cell proliferation and senescence, by downregulating the expression of p53, p21 and p16 (Neault et al., 2012; Phalke et al., 2012; Stein et al., 2012). PRMT6-deficient mouse embryonic fibroblasts (MEFs) undergo premature senescence, while PRMT6 knockout mice show no abnormal phenotype (Neault et al., 2012**).**

1.5 Identification of new histone PTMs by mass spectrometry

The work presented in Chapter 2 of this thesis was aimed at identifying new methylation sites on human histones. Traditionally, the identification of histone

PTMs has relied on two methods: 1) incorporation of radiolabeled isotopes followed by Edman degradation, or 2) the use of specific antibodies in immunoassays.

The first method is limited as the Edman degradation protocol can only be used if the N-terminal amino acid has not been chemically modified: the N-termini of mammalian H2A and H4 are acetylated, and therefore not easily sequenced (often referred to as “blocked” proteins). Moreover, Edman sequencing can typically only extend to about 30 residues since the efficiency of every cycle is below 100%, therefore making it impossible to identify PTMs affecting residues located further internally using this method. Antibody-based methods overcome these problems but present others, such as cross-reactivity of antibodies with different sites on the same or on another protein, and susceptibility to epitope occlusion, a phenomenon observed when PTMs near the epitope sterically prevent antibody binding. Most importantly, antibody-based techniques require an *a priori* knowledge of what to probe for, and are therefore unsuitable for unbiased analyses.

Mass spectrometry (MS) has recently been used as an alternative method for the discovery and the quantitative and unbiased analysis of histone PTMs (Garcia et al., 2007b). After separation of the peptide mixture by reverse-phase high performance liquid chromatography (RP-HPLC), MS measures the mass-to-charge (*m/z*) ratio of peptides based on their behavior in the gas phase of the mass spectrometer. Since peptide isomers have the same mass (e.g. ARTK vs. ATRK), a second fragmentation step, followed by *m/z* measurement of the

fragments, provides unambiguous identification of the peptide sequence. This step is key when trying to identify the precise localization of PTMs on specific residues. This process is achieved with tandem MS, where the instrument takes both a MS and MS/MS spectra containing the precursor ions and the fragmentation ions of a peptide, respectively. Fragmentation is obtained with collision-induced dissociation (CID), which results in cleavage of adjacent amino acids at the peptide bond (Bonaldi et al., 2004).

The use of MS methods has greatly extended our knowledge of histone PTMs. Two of the first MS discoveries of novel histone PTMs were the findings of methylation on H4R3 (Strahl et al., 2001) and H3K79 (Ng et al., 2002; van Leeuwen et al., 2002). More recent improvements in methods and instrumentation have made it possible to identify several dozens of novel modifications in single studies (Tan et al., 2011; Zhang et al., 2003).

Garcia and colleagues recently developed a method that allows for a quantitative assessment of the abundance of PTMs on core histones (Garcia et al., 2007a; Plazas-Mayorca et al., 2009). Their method is based on trypsin digestion of the histone sample to be analyzed after derivatization by propionic anhydride (**Figure 1.6**). Trypsin only cleaves at the C-termini of arginine and lysine residues if they are unmodified and not followed by a proline residue (Ong et al., 2004). Since histones are arginine- and lysine-rich, trypsin digestion of histones would result in small peptides that are difficult to retain on RP-HPLC columns and analyze by MS. By treating histones with propionic anhydride before trypsin digestion, all free amine groups — including the N-termini of

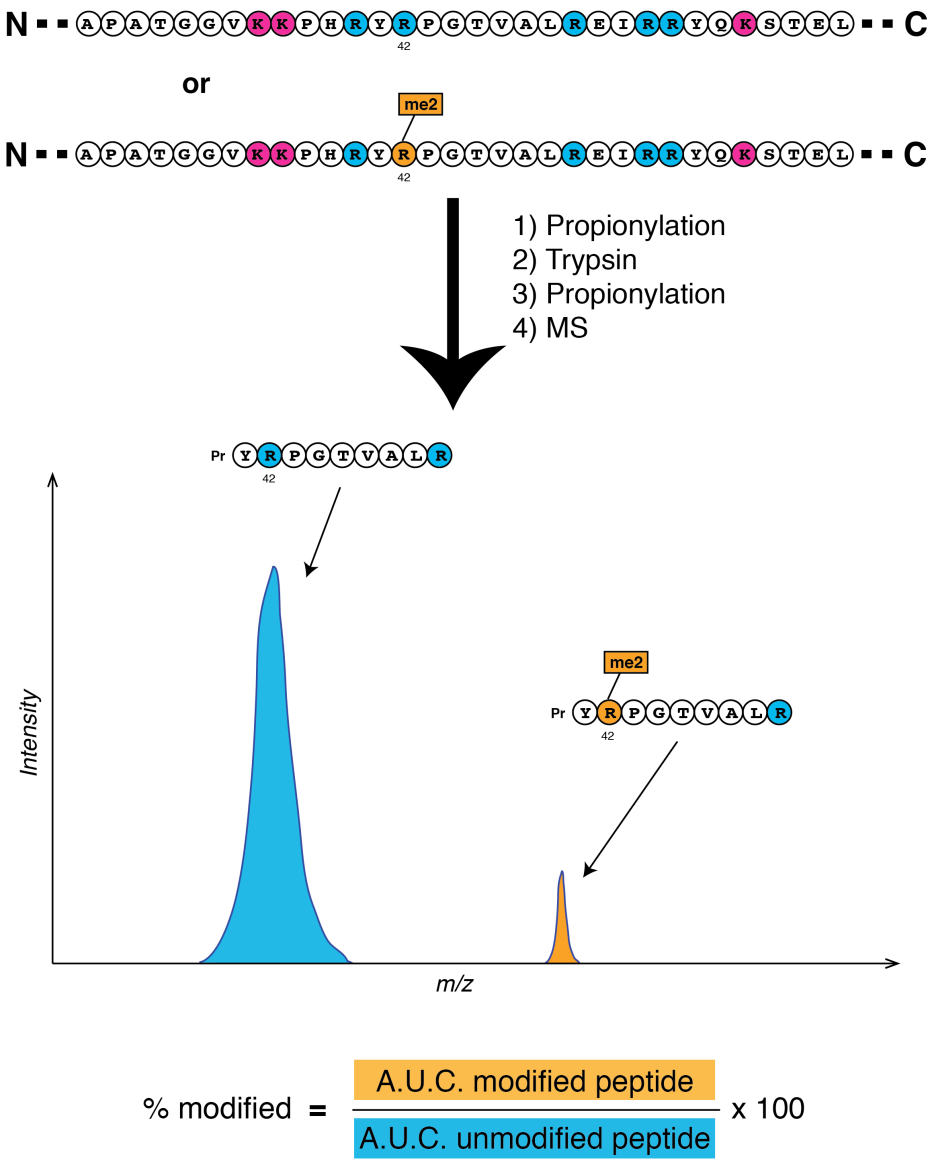

Figure 1.6: Schematic depiction of MS method for histone PTM quantification

Histones are propionylated to modify all the lysines in the sequence, therefore preventing cleavage by trypsin. Trypsinization results in cleavage at the C-termini of arginines. Another propionylation step modifies the free N-terminus. The figure shows a partial sequence of human histone H3, with detail on the tryptic peptide containing R42. Unmodified and modified (me2 in orange) peptides of the same sequence have different MS peaks because of their different masses. Cleavage does not occur C-terminal of R42 even when unmodified because R42 is followed by a proline. The relative amount of a peptide is estimated from the area under the curve (A.U.C.) for each peak.

peptides and ε-amino groups of unmodified and monomethylated lysine residues — are converted to propionyl amides. Therefore, trypsin digestion only induces proteolysis at the C-termini of arginine residues, unless these are methylated (Baldwin and Carnegie, 1971). Methylation of arginines, unless they are followed by prolines, generates a missed cut and a longer peptide. In addition, propionylation also reduces charges on treated peptides, which renders the histone peptides less hydrophilic. A further treatment with propionic anhydride is added after trypsinization. The resulting histone peptides can easily be resolved by RP-HPLC, resulting in MS spectra that are easy to interpret. The produced peptides are approximately the same length and their masses can be predicted. Therefore, PTMs within a certain sequence can easily be identified because of predictable mass shifts. Since peptides of similar length behave similarly in the gas phase, the relative abundance of unmodified and modified peptides can be quantified by comparing the areas under their MS peaks (**Figure 1.6**).

Using this method, Garcia and colleagues quantified several PTMs on histones (Dr. Benjamin Garcia, unpublished results). For example, acetylation of lysines in H3 and H4 is quite abundant, ranging from 5% to 30% depending on the site and cell type. Abundance of methylations on histone lysines is very variable depending on the site and cell type: H3K4me3 is in the 0.1-0.3% range; H3K27me3 is about 5-10%; H3K9 is trimethylated in about 15-20% of histones; about 70% of H4 is dimethylated on K20. Arginine methylation on histones is in general more rare and much closer to the detection limit of MS, which is about 0.01% for a PTM. For example, H4R3me1 is less than 0.1%. This might explain

why fewer methylated arginines than other types of modified residues have been identified and studied on histones.

1.6 Use of designer histones to study the function of specific PTMs

The main objective of the work presented in this thesis was to determine the direct effect of the methylation of a core residue in histone H3 on the process of transcription. For this aim, I took advantage of a technique called Expressed Protein Ligation (EPL) to generate homogeneously modified H3 proteins and used them in *in vitro* transcription assays. Traditionally, enzymatically-modified histones have been used in *in vitro* assays to measure the direct effects of the modification(s). For example, Roeder and colleagues showed that specific lysines, presumed targets of acetylation, and methylation of specific arginines in the N-tails of H3 and H4, catalyzed by the co-activators p300, CARM1 and PRMT1, are critical in bringing about robust transcription from chromatin templates (An et al., 2004). The authors assembled chromatin templates with wild type histones, or histones mutated on residues that are targeted by the co-activators, and compared their transcriptional output. This method allows for the quantification of the contribution of the PTMs themselves.

Mutations to alanine are frequently used because of the non-bulky and chemically inert nature of the residue. Some substitutions are engineered to minimize their structural effects: arginines are mutated to lysines and vice-versa, in order to maintain the basic character but abolish the modification potential. In

other cases, mutations that mimic a modified state are introduced: for example, glutamine is frequently used as an acetyl-lysine mimic. This method is highly effective but comes with several drawbacks: 1) histone modifying enzymes can target several residues at the same time, which makes it hard to study PTMs in isolation; 2) the efficiency of enzymatic modification varies by enzyme and experimental condition, making it impractical to compare effects of PTMs catalyzed by different enzymes; 3) the level of enzymatic modification of histones might not be high enough to result in a measurable effect on *in vitro* assays; 4) histone modifying enzymes could modify other proteins present in the assay mix and in turn affect their activity; 5) mutation of residues in histones might have direct effects on template properties that could affect the result of the *in vitro* assay used.

The use of EPL to generate designer histones makes it possible to overcome many of these problems (Allis and Muir, 2011; Chatterjee and Muir, 2010). EPL is a technique used to generate full-length proteins from synthetic peptides and expressed protein fragments. The synthetic peptides can include amino acids that are not directly incorporated via the genetic code, therefore permitting the incorporation of any histone modification of interest (Shogren-Knaak and Peterson, 2004). Most importantly, unlike enzymatically-modified histones, EPL provides homogeneously modified histones that can be assembled into nucleosomes and used in *in vitro* assays, bypassing the need for histone modifying enzymes. On the other hand, the disadvantage of this technique is that, since designer histones are homogeneously modified, the resulting

chromatin is also fully modified, a situation that does not reflect faithfully the situation observed *in vivo*, where histone PTMs are deposited at discrete positions. For example, this technique has been successfully used to demonstrate that acetylation on a single residue of H4 (Shogren-Knaak et al., 2006), or ubiquitylation of H2B (Fierz et al., 2011), prevent chromatin compaction.

1.7 Histone PTMs embedded in the nucleosome core

For nearly four decades, the study of histone modifications focused exclusively on those that occurred on the tail domains of the core histones. The main reason tail PTMs dominated the field is that the primary method for discovering histone modifications, Edman degradation, favored the analysis of the first 20-30 amino acids. Things changed in 2002, when the application of mass spectrometry to the study of histone modifications allowed for the discovery of the first novel site of histone modification outside of the tail, methylation of histone H3 lysine 79 (Ng et al., 2002; van Leeuwen et al., 2002).

Histone core PTMs have unique effects on chromatin function. They fall into three distinct classes listed and detailed below:

1) PTMs on the solute accessible face of the nucleosome

Tail modifications primarily act through *trans* mechanisms mediated by effector proteins. Some tail modifications, like acetylation or phosphorylation, can alter the charge of the tail and influence chromatin through electrostatic mechanisms. Similarly to what is observed with histone tail PTMs, modifications located on the solute accessible face of the nucleosome have the ability to alter

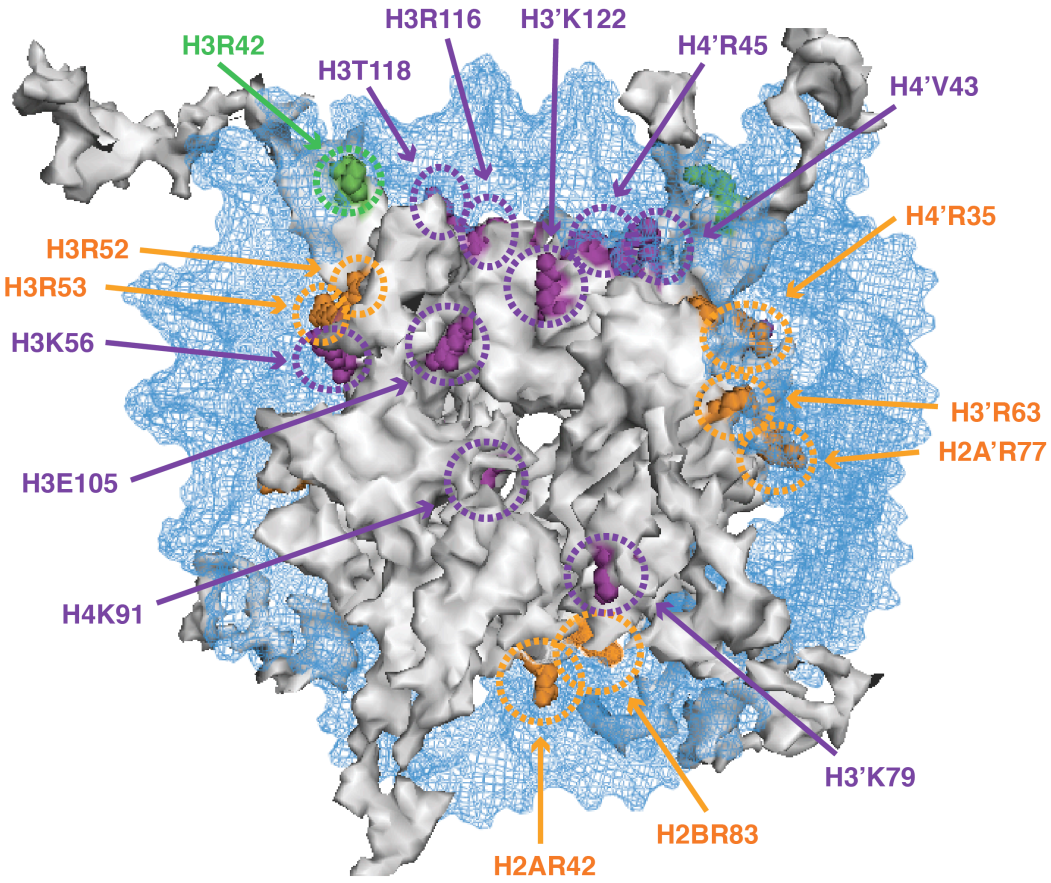

Figure 1.7: Some notable residues in the nucleosome core.
Surface rendition of the nucleosome structure (PDB code 1KX5). Octamer is colored in gray and DNA is colored in blue. Core residues that are mentioned in Section 1.7 are highlighted in purple. Surface arginines that have been shown to be methylated are highlighted in orange, H3R42 is highlighted in green.

higher order chromatin structure and chromatin-effector interactions. Histone H3K79 methylation is the best-characterized modification on the nucleosome face (**Figure 1.7**). This modification, mediated by methyltransferase Dot1, was shown to prevent the binding of telomeric heterochromatin protein Sir3 to chromatin (Altaf et al., 2007), contributing to loss of telomeric heterochromatin

(Ng et al., 2002; van Leeuwen et al., 2002). In higher eukaryotes, H3K79 methylation is also linked to transcriptional regulation and is enriched in the coding region of actively transcribed genes (Kouskouti and Talianidis, 2005), although the mechanism through which this PTM might affect transcriptional elongation is still unclear.

2) PTMs on the octamer lateral surface

Cosgrove and colleagues hypothesized in 2004 that covalent modifications on the nucleosome lateral surface could affect histone:DNA interactions (Cosgrove et al., 2004). This hypothesis led them to suggest a 'regulated nucleosome mobility' model, in which lateral surface PTMs lead to changes in histone:DNA affinity, which then result in more mobile nucleosomes. Mobile nucleosomes could be more readily displaced by proteins that must access DNA for processes like transcription, replication, etc.

The direct effects of lateral surface PTMs on nucleosome stability have been demonstrated in several cases. For example, H3K56 is located in the DNA entry/ exit region (**Figure 1.7**): acetylation of this residue lowers octamer binding affinity to DNA (Andrews et al., 2010), increases DNA unwrapping (Neumann et al., 2009), and enhances transcription factor binding within the nucleosome (Shimko et al., 2011). H3K56ac is essential for DNA replication (Xu et al., 2005), repair (Chen et al., 2008), and transcriptional activation (Williams et al., 2008). Another example is the acetylation of H3K122, a residue located at the dyad axis of the nucleosome (**Figure 1.7**), where histone-DNA binding reaches its maximum strength (see Section 1.2). H3K122ac can enhance the rate of nucleosome

disassembly upon mechanical stress (Simon et al., 2011) and stimulate transcription and histone eviction (Tropberger et al., 2013).

The importance of residues on the lateral surface in controlling nucleosome stability and mobility has also been shown by mutational analysis in *S. cerevisiae.* The amino acid substitutions H3-E105K, H3-R116H, H3-T118I, H4-V43I and H4-R45H (**Figure 1.7**) were identified as SWI/SNF-independent (*SIN*) mutants, as they partially relieve the requirement for the chromatin remodeling factor SWI/SNF for the activation of some genes (Kruger et al., 1995). All these residues are on the lateral surface at the nucleosome dyad axis, and their mutation results in decreased nucleosome stability and increased accessibility of nucleosomal DNA (Kurumizaka and Wolffe, 1997; Wechser et al., 1997).

3) PTMs at the histone-histone interfaces

Modifications at the histone-histone interface have the ability to disrupt intra-nucleosomal interactions, thereby altering nucleosome stability. For example, H4K91 is closely juxtaposed and likely forms a salt bridge with a glutamate in histone H2B (**Figure 1.7**) (Cosgrove et al., 2004). Mutation of H4K91 to alanine (K91A) renders chromatin more sensitive to micrococcal nuclease digestion and makes H2A/H2B dimers easier to be displaced from chromatin by salt (Ye et al., 2005). In addition, H4K91-acetylated histones co-purify with a histone deposition complex (Ye et al., 2005), suggesting a role for this PTM in modulating dimer-tetramer interactions during chromatin assembly.

1.8 Arginine 42 of histone H3

The work presented in this thesis was aimed at understanding how the post-translational modification of one arginine of histone H3 on the nucleosome lateral surface affects the process of transcription. We were able to identify with confidence the novel asymmetric dimethylation of arginine 42 in histone H3 (H3R42me2a), upon MS analysis of an antibody-enriched human histone sample (Chapter 2). H3R42 is at the entry/exit point of the DNA around the nucleosome (**Figure 1.8A**), and is a residue that is mostly conserved throughout evolution (**Figure 1.8B**). While most organisms contain an arginine at position 42 of H3, *S. cerevisiae* carries a lysine, an amino-acid change with functional conservation. Both arginine and lysine are basic residues and have the potential to create electrostatic interactions or hydrogen bonds with DNA, suggesting that this contact is structurally important.

I pursued the study of this particular residue for several reasons. First of all, the role of arginines situated within the globular domains of histones is still poorly understood, and in particular, if and how methylation in these domains might affect chromatin-templated processes remains unclear. Arginine residues are the most frequent hydrogen bond donors to backbone phosphate groups and to thymine, adenine, and guanine bases (Luscombe et al., 2001), and arginines in the core domains of H3 and H4 play essential roles in the folding of DNA into a nucleosome core particle (Ichimura et al., 1982). Intriguingly, addition of a methyl group to an arginine residue removes a potential hydrogen bond donor and adds steric bulk, suggesting a possible role in controlling DNA:histone interactions. In

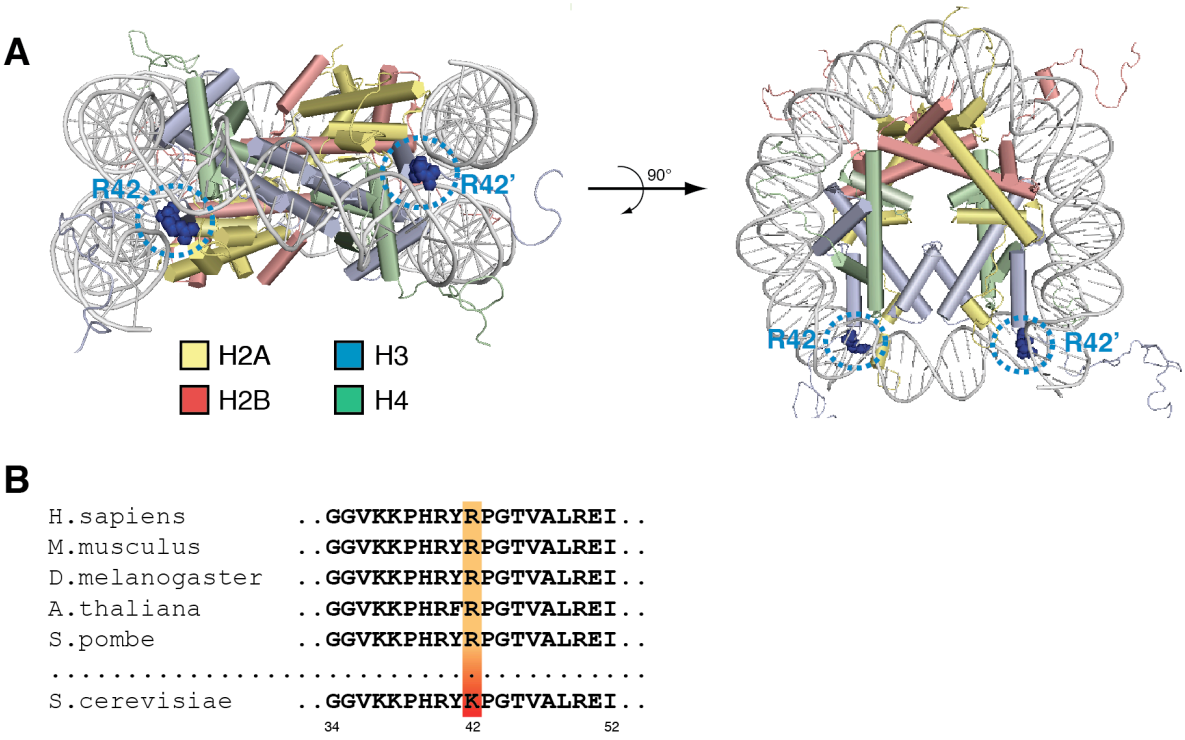

Figure 1.8: H3R42 in the nucleosome structure

A) Cartoon rendering of the *X.laevis* nucleosome highlighting histone H3 Arg 42 (circled dark blue spheres). Protein Data Bank ID: 1KX5. B) Sequence alignment of histone H3 from residue 34 to 52 from multiple eukaryotic species. The residue at position 42 is highlighted.

light of this, I hypothesized that methylation of H3R42 could be a mechanism used to modulate the interaction between DNA and the histone octamer.

Moreover, although several arginines on the DNA path in the nucleosome have been found to be methylated in large-scale proteomic studies (Cosgrove et al., 2004; Tan et al., 2011), no study to date has investigated the enzyme systems involved in depositing these modifications and their downstream effects. The previously identified methyl-arginines (H3R52, H3R53, H3R63, H4R35,

H2AR42, H2AR77 and H2BR83) are highlighted in orange on the *X. laevis* nucleosome structure of **Figure 1.7**. While methylation of all these residues could, in theory, disrupt critical histone:DNA interactions, H3R42 (green in **Figure 1.7**) appeared like a particularly interesting candidate because of the potential to also be interpreted by reader modules. Compared to the other arginine residues, H3R42 comes more upstream on the DNA path around the octamer, and is therefore in a more accessible position for enzymatic modification and recognition by specific binders.

In addition, mutational studies have demonstrated that residue 42 in H3 is important in controlling nucleosome stability. Mutation of arginine 42 to alanine (R42A) makes nucleosomes more mobile and better substrates for nucleosome remodeling enzymes *in vitro* (Somers and Owen-Hughes, 2009). Boeke and co-workers recently showed in *S. cerevisiae* H3 that mutation of lysine 42 to alanine (K42A), but not to arginine (K42R), results in increased transcriptional output, and that H3K42 is methylated *in vivo* (Hyland et al., 2011).

For these reasons, I decided to focus my work on the novel methylation of H3R42, a PTM with the potential of having both indirect, effector-mediated consequences, and direct effects on nucleosome stability. The work presented in this thesis shows that H3R42me2a has indeed a dual role in promoting transcriptional activation, both directly by affecting the biophysical properties of chromatin, and indirectly by protecting chromatin from histone deacetylation.

Chapter 2: Discovery of H3R42me2 and identification of enzymatic machinery

Although methylation of lysine residues in histones has been extensively studied, less attention has been paid to histone arginine methylation, in part because it is less abundant than its lysine counterparts (see Section 1.5). Despite its understudied status, arginine methylation is being increasingly appreciated as a critical epigenetic component in maintaining proper transcriptional regulation during organismal development (Chen et al., 1999; Phalke et al., 2012; Tee et al., 2010; Yadav et al., 2003). However, the biochemical mechanisms by which arginine methylation regulates transcription in a chromatin setting remains to be described in detail. For these reasons, I decided to focus on arginines, and in particular I sought to identify and characterize novel arginine methylations on mammalian histones.

2.1 Discovery of H3R42me2

Arginine methylation is a rare PTM in histones, and most of the known methylations on arginines are at the limit of detection by mass spectrometry (0.05% to 0.1%: Dr. Benjamin Garcia, unpublished results). When histones are analyzed by MS/MS to identify methylated arginines, the overwhelming majority of peptides from the sample is unmodified, and modified peptides are rarely detected. To overcome this problem, I first decided to use an immunoprecipitation (IP) step in order to enrich for histones with methylated arginines. Upon this

enrichment process, histones were subjected to MS/MS for identification of novel methylarginine marks. For the MS/MS analysis I established a collaboration with Gary LeRoy in the laboratory of Benjamin A. Garcia, then at Princeton University, who did all the MS/MS analyses presented in this thesis.

Mathias Mann and co-workers have reported a method to identify novel arginine methylation sites on proteins based on enriching with antibodies targeted to methylated residues followed by liquid chromatography-tandem mass spectrometry analysis (Ong et al., 2004). The authors used commercially available antibodies recognizing proteins monomethylated and dimethylated on arginine residues (Abcam, product code ab412) to immunoprecipitate proteins extracted from HeLa cells. Subsequent analysis by tandem mass spectrometry allowed these workers to identify 59 novel methylation sites on several proteins.

I chose to adapt their method for the discovery of methylarginine sites in chromatin-incorporated histones as outlined in **Figure 2.1A**. Histones from HeLa cells were extracted from a chromatin pellet derived from the classic Dignam and Roeder nuclear extraction protocol (Dignam et al., 1983). This step ensures that the PTMs observed are actually incorporated into chromatin and not only present pre-deposition. The extracted histones were immunoprecipitated with ab412 antibodies. After extensive washes, bound proteins were eluted and an aliquot was run on SDS-PAGE to check for recovery of histones after IP. Immunoblot with antibodies specific for H3R17me2a was performed as a control for enrichment of methylated arginines (ab412 could not be used for this control because in my hands it failed to function in western blots). **Figure 2.1B** confirms

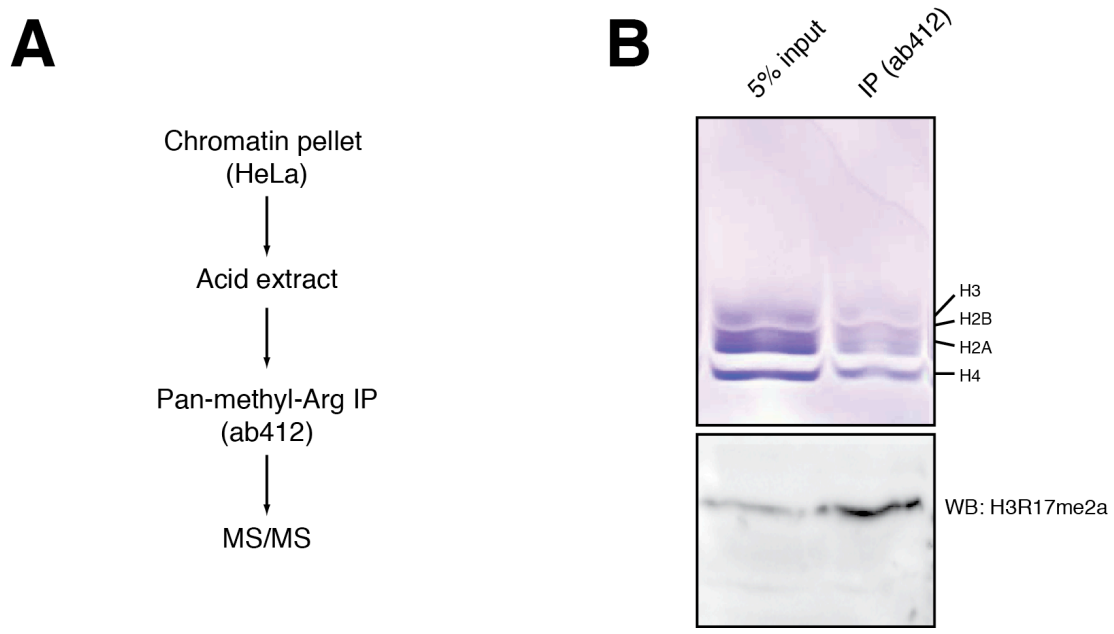

Figure 2.1: Antibody-enrichment for histones with methylated arginines
(**A**) Schematic representation of the antibody-based enrichment method used to identify novel methylated arginines on human histones (**B**) Upon antibody-enrichment, histones were run on SDS-PAGE side by side to 5% of the input material. Top panel: Coomassie staining reveals the tipical banding pattern of histones. Bottom panel: the level of H3R17me2a was measured by western blot.

that histones were successfully immunoprecipitated, and enriched for methylated arginines.

The immunoprecipitated material was then propionylated, trypsinized and analysed by tandem mass spectrometry. Several previously known sites of arginine methylation were identified (H4R3, H3R17, H3R26: data not shown). One novel site of arginine methylation on histone H3 was identified: **Figure 2.2** shows the MS/MS spectrum demonstrating the dimethylated tryptic peptide containing dimethylated arginine 42 (H3R42me2). No peptide corresponding to the mono-methylated form was detected. Since asymmetric and symmetric

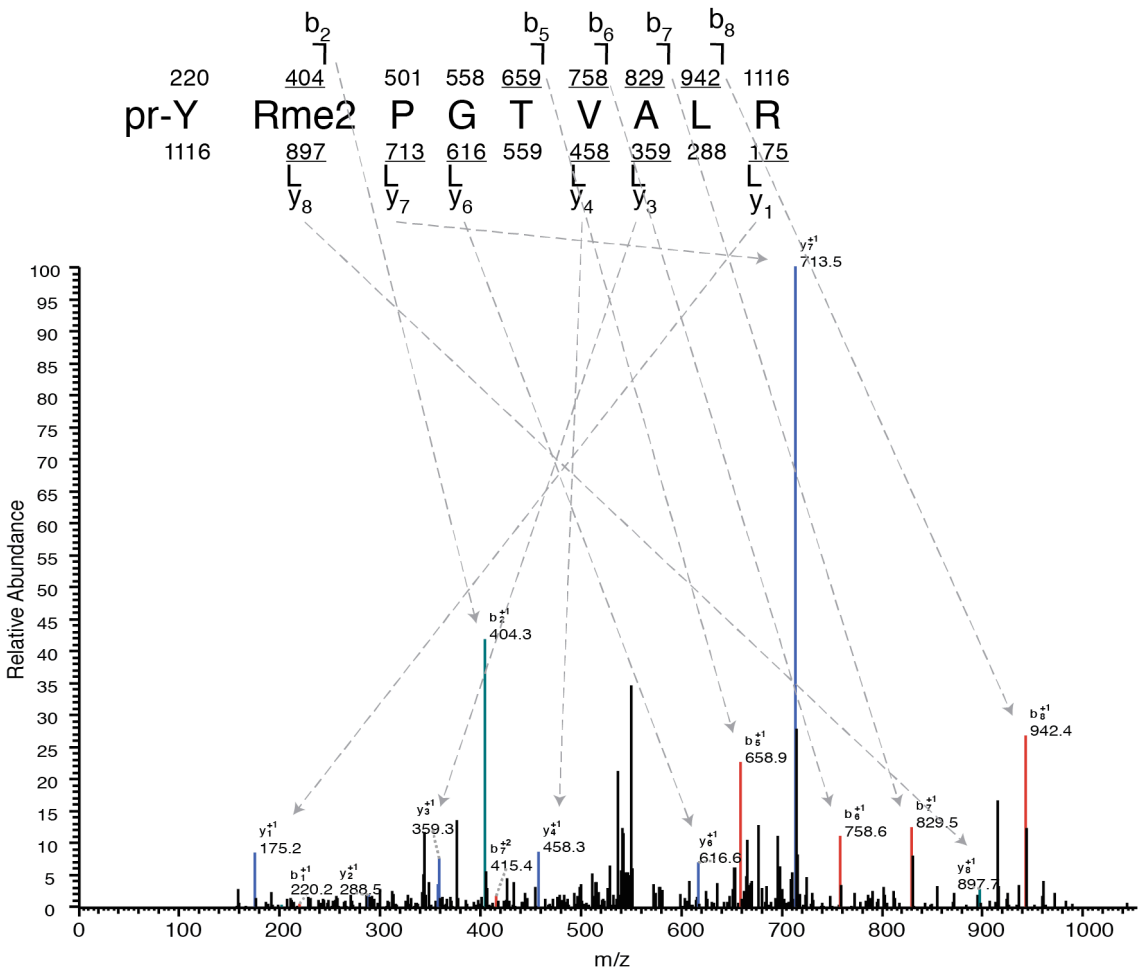

Figure 2.2: MS discovery of H3R42me2

MS/MS spectrum of the 2+ charged precursor ion at 558.831 *m/z* corresponding to the propionylated/triptic dimethylated peptide (a.a. 41-49) Pr-YRme2PGTVALR (Arg42 dimethylated) from histone H3. The sequence of the peptide containing is above; across the top are predicted b-type ions, which contain the amino terminus of the peptide, and across the bottom are predicted y-type ions, which contain the carboxyl terminus of the peptide. Those ions observed in the spectrum are underlined and indicated with an arrow. In the spectrum, the peaks corresponding to b ions are labeled in red and y ions in blue. Evidences for dimethylation of Arg42 are observed by the b2 ion at 404.3 m/z and the y8 ion at 897.7 m/z.

dimethylated arginine have the same mass, and since the antibody used for enrichment is not specific for either of the two forms, it was not possible to identify the symmetry of dimethylation.

2.2 Screening for writers

In order to investigate, and ideally identify the methyltransferase(s) responsible for bringing about methylation of H3R42, I first purified human enzymes PRMT1-2-3-5-6-7-8-9 and CARM1 and tested each for its ability to methylate a histone H3 peptide centered on R42 (residues 34 to 52) **Figure 2.3A**. Each enzyme was expressed as a Flag-HA tagged polypeptide in HEK293 cells and immunoprecipitated with anti-HA resin to avoid carryover of endogenous PRMT5 due to its affinity for M2/anti-Flag resins (Nishioka and Reinberg, 2003). Methylation was visualized via transfer of tritiated methyl groups from the donor SAM. Since peptide lengths in the 15-20 residues range are reported as viable PRMT substrates (Guccione et al., 2007; Migliori et al., 2012b), I chose to design a 19-mer centered around R42 where only three argines are present. I chose this length of peptides to minimize the number of other arginines present and at the same time leave enough residues so that an enzyme could recognize the sequence. On this first survey I chose less-stringent assay conditions (the *in vitro* methyltransferase reaction was incubated for 3 hours at 30°C) in order to minimize the chance for false negatives. As shown in **Figure 2.3B**, under these assay conditions, CARM1 and PRMT6 were able to methylate the H3 peptide substrate, but none of the other tested enzymes were

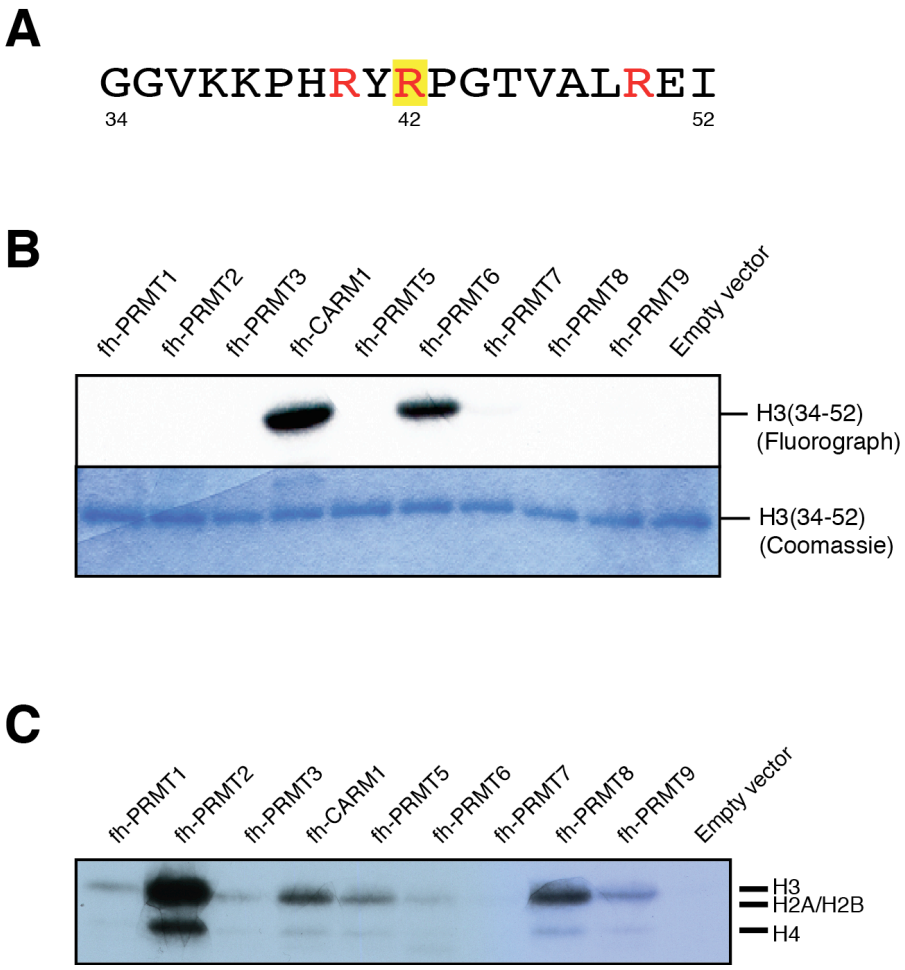

Figure 2.3: CARM1 and PRMT6 methylate H3(34-52)

(**A**) Amino acid sequence of H3 peptide (34-52). (**B**) H3(34-52) peptides or (**C**) full length recombinant human histones were incubated with immunoprecipitated Flag-HA-tagged human PRMT1, 2, 3, 5, 6, 7, 8, 9 or CARM1 in the presence of 3H-methyl-SAM and resolved by SDS-PAGE. Radioactive methyl incorporation is quantified by fluorography.

able to do so. As a control, the enzyme panel was also tested against recombinant human histones with the same assay conditions, and all displayed some enzymatic activity, albeit to varying degrees (**Figure 2.3C**).

These initial results reduced the number of candidates to test from nine to two likely candidates. One caveat of my work with short histone peptides is that the target residue can be one of three possible arginines in the substrate peptide sequence. As both CARM1 and PRMT6 are only capable of dimethylating asymmetrically, it seemed likely that the dimethylation of R42 observed by MS is asymmetric.

2.3 *In vitro* validation of writers

As the possibility remained that the methylations carried out by CARM1 and PRMT6 in **Figure 2.3** could be on arginine residues other than R42, I attempted to validate the site of methylation. Initial attempts to map the site of methylation by radioactive Edman degradation proved problematic because of the amino acid composition of the peptides used (data not shown). As an alternative I decided to use *in vitro* methyltransferase assays with peptide substrates.

I first verified that CARM1 and PRMT6 can methylate histone H3 outside of the tail region. Since both CARM1 and PRMT6 have been shown to be active toward histones and peptides as a GST-tagged, single polypeptide purified from *E. coli* (Cheng et al., 2012), both enzymes were expressed and purified from bacteria. Radioactive methyltransferase assays were then carried out using as substrates either H3(34-52) peptides, full length recombinant human H3, or an H3 deletion mutant missing the first 28 amino acids (H3 ΔN28). The deletion mutant was designed so that it would be devoid of all the previously known target

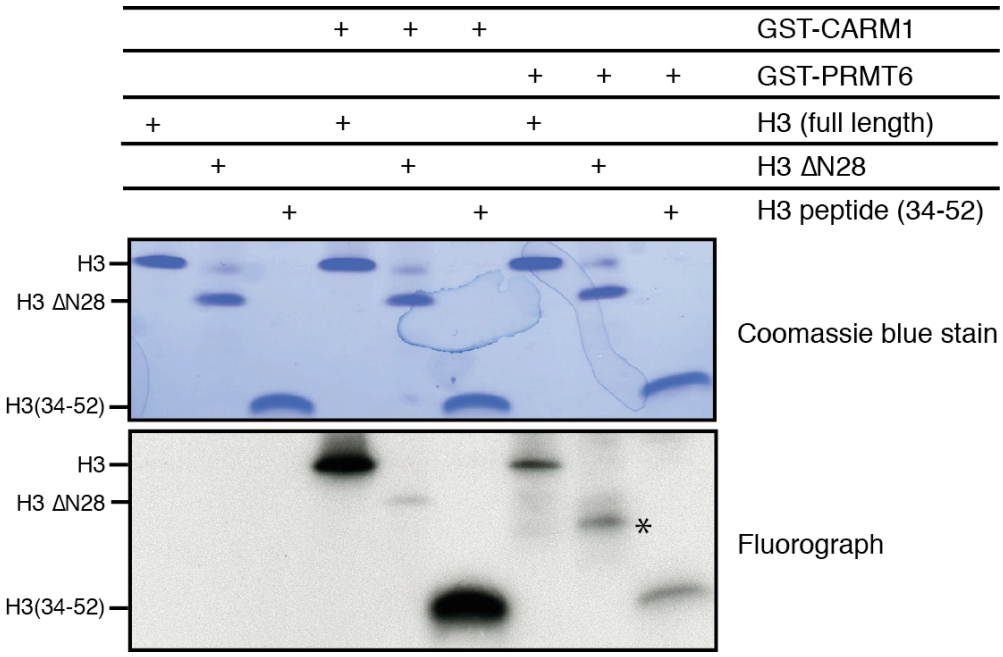

Figure 2.4: CARM1 and PRMT6 methylate non-tail residues of H3
Full length recombinant human H3, H3 ΔN28 or H3(34-52) were incubated with GST-tagged human CARM1 or PRMT6 in the presence of 3H-methyl-SAM and resolved by SDS-PAGE. The top panel shows the coomassie stain of the gel prior to being subjected to fluorography (bottom panel). Star indicates a radioactive band not corresponding to the substrate for the lane.

sites for CARM1 and PRMT6 (H3R2,R17,R26). I show in **Figure 2.4** that both enzymes were able to methylate all three substrates.

To confirm methylation on the R42 residue I carried out radioactive methyltransferase assays with CARM1, PRMT6 and PRMT1 (as negative control) on H3(34-52) peptides harbouring unmodified, mono- or di-methylated R42. Comparison of the activity toward the unmodified and dimethylated peptides is a good way to estimate enzyme specificity for a site of interest, since the dimethylated peptide is a blocked substrate and can't be further methylated on

the target residue. The H3R42me1 peptide was added as a further test for specificity, since PRMT6 has been shown to add a methyl group to a mono-methylated target more efficiently than an unmodified one (Hyllus et al., 2007; Lakowski and Frankel, 2008). **Figure 2.5** shows the incorporation of radioactive methyl groups onto the different peptides: both CARM1 and PRMT6 methylate R42me1 peptides better than unmodified H3(34-52) ones, while neither can methylate R42me2a peptides, indicating specificity for the R42 site. The higher activity toward the mono-methylated substrate is also in agreement with our observation that no mono-methylated R42 was observed from MS analysis. No methylation was measured for PRMT1, although the enzyme was active as shown by the robust methylation observed on the H4(1-20) peptide containing the known substrate H4R3 (Bedford and Clarke, 2009).

I also made sure that the conditions used for the enzymatic reactions just described (1 hour incubation and 1 µg of peptide substrate) were in the linear range for both enzymes. In the following titration experiments I kept both the amounts of purified enzyme (0.5 µg) and of radioactive SAM (1 µCi) constant, in keeping with standard published protocols (Cheng et al., 2012). I first performed time-course experiments using 1 µg of unmodified H3(34-52) peptide as a substrate and measuring the incorporated radioactivity at different time points. **Figure 2.6** shows that the incorporated radioactivity increases linearly between 30 minutes and 2 hours, validating the 1-hour reaction time used. Then I tested for dependance on substrate concentration using increasing amounts of unmodified H3(34-52) peptide. As shown in **Figure 2.7**, the incorporated

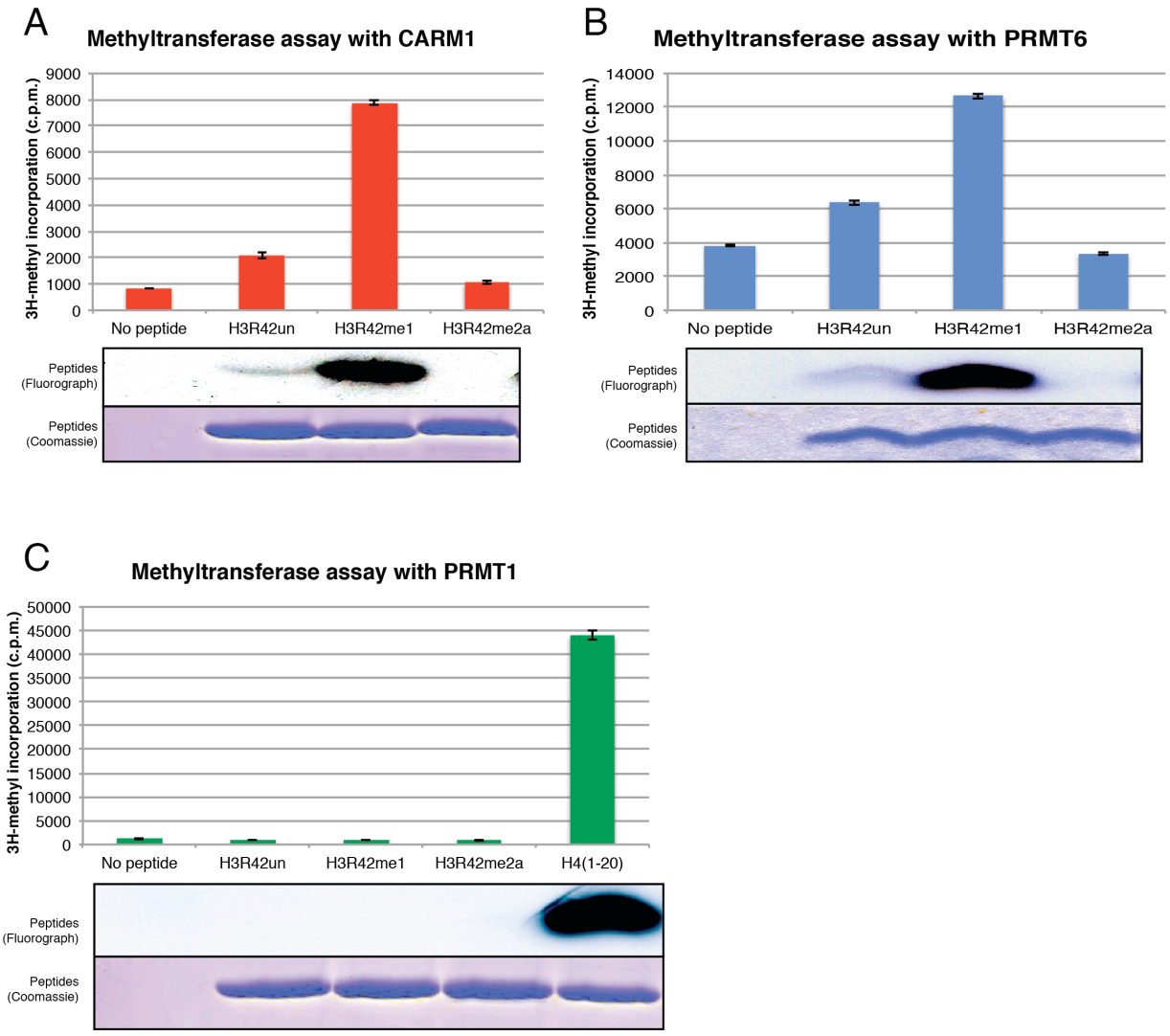

Figure 2.5: CARM1 and PRMT6, but not PRMT1, methylate H3R42 *in vitro*

Results of in vitro methyltransferase assays for CARM1 (A), PRMT6 (B) or PRMT1 (C). The peptide substrates used are indicated at the bottom of the graph. Top graph shows the levels (in cpm) of radioactive methyl incorporation for each peptide as measured by scintillation counting. The middle panel shows a representative fluorogram of the indicated substrates analyzed by 15% SDS-PAGE. Bottom panel shows coomassie staining for the same substrates.

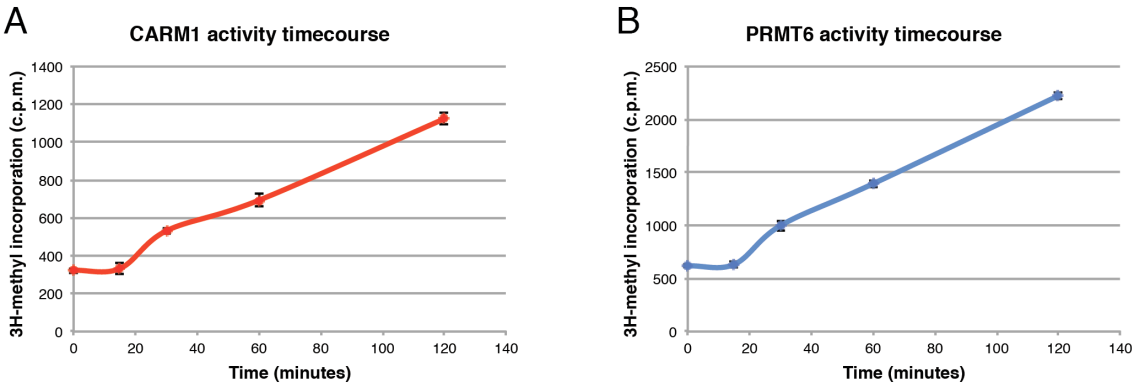

Figure 2.6: Time-course analysis

The graphs show the amount of radioactivity incorporated on H3(34-52) peptides after incubation with CARM1 (A) or PRMT6 (B), as a function of reaction time. Radioactivity was measured by scintillation counting of P81-absorbed reactions.

radioactivity increases linearly between 0.5 and 2 µg of substrate, again validating the previously used reaction condition.

Since both CARM1 and PRMT6 were known to methylate the H3 N-tail on H3R17 and H3R2, respectively (Bedford and Clarke, 2009), I repeated the radioactive methyltransferase assays including as a point of reference the unmodifed H3(1-20) peptide that carries one target site for both enzymes (R17 for CARM1 and R2 for PRMT6). As shown in **Figure 2.8**, CARM1 displays comparable activity toward unmodified H3(1-20) and H3(34-52) peptides, while PRMT6 higher activity toward H3(1-20). These results suggest that R42 might be a more physiological target for CARM1 and a secondary target for PRMT6.

Taken together, these initial results with histone peptides demonstrate that H3R42 is methylated *in vitro* by both CARM1 and PRMT6.

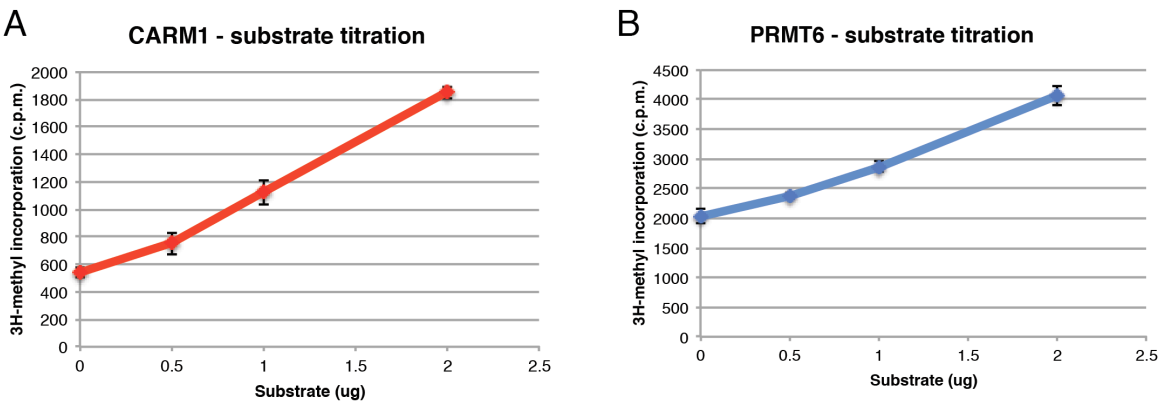

Figure 2.7: Substrate concentration analysis

The graphs show the amount of radioactivity incorporated on H3(34-52) peptides after incubation with CARM1 (A) or PRMT6 (B), as a function of substrate concentration. Radioactivity was measured by scintillation counting of P81-absorbed reactions.

2.4 *In vivo* validation of writers

To further test the CARM1/PRMT6-H3R42 hypothesis *in vivo*, I decided to see whether perturbations in the expression of CARM1 or PRMT6 would affect the levels of H3R42me2a. Despite several immunization attempts, we have not been able to obtain reliable and specific antibodies against H3R42me2a. Therefore, it is not possible to quantify easily the methylation levels with a simple western blot. One reliable way to quantify H3R42me2a is by using mass spectrometry and comparing the peak areas corresponding to the dimethylated and unmodified R42 peptides after propionylation and trypsin digestion (see Section ???).

To this end I performed siRNA knockdown of CARM1, PRMT6, or both, in HEK293 cells and acid extracted histones after 72 hours of siRNA treatment.

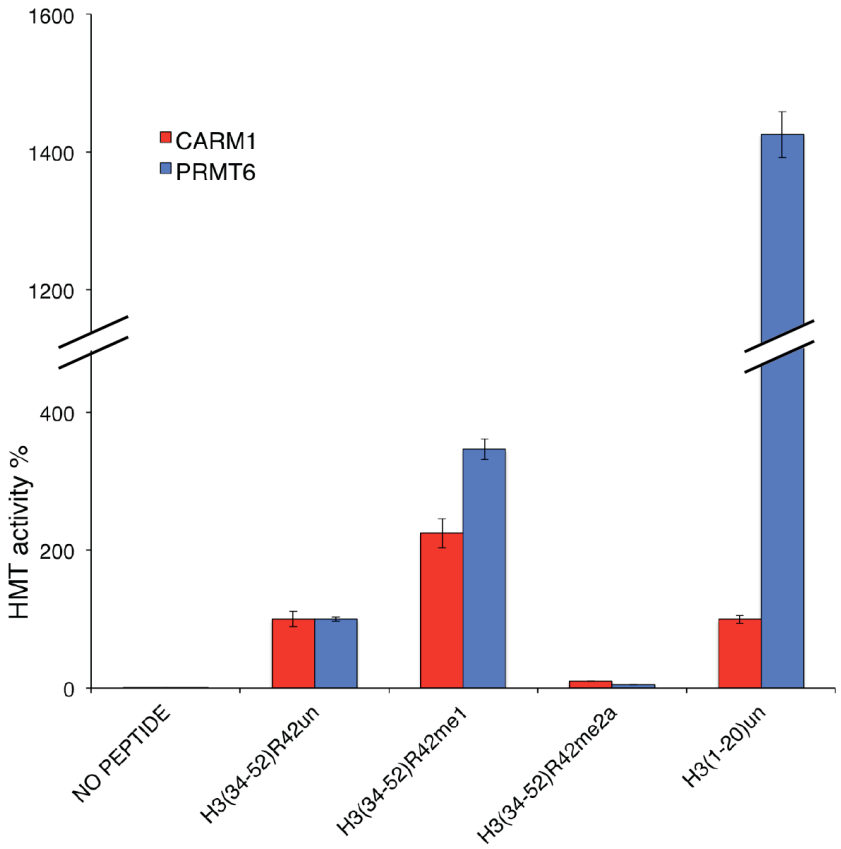

Figure 2.8: Comparison of activity toward H3R42 and previously known substrates

Comparison of methyltransferase activity against different peptide substrates between CARM1 and PRMT6. Activity was measured by scintillation counting in triplicate experiments and is expressed as percentage of the activity measured for H3(34-52) peptides. Baseline (0%) was set as the activity measured in no substrate controls (no peptide).

H3R42me2 levels were determined by MS, relative to cells treated with control siRNA. As shown in **Figure 2.9**, the knockdown of CARM1 and PRMT6 was effective in reducing the abundance of both enzymes. CARM1 siRNA alone resulted in a slightly larger reduction of H3R42me2 compared to PRMT6 siRNA alone, which is in line with the previous results suggesting that R42 might be a

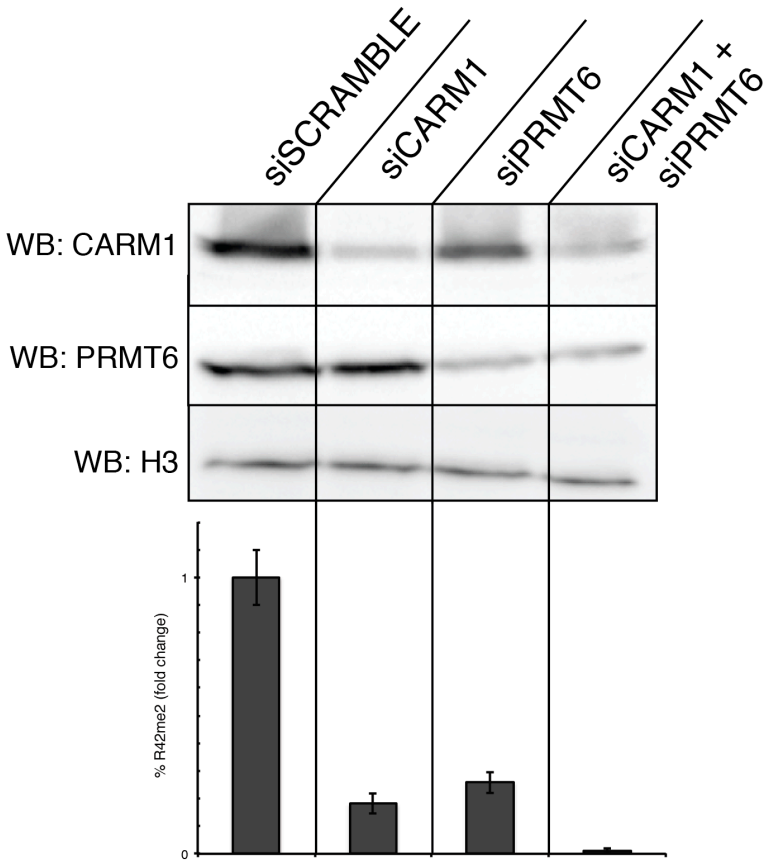

Figure 2.9: Knockdown of CARM1 and PRMT6 reduces H3R42me2a *in vivo*
Top panel shows the levels of CARM1 and PRMT6 measured by western blot in HEK293 extracts after treatment with either control siRNA or siRNAs against CARM1, PRMT6, or both. H3 levels are shown as loading control. Bottom graph shows the levels of H3R42 methylation measured by MS in acid extracts from the same cells. The percentage of H3R42 methylation for each sample is expressed in fold changes relative to the siSCRAMBLE control sample.

more physiological target for CARM1 and a secondary target for PRMT6. The double knockdown resulted in almost undetectable levels of the mark.

In addition, I tested whether overexpression of the enzymes would result in increased methylation of H3R42. For this I generated HEK293 cell lines stably

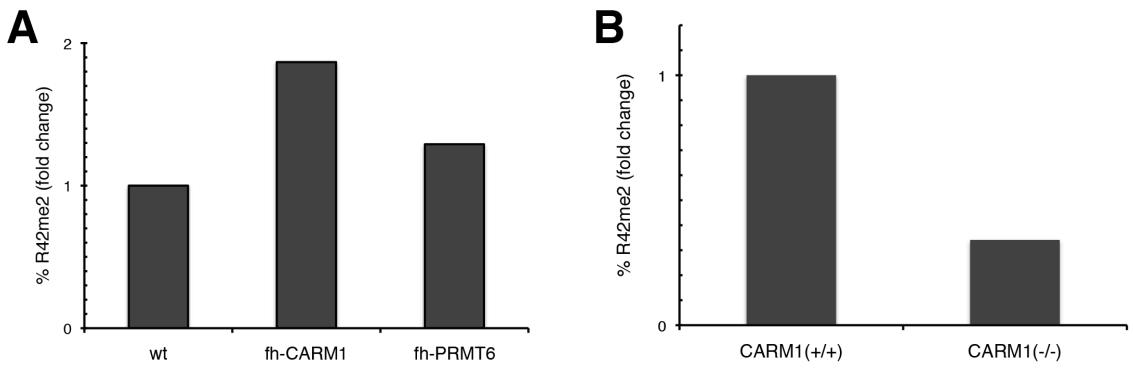

Figure 2.10: Perturbation in the levels of CARM1 and PRMT6 affects H3R42me2a *in vivo*

(**A**) Levels of H3R42me2 were measured by MS in acid extracts from HEK293 either untransfected (wt), or overexpressing CARM1 or PRMT6. The results are expressed in fold changes relative to the untransfected (wt) sample. (**B**) Levels of H3R42 methylation were measured by MS in acid extracts from CARM1(+/+) or CARM1(-/-) MEFs. The results are expressed in fold changes relative to the CARM1(+/+) sample.

overexpressing CARM1 or PRMT6. The acid extracted histones were analysed by MS. **Figure 2.10A** shows that H3R42me2 levels increase significantly with overexpression of either enzyme, although overexpression of CARM1 resulted in a bigger effect than PRMT6, again validating the preferential of CARM1 for H3R42me2a in comparison to PRMT6. Finally, I took advantage of the existence of CARM1 -/- mouse embryonic fibroblasts (MEFs) (Yadav et al., 2003), and compared the levels of R42 methylation in acid extracted histones from CARM1 +/+ and CARM1 -/- MEFs. Deletion of CARM1 results in marked decrease in H3R42me2 levels, further supporting a role *in vivo* for this enzyme in modifying H3R42 (**Figure 2.10B**).

Taken together these results demonstrate that CARM1 and PRMT6 methylate H3R42 *in vivo*, and that the two enzymes regulate the global level of H3R42me2a.

2.5 Screening for H3R42 deimination

The level of most histone PTMs is maintained by an equilibrium between writer and eraser enzymes (Allis et al., 2007). With the experiments presented in the previous sections of this chapter I identify two enzymes that methylate H3R42 *in vivo* and *in vitro.*

As described in Section 1.4, deimination by PAD enzymes is the only known mechanism that can counteract arginine methylation (Chang et al., 2007; Cuthbert et al., 2004; Wang et al., 2004; Webby et al., 2009). I therefore decided to test whether deimination could be used to regulate the methylation levels of H3R42.

Given the identification of CARM1 and PRMT6 as the methyltransferases responsible for H3R42 methylation, and since PAD4 has been shown to target for deimination residues that can be methylated by both PRMT6 and CARM1 (H3R2 and R17, respectively) (Cuthbert et al., 2004), it seemed reasonable to test PAD4 as a candidate for deiminating H3R42.

Purified PAD4 was incubated with either H3(34-52), or H3(34-52)R42me2a (negative control: PAD4 cannot deiminate dimethylated residues), or full length human H3 (positive control). This *in vitro* citrullination reaction was subjected to western blot with anti-citrulline antibodies. PAD4 did not deiminate residues in the

region of H3 encompassing R42, while it was fully active against full length H3, suggesting that either other PAD enzymes or different mechanisms are involved in negatively regulating H3R42me2a (**Figure 2.11**).

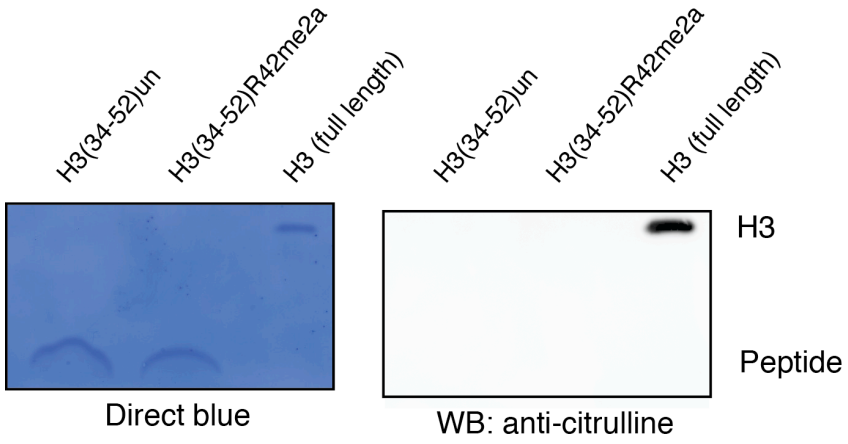

Figure 2.11: H3R42 is not a target for PAD4

Purified PAD4 was incubated with unmodified or dimethylated H3(34-52) peptides or full length H3 (positive control). Citrullination was detected by western blot.

Chapter 3. Direct effects of H3R42me2a on *in vitro* transcription

The results presented in the previous chapter support a novel role for methyltransferases CARM1 and PRMT6 in regulating the level of H3R42 methylation, a site that differs from the other better-characterized sites of methylation in the H3 N-tail (R2, R17 and R26). In this chapter I will describe experiments aimed at understanding the function of this novel PTM, and in particular its contribution to transcriptional activation.

3.1 Rationale for choosing to study H3R42me2a in the process of transcriptional activation

Several lines of evidence suggest that methylation of H3R42 might be involved in transcriptional regulation. 1) CARM1 is a well-characterized transcriptional co-activator (An et al., 2004; Chen et al., 1999), and PRMT6, albeit being initially associated with transcriptional repression (Guccione et al., 2007; Hyllus et al., 2007; Iberg et al., 2007; Kirmizis et al., 2007), has been more recently shown to be involved in activation of a subset of target genes (Harrison et al., 2010). 2) Mutational studies have implicated the importance of CARM1 activity on target arginines in H3 N-tail with direct stimulatory effects on *in vitro* transcription from chromatinized templates (An et al., 2004). 3) H3K42 in *S. cerevisiae* is methylated *in vivo* and mutation to alanine (K42A) results in increased transcriptional output (Hyland et al., 2011). 4) H3R42 is in a critical

position within the nucleosome (North et al., 2012; Somers and Owen-Hughes, 2009) and it can hypothesized that methylation might disrupt critical protein-DNA contacts. For all these reasons, in my effort to understand the function of this novel histone PTM, I first asked whether H3R42me2a could have a direct effect on transcription.

It seemed clear that the best way to pinpoint the effect of a single PTM on transcriptional activation would be to study it with *in vitro* transcription assays on chromatinized templates. In 1979, the laboratory of Robert Roeder at The Rockefeller University reproduced, using a naked DNA template, the accurate transcription of an mRNA-encoding gene in a test tube (Weil et al., 1979). It was later discovered that chromatinization of the DNA template prevents transcriptional initiation (Lorch et al., 1987; Workman and Roeder, 1987). As a result, chromatin-based transcription systems have been developed that are able to simulate *in vitro* the barrier to transcriptional activation imposed by chromatin (An and Roeder, 2004).

The system that was used for this thesis is based on assembling a chromatin template with purified assembly factors and recombinant histones (An and Roeder, 2004). The general assay scheme is shown in **Figure 3.1A**. The DNA template resembles the model in **Figure 3.1B**: activator binding sites upstream of a TATA box element are flanked by nucleosome positioning sequences to allow for precise nucleosomal deposition. Chromatinization of the template is obtained with the ATP-dependent ACF system introduced by Kadonaga and colleagues (Ito et al., 1999), which uses three recombinant proteins (Acf1, ISWI, and NAP1)

and generates a chromatin template with regularly spaced nucleosomes. The use of recombinant assembly factors rather than insect or frog extracts allows the use of recombinant octamers devoid of any modification. The transcription reaction is strictly dependent on addition of specific DNA binding activators, and

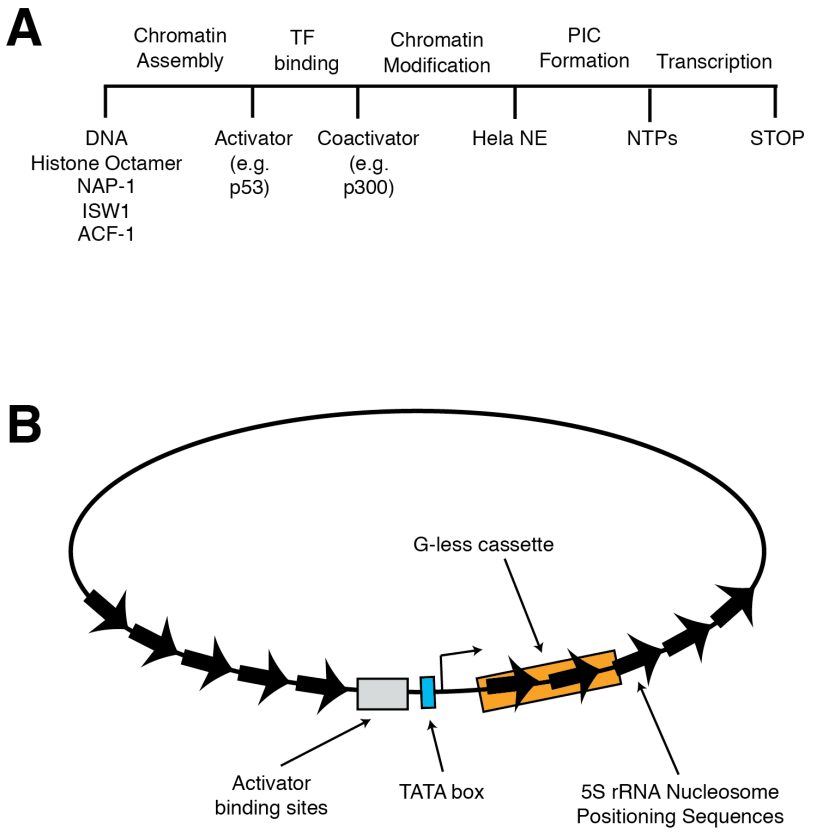

Figure 3.1: General procedure of *in vitro* transcription assays

(**A**) Schematic summary of chromatin assembly, modification, and transcription protocol. The chromatin templates are assembled with recombinant octamers using NAP1 and ACF/ISWI assembling system. After DNA-binding activators are bound to the template, histone modifying coactivators are added with their respective cofactors. HeLa nuclear extracts provide the machinery for the transcription reaction, which starts after addition of NTPs (**B**) Schematic representation of the template used in transcription assays. Adapted from (An and Roeder, 2004).

the transcription machinery is provided by addition of nuclear extract. A G-less cassette downstream of the core promoter allows direct analysis of the synthesized RNA by autoradiography. Since histones are of recombinant origin, mutant histones (or designer histones, see Section 1.6) can be used in conjunction with histone modifying cofactors to allow for functional analysis of specific histone modifications. Given the almost complete control on the experimental conditions, these assays are perfectly suited to quantify the effect of H3R42me2a on transcription.

I initially set out to expand on the work led by Woojin An, then a post-doctoral associate in the Roeder laboratory (An et al., 2004). This study showed that CARM1 stimulates p53-dependent transcription *in vitro*, and that the stimulatory effect of CARM1 is partially lost when H3R2, R17 and R26 are mutated to glutamine. Since I show that R42 is a target for CARM1, I decided to ask whether R42 mutation could impair CARM1-dependent transcriptional stimulation. I then took advantage of designer histones homogeneously dimethylated on H3R42. This set of experiments was made possible by the generous contributions of Dr. Xiangdong Lu in the Roeder laboratory at the Rockefeller University, who performed the transcription assays presented in this thesis, and Sam Pollock, an undergraduate student in the Muir laboratory at Princeton University, who synthesized the designer H3(R42me2a) molecule.

3.2 CARM1 methylates R42 in nucleosomes

In Chapter 2 I have shown that CARM1 controls the level of R42 methylation *in vivo*, and that it methylates R42 on peptide substrates *in vitro*. Before performing transcription experiments on chromatinized templates, I needed to confirm that CARM1 could indeed methylate R42 in the context of the nucleosome. For this purpose I assembled octamer and mononucleosome substrates from recombinant human histones (**Figure 3.2**). Briefly, N-terminal 6xHis-tagged histones were expressed in *E. coli*, extracted from inclusion bodies and purified by Ni-NTA affinity resin. Denatured, purified histones were combined in dialysis buttons such that H3 and H4 were slightly limiting and dialyzed into high salt buffer. TEV or PreScission proteases were used to remove the 6xHis tags. Untagged octamers were purified from unincorporated dimers, individual histones and proteases by Superdex 200 size exclusion chromatography. Fractions containing octamers were pooled and verified by SDS-PAGE.

Mononucleosomes were formed by combining purified octamers with 153 bp dsDNA corresponding to the 601 strong positioning sequence (Lowary and Widom, 1998), followed by gradient dialysis from 2M NaCl to 0.1M NaCl over approximately 30 hours, as described in (Ruthenburg et al., 2011). Assemblies were checked for proper DNA incorporation by native 5% polyacrylamide gel electrophoresis and ethidium bromide staining (**Figure 3.3**).

Recombinant CARM1 was incubated with equal amounts of either recombinant octamers or mononucleosomes with SAM as a methyl-donor. One small aliquot of each reaction was incubated with radioactive SAM as a control

Figure 3.2: Assembly and purification of recombinant octamers

Purified recombinant 6xHis tagged human histones were combined in denaturing buffer and dyalized into high salt buffer to assemble octamers. The tags used for purification were removed with TEV and PreScission proteases and octamers were further purified sith Superdex 200 size exclusion FPLC. The resulting chromatogram is shown, A280 absorbance graphed as a function of time. Octamer peak fractions were pooled as indicated (red box) and analyzed by SDS/PAGE and Coomassie staining

Figure 3.2

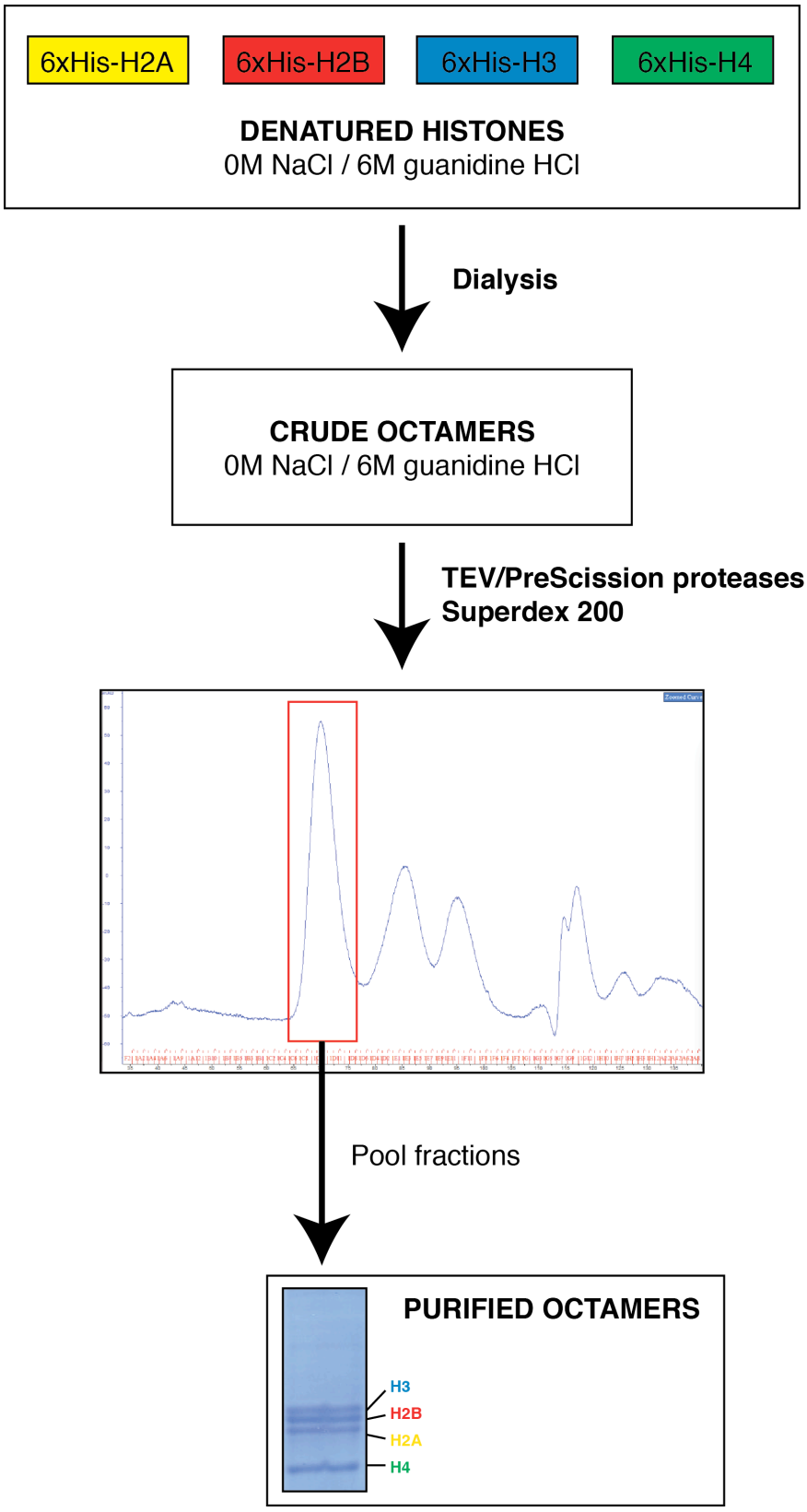
6xHis-H2A
6xHis-H2B
6xHis-H3
6xHis-H4
DENATURED HISTONES
0M NaCl / 6M guanidine HCl
Dialysis
CRUDE OCTAMERS
0M NaCl / 6M guanidine HCl
TEV/PreScission proteases
Superdex 200
Pool fractions
PURIFIED OCTAMERS
H3
H2B
H2A
H4

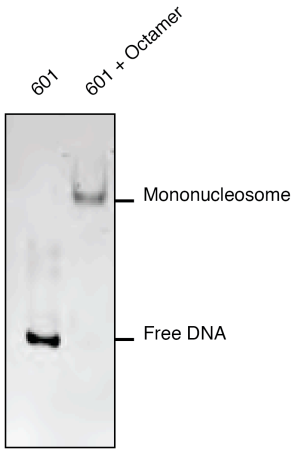

Figure 3.3: Characterization of nucleosome assembly

Mononucleosome assembly quality was assessed by 5% native PAGE and EtBr staining. The faster migrating band is the uncomplexed 601 DNA fragment (left lane), while the assembled nucleosomes is the slower migrating band on the right.

for methyltransferase activity and is shown in **Figure 3.4A**. The reaction products were analyzed by MS/MS for R42 methylation: H3R42me2a was detected from both the octamer and nucleosome reactions, although methylation of R42 in the nucleosome context was several folds less efficient than in octamer form (**Figure 3.4B**). This difference in efficiency most likely reflects the barrier imposed by the DNA in the nucleosome structure. The apparent disconnect between the incorporated radioactivity in **Figure 3.4A** and the levels of H3R42 methylation of **Figure 3.4B** can be explained by CARM1 targeting other arginines, most likely H3R17 and H3R26. PRMT6 was not tested since this experiment was done as a preliminary step to transcription assays using CARM1 as a co-activator, but will be tested in future experiments.

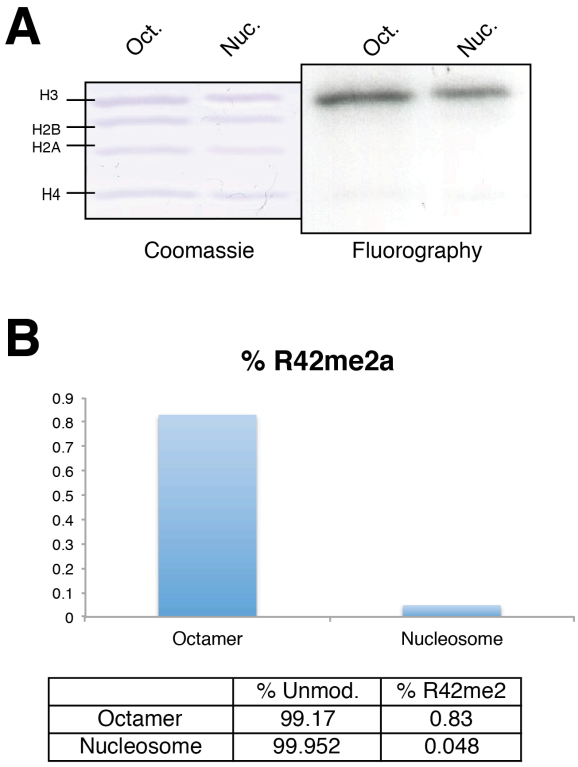

	% Unmod.	% R42me2
Octamer	99.17	0.83
Nucleosome	99.952	0.048

Figure 3.4: CARM1 methylates R42 in nucleosomes

(**A**) Left panel shows coomassie staining for the octamer (Oct.) and nucleosome (Nuc.) substrates after methltransferase reaction with CARM1; right panel shows the fluorogram of the indicated substrates. (**B**) Graph shows the relative abunbdance of R42me2a (in %) in the substrate as in (A). The exact amounts are also shown in the table below.

3.3 Effects of H3R42 mutations on transcription

With the knowledge that CARM1 can methylate H3R42 in the context of the nucleosome, I mutagenized the H3 sequence to generate arginine to lysine (R42K) or alanine (R42A) mutations. While both mutant residues cannot be modified by CARM1, R42K is a more conservative mutation since the potential

interaction with the DNA backbone is preserved due to the retention of the positive charge, while R42A also neutralizes the charge of the residue. Mutant histones were purified and assembled into octamers as described in the previous section.

Equal amounts of purified mutant and wild type octamers were used to reconstitute chromatin templates onto the plasmid DNA template illustrated in **Figure 3.5A** using a recombinant ACF/NAP1 system. The assay scheme used is the one in **Figure 3.1A**: p53 was used as activator and p300 as co-activator as in (An et al., 2004). The results of the transcription experiment are in **Figure 3.5B**: no transcription was observed in the absence of activator (lane 1). Minimal transcription was observed on the wild type template with p53 (lane 2), while mutations of R42 increased the transcription output, with R42A having a greater effect than R42K (lane 3 and 4). Lane 5 to 7 represent reactions with both p53 and p300: as expected, p300 stimulated transcription from the wild type template (lane 5) and to a greater extent from the two mutant templates (lane 6 and 7).

These results show that mutation of H3R42 to lysine or alanine make chromatin templates more permissive to transcription. This might be due to the fact that arginine interacts with DNA better than lysine or alanine (Luscombe et al., 2001), creating a more permissive chromatin template. The bigger effect observed with the R42A mutation compared to R42K might account for the loss of positive charge. The increased transcription of the two mutants with p300 compared to the wild type template could be explained by the fact that mutant nucleosomes might be easier to unwrap, therefore exposing some of the internal

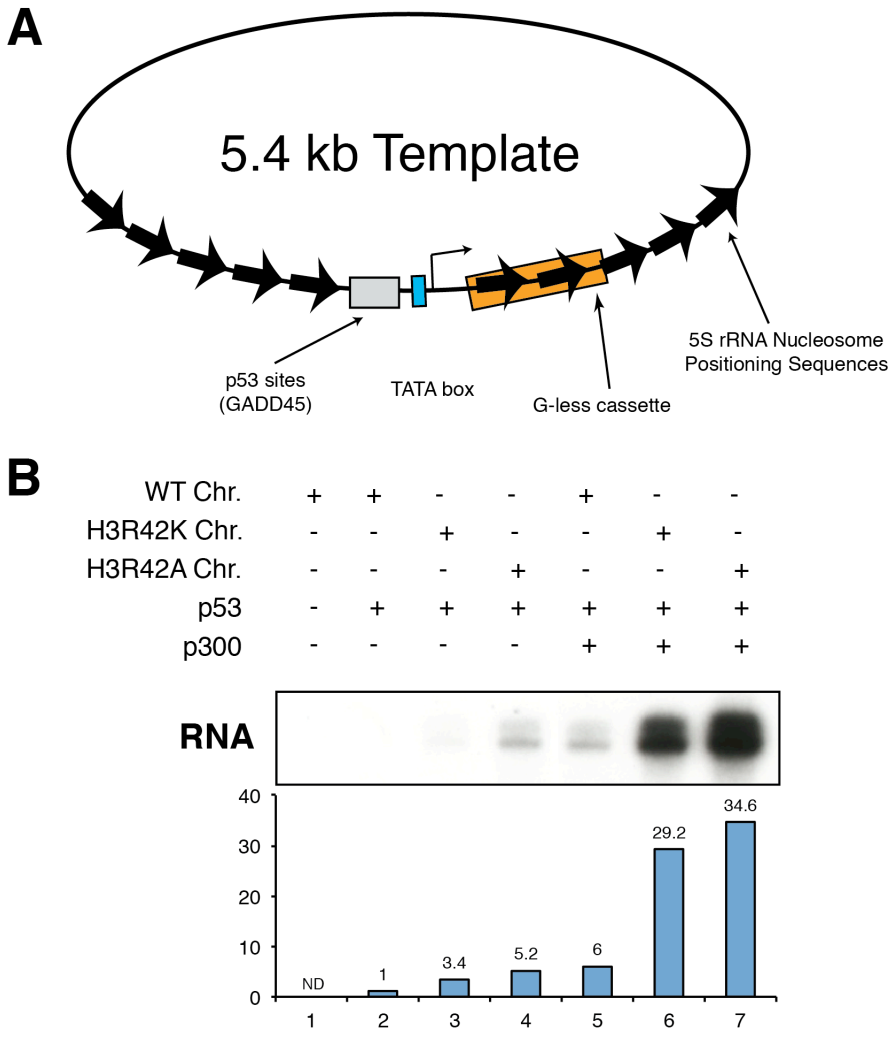

Figure 3.5: Mutations of R42 affect *in vitro* transcription

(**A**) Schematic representation of the template used in transcription assays. It contains an adenovirus major late promoter, a tandem of five p53 binding sites and nucleosome positioning sequences. (**B**) p53-dependent, p300-mediated transcription activation in the presence of wild type or mutant H3R42A/K templates. Top panel shows autoradiograph of the P32-labeled transcripts. The bottom graph shows the densitometric quantification of the transcripts. Transcription assay performed by Dr. Xiangdong Lu.

targets of p300 for easier acetylation. This speculation could be tested by incubating p300 with mutant or wild-type mononucleosomes, and quantifying by MS the different sites of acetylation.

Although this experiment demonstrates the importance of R42 in transcriptional activation, I felt that this system would not be optimal for analysing the direct effect of methylation of R42 by CARM1. To do so, we would have to compare the gain in transcription upon CARM1 addition between different templates, and since different templates have different basal activities, I felt that the comparison would not be fair. As a consequence, I decided to bypass the need for CARM1 methylation altogether and use designer histones pre-methylated on R42. In addition to not requiring enzymatic reaction, designer histones are homogeneously modified, therefore maximizing the likelihood of observing an effect of the modification in transcription assays.

3.4 Generation of designer H3R42me2a histones

Generating H3R42me2a designer histones is technically challenging because of the central location of the modification within the histone. The standard strategy for generating designer histones is based on a single ligation of one synthetic peptide harbouring the PTM of interest and one recombinant segment containing the remaining histone sequence (Shogren-Knaak and Peterson, 2004). Asymmetric dimethyl arginine is only available as an Fmoc-protected building block, and the Fmoc protection strategy is not reliable over long peptides (Larsen and Holm, 1994). Because of the central location of the modification, we

believed the best synthetic route to generate H3R42me2a designer histones would involve covalently ligating three polypeptide segments rather than two. A two-ligation strategy has been previously utilized to generate H3K56ac by ligating 3 peptides of synthetic origin (Shimko et al., 2011).

The semi-synthetic strategy utilized to generate designer histone H3 proteins harboring pre-modified R42me2a is illustrated in **Figure 3.6**. In this strategy, one segment is obtained using solid-phase peptide synthesis (SPPS) with a Boc protection strategy, one using SPPS with an Fmoc protection strategy, and one would be of recombinant origin. Particular attention was paid when selecting the appropriate ligation junctions, in order to obtain a "scar-less" product. Native chemical ligation requires an N-terminal cysteine for the reaction to occur: this leaves a residual cysteine at the ligation site. Unfortunately the only cysteine in human H3.2 is present at position 110, therefore not useful for this ligation strategy. A desulphurization reaction can be used to convert ligation-site cysteines to alanines (Wan and Danishefsky, 2007), such that alanines can be considered potential ligation sites. Given these considerations, we chose A29 and A47 as ligation sites that allow generation of fully native H3 with pre-modified R42.

The recombinant segment (47- 135) was expressed in *E.* coli and purified from inclusion bodies. Alanine 47 was mutated to cysteine to allow subsequent ligation (A47C). Taking advantage of the generally benign mutation of the only cysteine in H3.2 to alanine (Luger et al., 1999a), a C110A mutation was engineered to prevent problems with the ligation steps. No protein expression

Figure 3.6: Generation of semi-synthetic H3R42me2a protein.

Schematic representation of the synthetic scheme utilized. See Materials and Methods for details. ① and ②: solid phase peptide synthesis of H3(1-28) and H3(29-46;A29C,R42me2a); ③ ligation of the two synthetic peptides to generate H3(1-46;A29C,R42me2a); ④ final ligation step of the recombinant fragment H3(47-135;A47C,C110A) to H3(1-46;A29C,R42me2a) followed by desulfurization to convert cysteines to alanines. Residue 42 is highlighted in yellow. Synthesis was carried out by Sam Pollock in the Muir Laboratory.

Figure 3.6

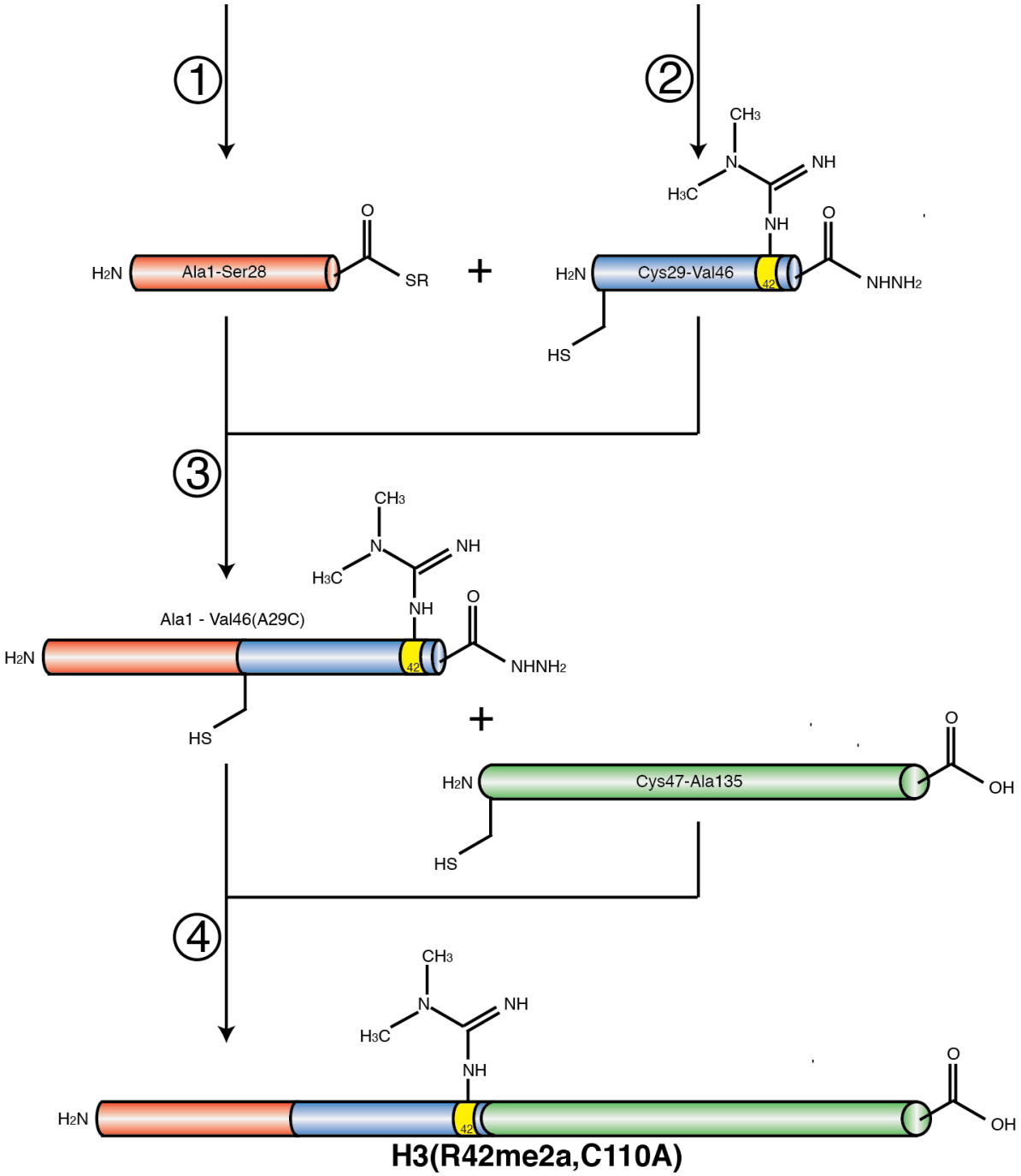
①
②
③
④
H2N
Ala1-Ser28
SR
O
+
CH3
N
NH
H3C
NH
O
H2N
Cys29-Val46
42
NHNH2
HS
CH3
N
NH
H3C
NH
O
Ala1 - Val46(A29C)
H2N
42
NHNH2
HS
+
H2N
Cys47-Ala135
O
OH
HS
CH3
N
NH
H3C
NH
O
H2N
42
OH
H3(R42me2a,C110A)

was observed with the standard 6xHis tag used for purifying full-length histones. A longer construct with a 6xHis-SUMO tag resulted in successful expression. After purification, the tag was cleaved with overnight treatment with SUMO protease. Peptide 1 was synthesized corresponding to residues 1-28 of H3. Peptide 2 was synthesized corresponding to residues 29-46, bearing R42me2a, and an A29C mutation. Each segment was verified by MS analysis.

In the first step of the synthesis, peptide 1 was ligated to peptide 2, to give H3(1-46;A29C,R42me2a). This intermediate product was purified and ligated to recombinant fragment H3(47-135,A47C) to give H3R42me2a(A29,47C;C110A), which was then purified by HPLC chromatography. In the final step, a desulphurization reaction was used to convert the two cysteine residues to the native alanine residues present in H3. After HPLC purification, the production of the desired product was verified by mass spectrometry (**Figure 3.7**). The final yield of purified designer histone was about 0.4 mg.

3.5 Preparation of designer octamers and chromatin templates

Semi-synthetic H3R42me2a was incorporated into core histone octamers with wild-type recombinant human H2A, H2B and H4 by salt dialysis as described in section 3.2. Removal of the 6xHis tags used for purification of H2A, H2B and H4 was carried out by digesting with TEV and PreScission proteases overnight. Untagged designer octamers were purified by Superdex 200 size exclusion chromatography and confirmed by SDS-PAGE (**Figure 3.8**). Control unmodified histone octamers were formed containing recombinant human H3.2(C110A).

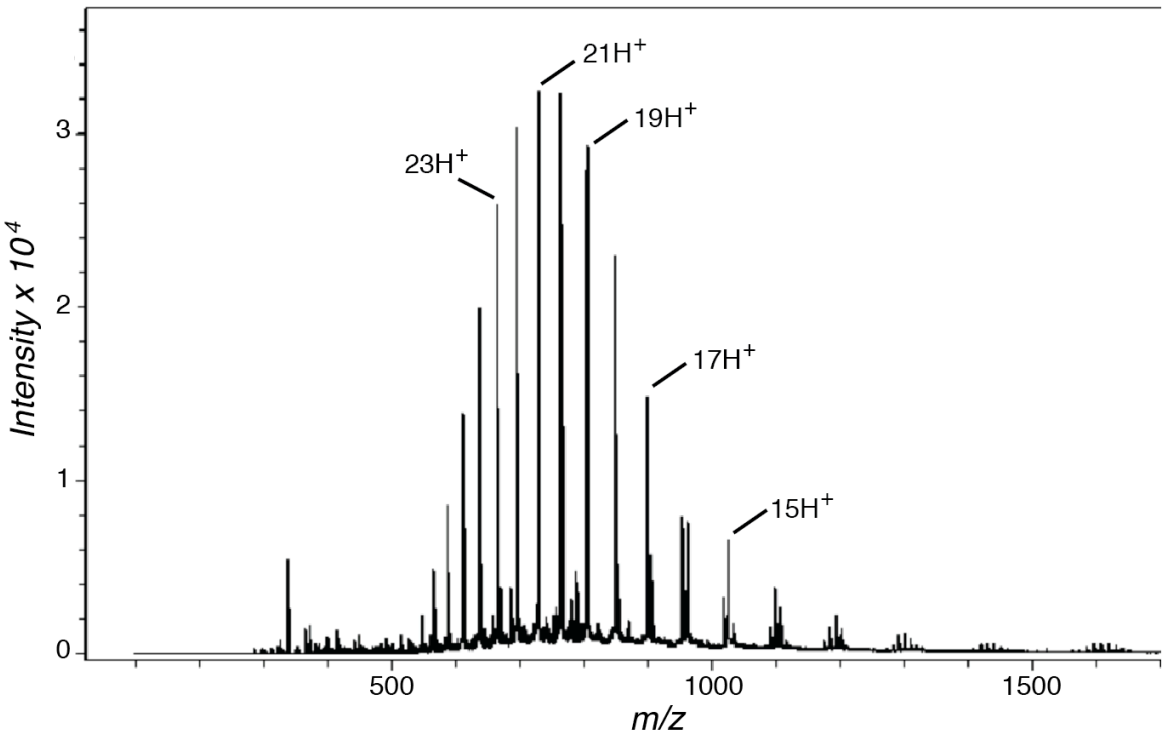

Figure 3.7: Confirmation of the production of H3(R42me2a)

Electrospray ionization mass spectrometry (ESI–MS) spectrum of purified H3(R42me2a). Charge states are labelled. $(M+H)^+$ observed: 15,252 ± 4 Da; expected: 15,252 Da. MS characterization carried out by Sam Pollock.

Unmodified and designer octamers were run side by side on SDS-PAGE to confirm equivalent protein composition (**Figure 3.9A**).

Equal amounts of purified octamers were used to reconstitute chromatin templates onto the 5.4 kb plasmid DNA template described in Section 3.3 (**Figure 3.5A**) using the ACF system as described previously. Characterization of assembled chromatin templates by incomplete micrococcal nuclease digestion and agarose gel electrophoresis revealed a 200 bp ladder of kinetic intermediates with both input octamers although the methylated input is lightly loaded compared to the unmodified one (**Figure 3.9B**), confirming that the quality

of both unmodified and R42me2a chromatin is similar, and that R42 methylation does not prevent assembly of octamers into chromatin.

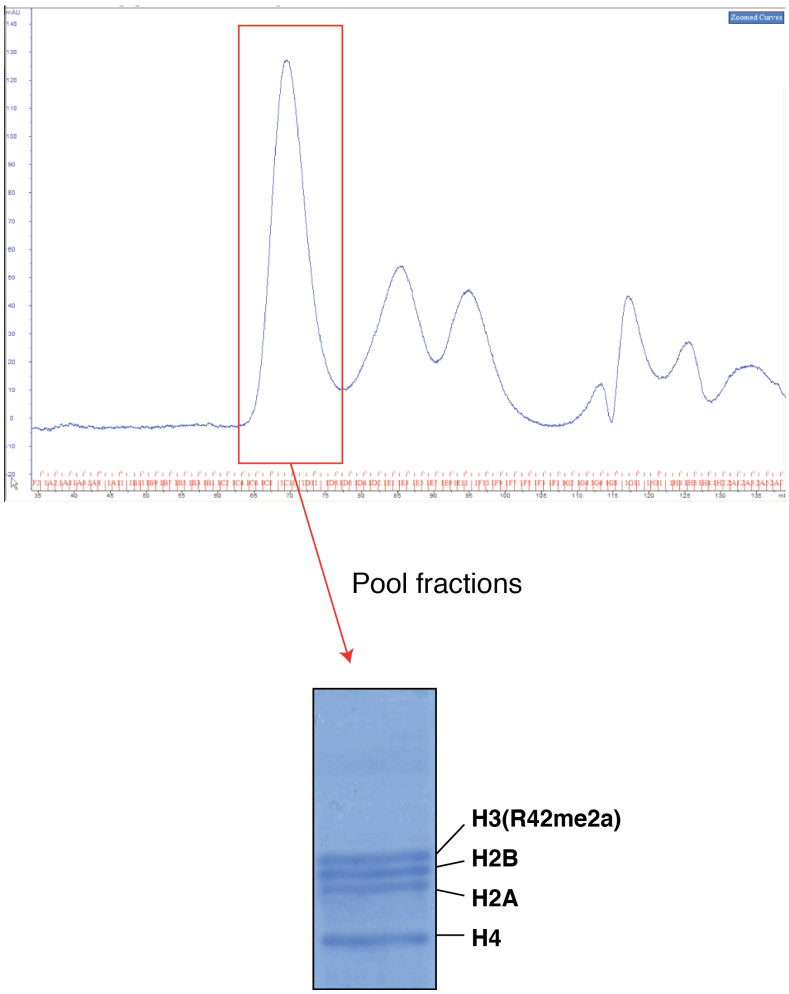

Figure 3.8: Purification of designer octamers

H3(R42me2a) and recombinant H2A, H2B and H4 were assembled into octamers and purified by Superdex 200 size exclusion FPLC. The resulting chromatogram is shown, A280 absorbance graphed as a function of time. Octamer peak fractions were pooled as indicated (red box) and analyzed by SDS/PAGE and Coomassie staining

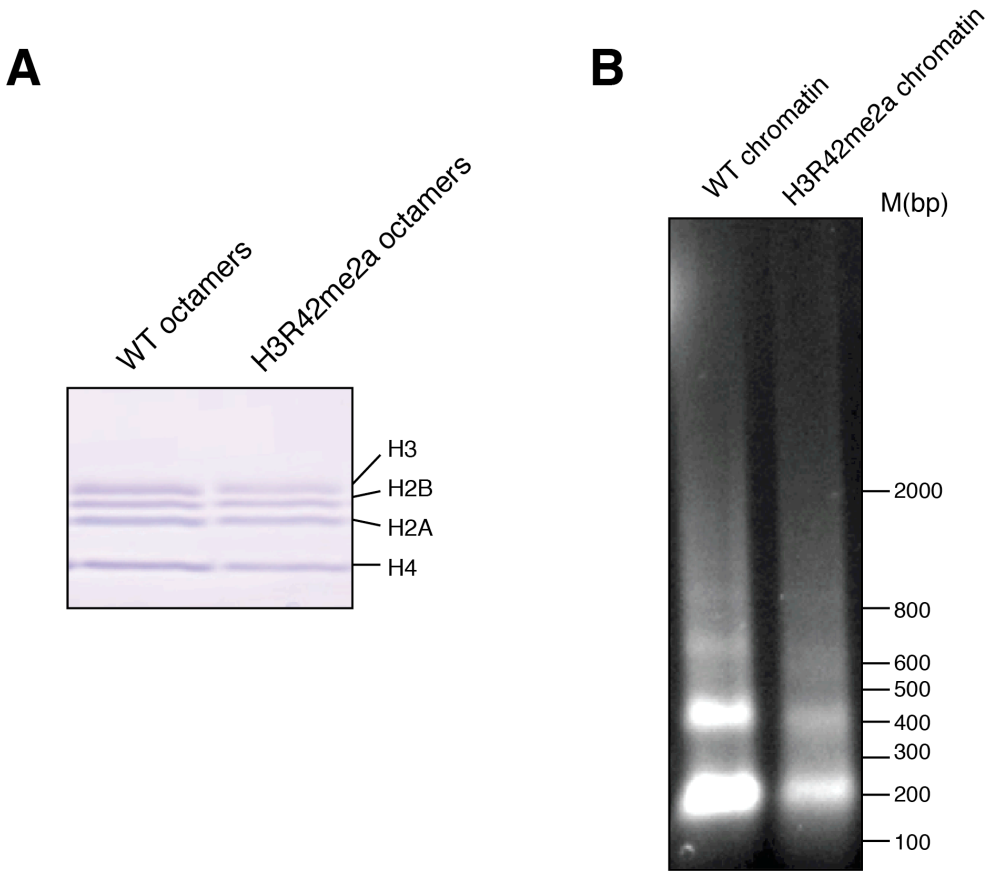

Figure 3.9: Chromatin template assembly with wild type and designer octamers

(**A**) Reconstituted octamer samples were analysed by SDS–polyacrylamide gel electrophoresis (SDS–PAGE) and staining with Coomassie blue. (**B**) Assembled chromatin was partially digested with MNase, and the recovered DNA was detected as described (An and Roeder, 2004). Chromatin assembly and MNase digestion was carried out by Dr. Xiangdong Lu.

3.6 Effect of H3R42me2a on *in vitro* transcription

Designer and unmodified chromatin templates were then used in the activator-dependent *in vitro* transcription system described in detail in Section 3.3 and illustrated in **Figure 3.5B**. By using the designer R42me2a template we

tested whether H3R42me2a can act together with p300 activity and stimulate transcription directly. As shown in **Figure 3.10**, in the presence of both p53 and p300 a 3-fold increase in transcription was observed from R42me2a over unmodified templates (compare lane 6 with lane 5). The reaction in absence of p300 was also performed: in these conditions R42 methylation resulted in a considerable (6-fold) increase in transcription versus unmodified template (compare lane 4 with lane 3). In the absence of activator p53 no transcription

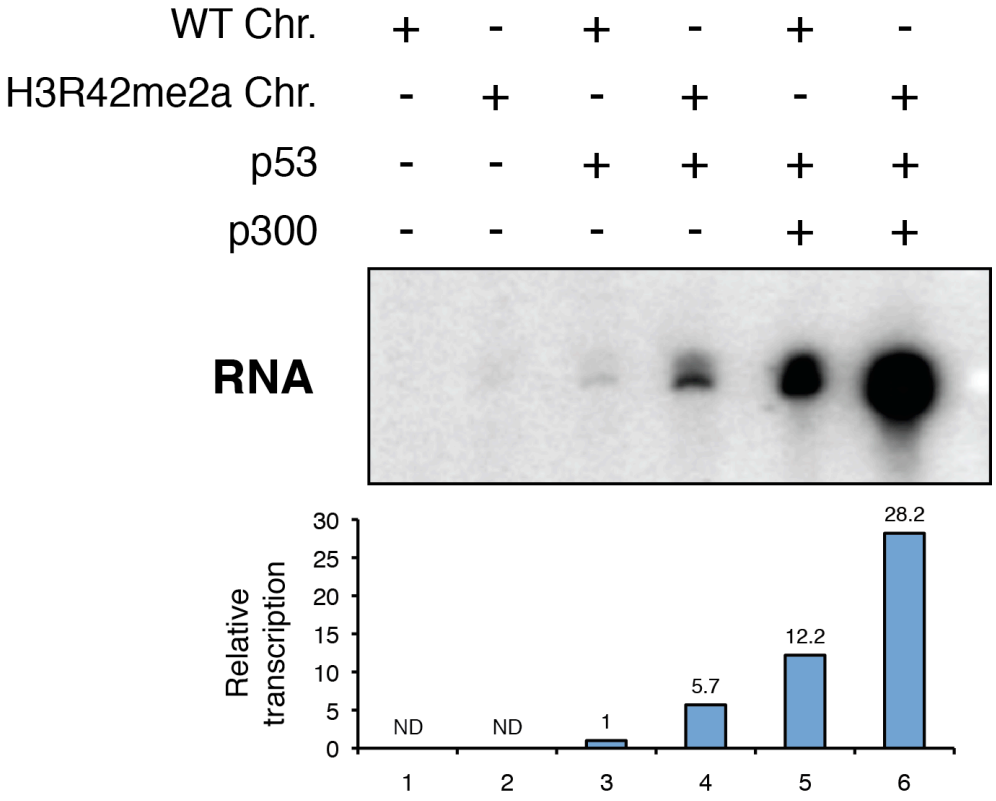

Figure 3.10: H3R42me2a stimulates transcription *in vitro*.
p53-dependent, p300-mediated transcription activation in the presence or absence of H3R42 asymmetric dimethylation. Top panel shows the autoradiograph of the P32-labeled transcripts. The bottom graph shows the densitometric quantification of the transcripts. Transcription assay performed by Dr. Xiangdong Lu.

was observed (lanes 1 and 2). In light of the results presented in the next Chapter, it is important to point out that the experiments shown here were carried out in the presence of the HDAC inhibitor sodium butyrate.

Taken together, these results demonstrate that methylation of H3R42 directly stimulates transcription *in vitro,* alone or in combination with the activity of co-activator p300. To my knowledge this is the first time that a methylation in the nucleosome core is demonstrated to have such an effect. Natural extensions of these results will be to understand whether H3R42me2a also weakens the interaction with DNA and/or enhances the activity of nucleosome remodelling enzymes.

Chapter 4. Effector-mediated consequences of H3R42 methylation

Histone PTMs often result in promoting or blocking the recruitment of binding proteins to chromatin in what has been described as *trans* mechanisms (Allis et al., 2007). In Chapter 3, I described a direct effect of H3R42 methylation on transcriptional activation. The fact that this modification can directly influence the properties of chromatin does not rule out the possibility that this modification could have effector-mediated effects. In this Chapter, I describe experiments aimed at uncovering some of these effects.

4.1 Investigation of a possible crosstalk with phosphorylation of H3Y41 by tyrosine-protein kinase JAK2

It has been proposed that pairs of neighboring modifiable residues in histones might not act independently but rather form cassettes ("binary switches") where modification of each site depends on the other, and modification on one or the other residue will influence the recognition and binding of modules to the cassette (Fischle et al., 2003). For example, HP1 association with H3K9me3 is required for its localization to heterochromatin (Lachner et al., 2001). H3S10, adjacent to K9, is phosphorylated in M-phase by Aurora B kinase. HP1 binding to H3K9me3 is incompatible with H3S10phos, and this explains the observed dissociation of HP1 from chromatin during mitosis (despite no significant change in H3K9me3 levels) (Fischle et al., 2005; Hirota et al., 2005). This binary switch is

also played out at the enzyme level, with H3S10phos inhibiting H3K9 methylation by methyltransferase SUV39, and H3K9me3 inhibiting H3S10 phosphorylation by Aurora B (Rea et al., 2000) (**Figure 4.1**).

Since H3R42 is adjacent to the phospho-acceptor tyrosine 41 (H3Y41) (**Figure 4.1**), I asked whether these two residues could constitute a cassette, as K9 and S10 do. Phosphorylation of H3Y41 by the kinase JAK2 prevents the binding of the chromo-shadow domain in Heterochromatin Protein 1α (HP1α) to this region of H3, therefore preventing silencing of JAK2 target genes (Dawson et al., 2009).

I first tested whether H3R42 methylation affects the kinase activity of JAK2 by radioactive kinase assays on peptide substrates. Unmodified H3(34-52) peptides were effectively phosphorylated by recombinant JAK2, while mono- or dimethylation on R42 completely inhibited the activity (**Figure 4.2A**).

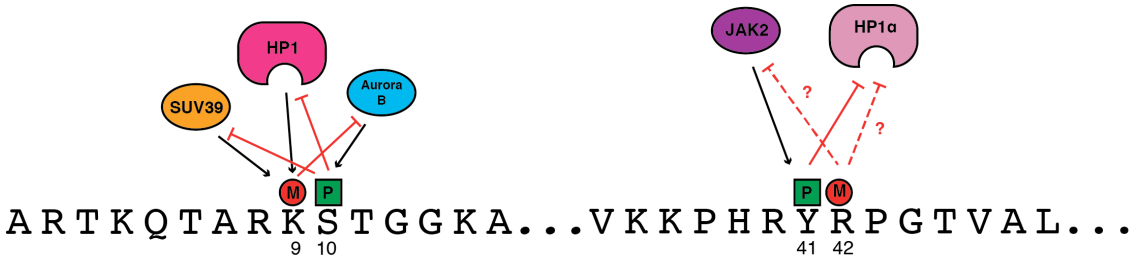

Figure 4.1: Binary switches in histone H3

The partial sequence of human histone H3 is shown with highlighted the demonstrated K9/S10 binary switch and the putative Y41/R42 binary switch. Dotted lines with question marks indicate relationships that were tested experimentally in this thesis. Methylation is indicated with red M, phosphorylation with green P.

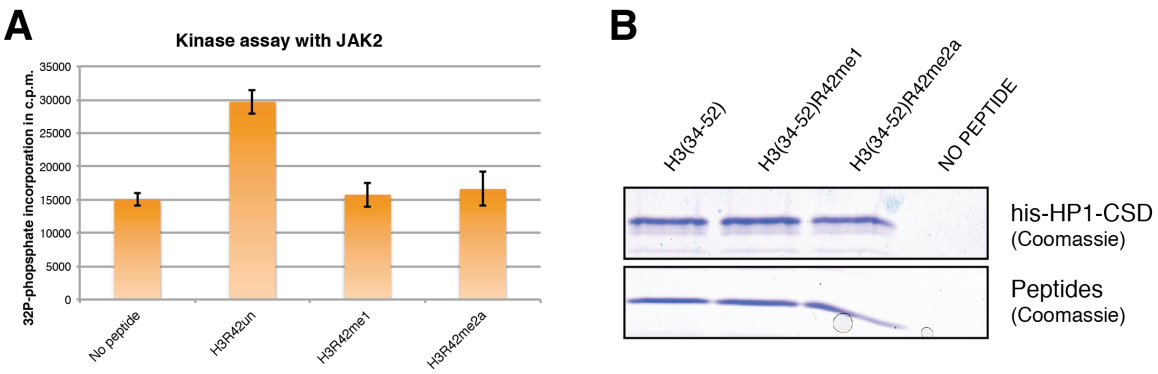

Figure 4.2: R42 methylation affects JAK2 activity but not HP1α binding

A) JAK2 activity was measured by quantifying the amounts of P32-phosphate deposited onto the peptide substrates indicated at the bottom of the graph . **B)** The recombinant chromoshadow domain (CSD) from HP1α was subjected to peptide pull-down with the biotinylated peptide indicated on top of the panels. After SDS-PAGE, proteins were stained by Coomassie.

I then tested whether the binding of the chromo-shadow domain of HP1α was sensitive to H3R42 methylation. I purified the bacterially expressed 6xHis-tagged domain and used it in peptide pull-down experiments. Biotinylated H3(34-52) peptides (unmodified or methylated on R42) were conjugated to streptavidin beads and used as baits. The result in **Figure 4.2B** shows that the chromo-shadow domain of HP1α binds to H3 peptides irrespective of methylation on R42.

Taken together, these results suggest a possible interplay between Y41phos and R42me2, where R42 methylation might locally prevent JAK2 activity without affecting HP1α recruitment. Unfortunately, given the lack of reliable antibodies for

R42me2a to be used in functional and genomic studies, I did not further investigate this putative crosstalk.

4.2 Identification of binders: candidate approach.

In contrast with the large number of proteins that specifically bind to methylated lysines, only two domains are known to recognize methylated arginines on histones. WDR5 has been shown to bind with its WD40 domain to symmetrically dimethylated H3R2 (H3R2me2s), a mark deposited by PRMT5 and PRMT7 (Migliori et al., 2012b). The Tudor domain protein TDRD3 has been identified as a specific binder of asymmetric dimethyl arginine on histones; in particular, TDRD3 binds H3R2me2a and H3R17me2a, two modifications catalyzed by the enzymes PRMT6 and CARM1, respectively (Liu et al., 2012; Yang et al., 2010).

Since my data demonstrates that R42 is dimethylated asymmetrically by CARM1 and PRMT6, I tested whether TDRD3 could also bind H3R42me2a. For this purpose, I purified bacterially expressed GST-tagged Tudor domain from TDRD3 and used it in peptide pull-down experiments with biotinylated H3 peptides. H3R17me2a peptides were used as positive control. I confirmed that the Tudor domain of TDRD3 binds very effectively to peptides containing H3R17me2a. On the other hand, no binding was observed for modified or unmodified H3R42 peptides (**Figure 4.3**). This result indicates that TDRD3 is not a reader of H3R42me2a.

4.3 Identification of binders: an unbiased approach.

Since the candidate approach described in the previous section did not prove successful, I opted for an unbiased approach and used peptide pull-down assays in my search for R42 binders. Our laboratory and others have successfully used this method to identify histone PTM readers (Wysocka, 2006; Wysocka et al., 2005; Wysocka et al., 2006). Biotinylated histone peptides that are either unmodified or modified on the residue of interest are immobilized on avidin beads and incubated with nuclear extracts (**Figure 4.4**). After incubation and extensive washes, bound proteins are eluted from the beads and resolved by SDS–PAGE. Proteins differentially present in one of the two lanes are identified by mass spectrometry. Since unmodified and modified pull-downs are always carried out side by side, this method allows identification of effectors that either bind to

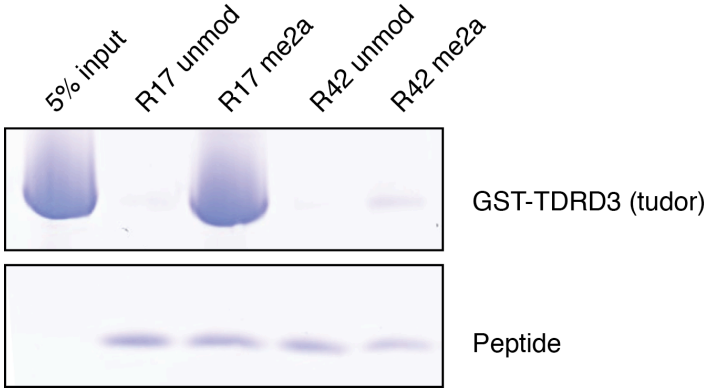

Figure 4.3: TDRD3 does not bind to H3R42me2a

The recombinant tudor domain from TDRD3 was subjected to peptide pull-down with the biotinylated peptide indicated on top of the panels. After SDS-PAGE, proteins were stained by Coomassie.

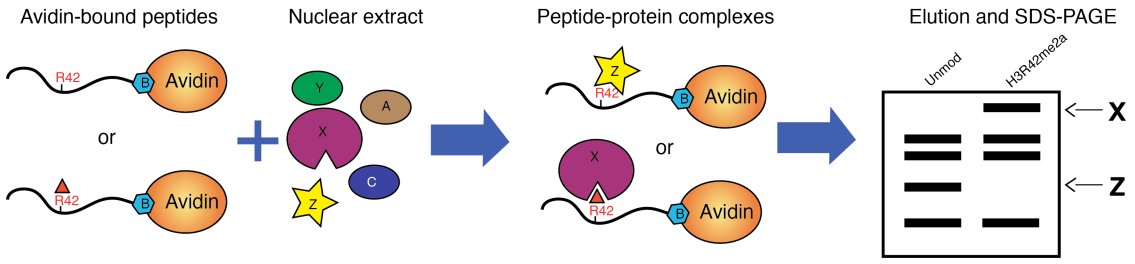

Figure 4.4: Schematics of the peptide pull-down assay.
Biotinylated histone peptides either unmodified, or modified at R42 are immobilized on avidin beads and incubated with extract. Specific effector proteins bind to histone peptides in a modification-sensitive manner. Bound proteins are then eluted from the avidin beads, and resolved by SDS–PAGE. Candidate readers are enriched in the modified (factor X), or unmodified (factor Z) peptide pull-down lane. Adapted from (Wysocka, 2006).

(factor X in **Figure 4.4**) or are blocked by (factor Z in **Figure 4.4**) methylation on H3R42.

I first carried out the pull-down experiment following standard protocols (Wysocka, 2006) and incubating the resin-bound peptides with pre-cleared nuclear extracts from HeLa cells. As shown in **Figure 4.5A**, this method did not result in any differentially represented band. I reasoned that the peptides used (residues 34-52 of H3) are positively charged and could therefore interact with nucleic acids present in the nuclear extract. The nucleic acids might in turn act as a bridge and bind to many DNA/RNA-interacting nuclear proteins and result in a high background, preventing the identification of putative R42 binders. To overcome this problem I treated the nuclear extracts with RNAse and ethidium bromide prior to incubation with the peptides, following a protocol introduced by

Peter Lewis, a post-doctoral associate from our laboratory. With this modified protocol, several bands appeared enriched in the pull-down lane of the unmodified peptide (**Figure 4.5B**). The experiments were repeated three times with independent extracts, and enriched bands (together with corresponding molecular weight bands from the modified pull-down) were sent for MS analysis at the Proteomics Resource Center of The Rockefeller University. Two

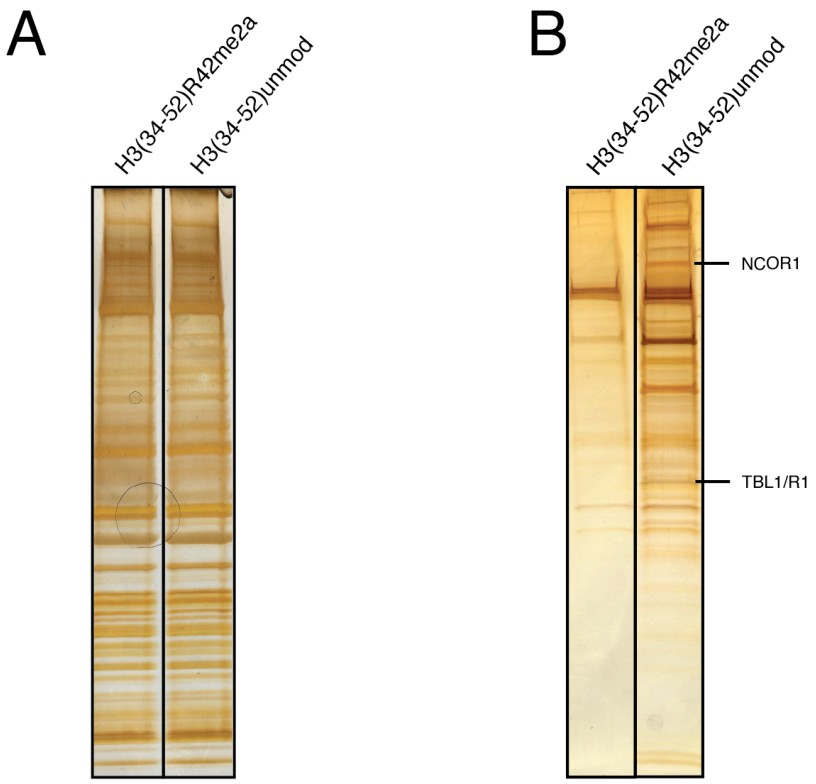

Figure 4.5: Unbiased peptide pull-down assays.

Proteins recovered after peptide pull-down with R42me2a or unmodified histone peptides were resolved by SDS-PAGE and silver stained. (**A**) shows a representative experiment using untreated nuclear extracts, (**B**) shows a representative experiment with nuclear extract pretreated with RNAse and EtBr. The bands corresponding to NCOR1 and TBL1/R1 are highlighted.

Table 4.1: List of factors identified by MS after peptide pull-down

Protein name	Function	Enriched?
Cdc5-like protein	Cell cycle control	Yes, unmodified
E3 ubiquitin-protein ligase HUWE1	Protein degradation	No
E3 ubiquitin-protein ligase UBR	Protein degradation	No
E3 ubiquitin-protein ligase UBR5	Protein degradation	No
Intron-binding protein aquarius	RNA splicing	Yes, unmodified
Pre-mRNA-splicing factor SYF1	RNA splicing	Yes, unmodified
Pre-mRNA-processing factor 19	RNA splicing	Yes, unmodified
Nuclear receptor co-repressor 1 (NCOR1)	Transcriptional repression	Yes, unmodified
F-box-like/WD repeat-containing protein TBL1	Transcriptional repression	Yes, unmodified
F-box-like/WD repeat-containing protein TBLR1	Transcriptional repression	Yes, unmodified
SWI/SNF complex subunit SMARCC2	Nucleosome remodeling	No

polypeptides were consistently present in the unmodified peptide pull-down and not in the H3R42me2a one in all three replicates. These proteins were identified by MS as NCOR1 and TBL1/TBLR1 (highlighted in **Figure 4.5B**). All the proteins that were identified with high degree of confidence in these experiments are listed in **Table 4.1**.

NCOR1 and TBL1/R1 made interesting candidates for follow-up experiments because they both belong to the N-CoR co-repressive complex. This complex represses the expression of target genes through the histone de-acetylase activity of its subunit HDAC3, and is recruited to chromatin by several transcription factors, including nuclear hormone receptors (Perissi et al., 2010). Since the experiments presented in Chapter 3 suggested a role for H3R42me2a in transcriptional activation, it seemed plausible that methylation of R42 might prevent the binding of a repressive complex like N-CoR to chromatin. The experiments presented in the next sections are aimed at validating the binding

result and at understanding the mechanisms through which this interaction might affect gene expression.

4.4 Validation of H3:NCoR interaction

To validate the binding of the NCoR complex to unmodified R42 peptides, I repeated the peptide pull-down experiments from nuclear extracts as described previously. The resulting samples were run on SDS-PAGE and blotting was performed with antibodies specific to NCOR1. H2B, H3 and H4 N-terminal peptides were used as controls. The result shown in **Figure 4.6A** confirms that NCoR selectively binds to unmodified H3(34-52), and not to R42me2a peptides or any of the control peptides.

To rule out the possibility that the binding observed might be an artifact due to the inherent complexity of the crude nuclear extract, and not be a direct interaction, I asked whether a purified N-CoR complex would show the same binding specificity. I obtained affinity-purified human NCoR complex from Dr. Tomoyoshi Nakadai, a post-doctoral associate from the Roeder laboratory at The Rockefeller University. Briefly, Flag-tagged NCOR1 was overexpressed in HeLa cells, purified using M2 anti-Flag affinity resin, and eluted with 3xFlag peptides. The purified complex was confirmed by MS analysis (**Figure 4.6B**). When used in peptide binding experiments, the purified complex recapitulated the binding pattern observed with nuclear extracts (**Figure 4.6C**).

Taken together these results validate that the N-CoR complex interacts *in vitro* with H3 peptides containing R42, and that methylation on this residue

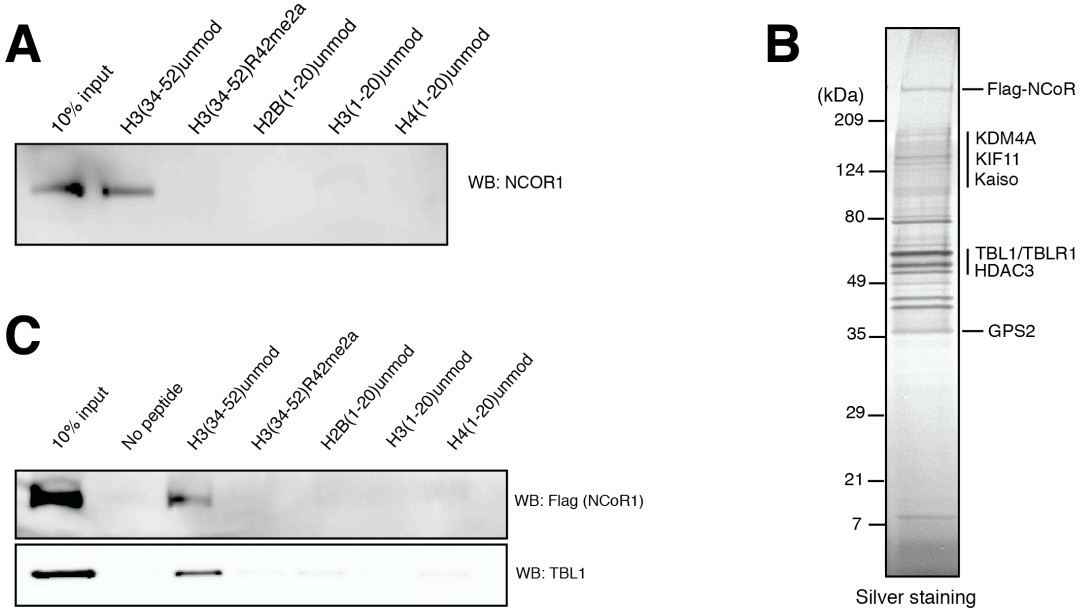

Figure 4.6: H3R42me2a prevents binding of the NCoR complex to H3.
(**A**) Recovery of NCOR1 after peptide pull-down from HeLa nuclear extract, assayed by western blot. The peptides utilized are indicated at the top of the panel. (**B**) Protein composition of the affinity-purified NCoR complex. Proteins were resolved by SDS-PAGE and silver stained. (**C**) Recovery of affinity-purified NCoR complex after pull-down with the peptides indicated at the top of the panel. Western blot (WB) probed with anti-Flag (NCOR1) and anti-TBL1 antibodies.

abolishes the binding. Interestingly, although a previous report had shown binding of N-CoR to H2B or H4 N-tail peptides (Yoon et al., 2003), I was not able to reproduce these results. This could be explained by differences in washing conditions used in pull-down experiments, or by differences in protein preparations.

4.5 Molecular basis of H3:NCoR interaction

With data suggesting a direct interaction between N-CoR and H3, I sought to investigate which protein domain(s) within the complex could mediate this interaction. I used the SMART protein domain prediction algorithm (http://smart.embl-heidelberg.de/) and interrogated the sequences of each known subunit of the complex for the presence of known histone binding domains.

The subunits TBL1 and TBLR1, two highly similar components of N-CoR, both contain 7-blade WD40-repeat domains (**Figure 4.7A**). I chose these domains as candidate binders since several WD40-repeat domains have been shown to specifically recognize the methylation states of histone arginines (Migliori et al., 2012a).

To test the binding of the WD40 domains, I expressed both in *E. coli* and purified them as GST-tagged recombinant proteins. When used in peptide pull-down experiments (**Figure 4.7B**), both domains behaved similarly: they displayed binding to unmodified R42 peptides, but not to methylated R42 peptides or control peptides. To rule out the possibility that the binding observed might be a result of stickiness due to improper folding of the bacterially-produced proteins, I synthesized the same protein domains *in vitro* using reticulocyte lysates, and labeled them with 35S-methionine. Peptide pull-down followed by SDS-PAGE and autoradiography (**Figure 4.7C**) confirmed binding of both domains to unmodified R42 peptides.

The data presented in this section demonstrates a direct interaction of the WD40 domains in TBL1 and TBLR1 with an internal H3 peptide centered on R42.

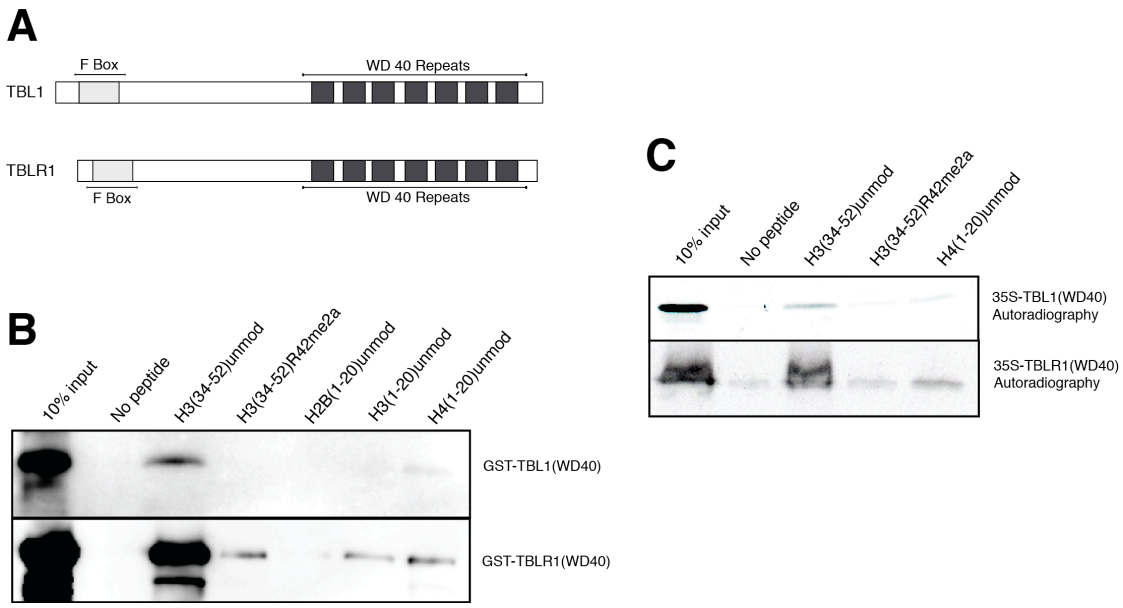

Figure 4.7: WD40 domain in TBL1 bind to H3(34-52)

(**A**) Domain structure of TBL1 and TBLR1. (**B**) Peptide pull-down of recombinant WD40-repeat domains from TBL1 and TBLR1. The proteins were resolved by SDS-PAGE and visualized by anti-GST western blot. (**C**) Peptide pull-down of *in vitro*-translated WD40-repeat domains from TBL1 and TBLR1. The radiolabeled protein is visualized by autoradiography after SDS-PAGE.

The binding appears to be sensitive to R42 methylation, providing an effector-mediated role for this new modification. In addition to the C-terminal WD40 domain, TBL1/R1 contain an N-terminal tetramerization domain. The tetrameric nature of TBL1/R1 suggests that the proteins may serve as a scaffold for a multivalent chromatin-targeted repressive complex that also contains HDAC activity. Indeed, comparison of the predicted size of the complex with a di-nucleosome also suggests that the complex may be able to simultaneously target HDAC3 activity to multiple nucleosomes (Watson et al., 2012) (**Figure 4.8**).

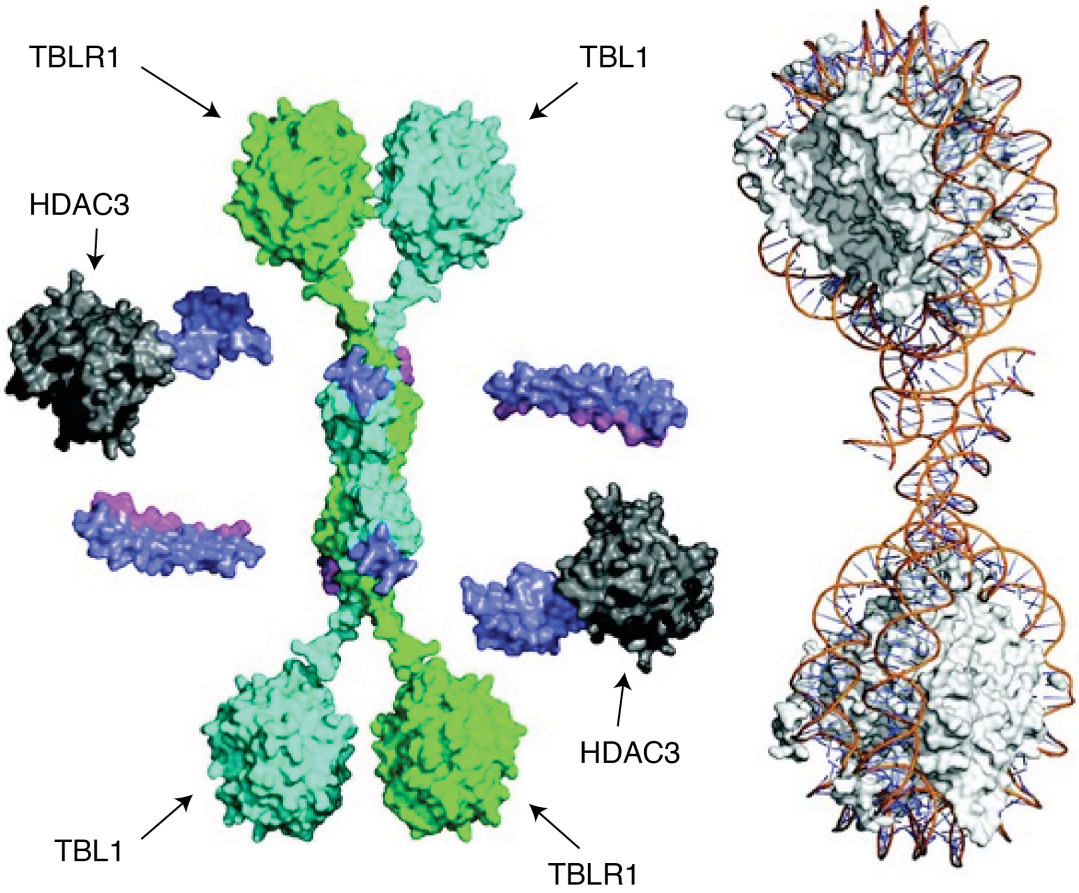

Figure 4.8: Model of NCoR complex binding to nucleosomes

Synthesis of the structural data to yield a global illustrative model of the core NCoR complex including WD40 domains for TBL1 (green & cyan disks), HDAC (grey) and NCOR (purple). A di-nucleosome is shown to the right to illustrate the relative scale of the chromatin substrate, suggesting binding to two adjacent nucleosomes. Adapted from (Watson et al., 2012).

4.6 Effects of binding on complex recruitment and activity

As described in Chapter 1, histone PTMs that act *in trans* can influence either the recruitment of effector proteins to chromatin or the enzymatic activity of effector proteins on chromatin.

I first asked whether the observed negative effect of R42me2a on N-CoR binding to H3 peptides affected the overall chromatin recruitment of the complex. To this end, I compared the nuclear salt extraction properties of N-CoR in cells with different levels of H3R42me2a. Since CARM1 appeared to play a dominant role in controlling the levels of this modification (as discussed in Chapter 2) I chose to compare CARM1 +/+ and -/- MEFs. The double-negative cells showed in fact over 50% reduction in R42 methylation by MS (**Figure 2.10B**). Briefly, I isolated nuclei by hypotonic lysis from CARM1 +/+ and -/- MEFs, and incubated them with buffer containing increasing amounts of NaCl to sequentially extract proteins from chromatin. Western blot for NCOR1 was carried out to follow the extraction profile of the complex (**Figure 4.9**). Immunoblots for WDR5 and H3 were used as controls. The extraction profile for NCOR1 does not differ in either cell line, suggesting that H3R42 methylation may not influence the recruitment of N-CoR to chromatin. This is consistent with the report of N-CoR being recruited to chromatin via interaction with several DNA-binding transcription factors (Perissi et al., 2010).

In light of this I asked whether binding of N-CoR to H3 could allosterically affect the enzymatic activity of HDAC3 within the complex. This would be similar

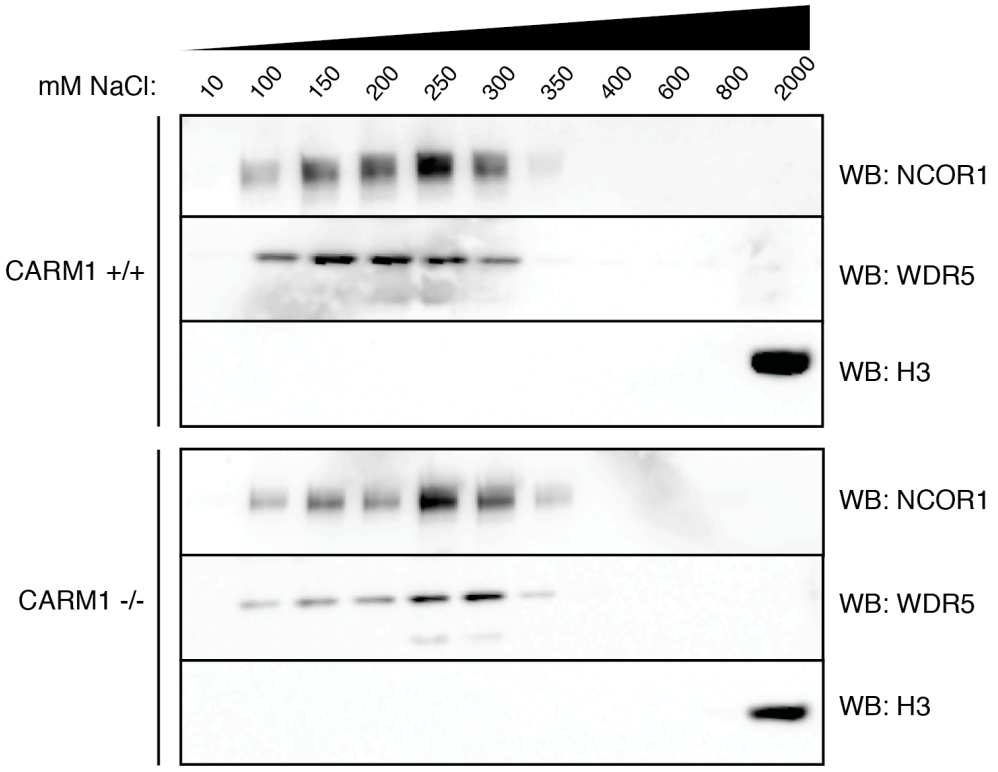

Figure 4.9: Salt extraction properties of N-CoR.

Western blot (WB) for NCOR1, WDR5 and H3 after sequential salt extraction from nuclei purified either from CARM1 +/+ or CARM1-/- MEFs.

to the situation reported for the PRC2 histone methyltransferase complex, where the WD40-repeat subunit Eed binds to H3K27me3 peptides and increases the methyltransferase activity of the complex (Margueron et al., 2009). To test this hypothesis, I measured HDAC activity with commercially-available fluorescent HDAC activity assays (Active Motif catalog # 56200), using affinity-purified N-CoR complex and addition *in trans* of increasing amounts of unmodified or R42me2a H3(34-52) peptides, or of H4(1-20) peptide as a control. The fluorescent assay kit utilizes a proprietary short peptide substrate that contains

an acetylated lysine optimized for HDAC3 (as well as other HDACs). Once the substrate is deacetylated, the lysine residue reacts with a developing solution releasing a fluorescent product, which can be quantified using a fluorescent plate reader. As shown in **Figure 4.10A**, addition of unmodified H3(34-52), but not the other two tested peptides, caused a concentration-dependent increase in the HDAC activity of the complex.

I then asked whether this stimulatory effect translated into different levels of acetylation *in vivo*. To do this, I compared by western blot the levels of histone lysine acetylation in CARM1 +/+ and -/- MEFs. In agreement with the observed

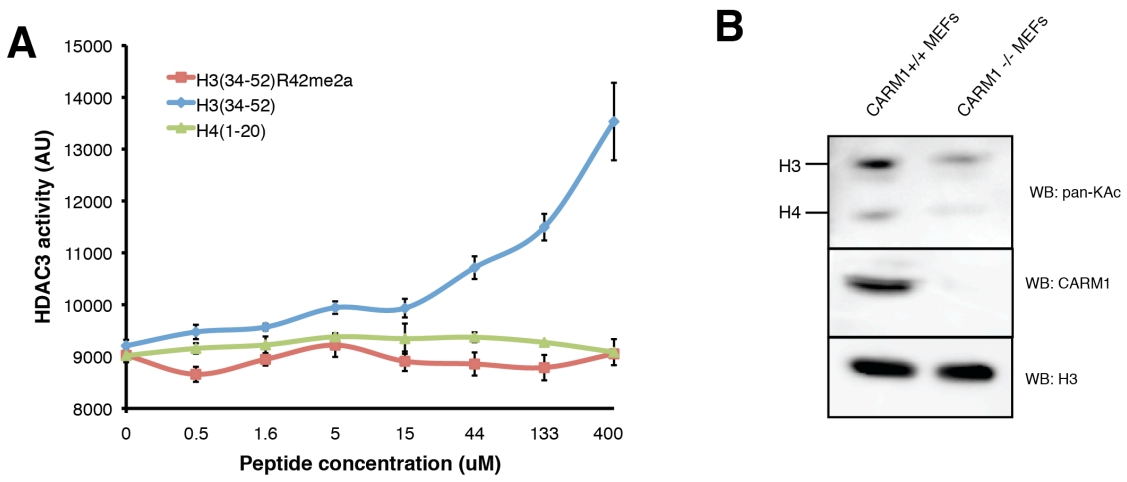

Figure 4.10: H3R42me2a prevents stimulation of N-CoR

(**A**) HDAC activity of purified NCoR complex with increasing amounts of H3 peptides added *in trans,* measured by fluorescence. (**B**) Levels of acetylated histones, CARM1 and H3 in extracts from CARM1 +/+ or CARM1-/- MEFs measured by anti-Kac western blot. Middle panel confirms absence of CARM1 in CARM1-/- MEFs. Western blot for H3 in the bottom panel is a control for loading.

stimulation of HDAC activity upon H3 binding, I observed that the amounts of acetylated lysines on histone H3 and H4 are larger in CARM1 +/+ than in CARM1 -/- MEFs (**Figure 4.10B**).

Taken together, these results suggest a role for H3R42me2a in protecting chromatin from deacetylation, by negating a stimulatory effect on the HDAC complex N-CoR. Although preliminary, this observation is potentially very interesting and provides a novel mechanism through which histone acetylation levels can be regulated.

Chapter 5. Discussion

Methylation of arginines on histone tails has been linked to both transcriptional activation and repression (Bedford and Clarke, 2009). The experiments presented in this thesis show for the first time that a methylated arginine at the interface between DNA and histones, H3R42, targeted by methyltransferases CARM1 and PRMT6, has a dual transcriptional activating role: H3R42me2a both prevents histone deacetylation and affects the biophysical properties of chromatin, making it easier to be transcribed in *in vitro* transcription assays. While uncertainties remain as to the actual mechanisms that bring about these dual effects, these findings call attention to H3R42 methylation as influencing both enzyme activities and substrate properties in the promotion of transcriptional activation.

5.1 Methylation of residue 42 of histone H3 is conserved through evolution

In Chapter 2 I used an antibody-enrichment strategy combined with mass spectrometry to identify novel arginine methylation sites in human histones. The rationale for using an enrichment step was based on the notion that arginine methylation is a rare PTM in histones. This approach led me to the identification of dimethylated arginine 42 of histone H3 (H3R42) in both human and mouse cells, a residue at the DNA entry/exit region of the nucleosome (**Figure 2.2** and **2.10**).

Histones are among the most conserved proteins in eukaryotes (Malik and Henikoff, 2003). Residue 42 in histone H3 shows an amino-acid change with functional conservation: *S. cerevisiae* "evolved" a lysine at this position while most other organisms have arginine (**Figure 1.8B**). Both arginine and lysine are basic residues and have the potential to create electrostatic interactions or hydrogen bonds with DNA, suggesting that this contact is structurally important. Upon discovery of the H3R42me2 mark, I hypothesized that, given the particular location within the nucleosome structure, this modification could play a role in transcriptional activation. My hypothesis was further supported by work from Boeke and colleagues (Hyland et al., 2011): they, in fact, discovered that H3K42 is dimethylated in budding yeast as well, and that mutation to alanine (K42A) results in a widespread increase in transcription. These findings, together with mine, suggest that methylation of residue 42 in histone H3, whether that residue is a lysine or an arginine, is a conserved and important regulatory modification that may modulate the tightness of interaction between DNA and the histone octamer.

Since organisms as phylogenetically distant as yeast and humans maintained methylation of residue 42 in H3 as a mechanism to modulate transcription, it will be interesting to see if this PTM can also be found in other organisms.

5.2 Both CARM1 and PRMT6 methylate R42 *in vivo.*

In Chapter 2 of this thesis I demonstrated that CARM1 and PRMT6 can methylate H3R42 *in vitro* on peptide substrates (**Figures 2.5** and **2.8**), and that

both enzymes regulate the level of H3R42me2a *in vivo* (**Figures 2.9** and **2.10**). The two identified methyltransferases fit with the initial hypothesis that H3R42me2a is a mark involved in transcriptional activation. CARM1 was originally identified as a transcriptional co-activator for nuclear steroid receptors (Chen et al., 1999) and its positive role in transcriptional activation is well established (An et al., 2004). On the other hand, PRMT6 activity has generally been associated with transcriptional repression (Guccione et al., 2007; Hyllus et al., 2007; Iberg et al., 2007), although more recently it has been reported that PRMT6 can positively regulate a group of nuclear receptor target genes (Harrison et al., 2010).

My data demonstrates that both enzymes are important in controlling the overall level of R42 methylation *in vivo.* Given this overlap, an outstanding question remains: do both enzymes target the same or different genomic locations? Or is there a cell-specificity for the use of either enzyme? Or a time-specificity in the cell cycle? Interestingly, the activity of CARM1 on H3R17 has been shown to increase in M phase (Sakabe and Hart, 2010), it is therefore possible that methylation of H3R42 might follow a similar behaviour. The lack of a specific antibody for H3R42me2a prevented me from answering these questions. Should this reagent become available, it would be very interesting to map H3R42me2a in the genome and study how the localization of this PTM is affected by CARM1/PRMT6 knockdown/overexpression. It is possible that redundancy exists between the two enzymes and that the activity of one might influence the activity of the other.

At the enzyme level, it also remains unclear whether CARM1 and PRMT6 deposit methyl groups on their tail sites and R42 at the same time. This could be addressed with *in vitro* methylation experiments on recombinant nucleosomes followed by MS analysis to quantify all the modifications. Unfortunately both H3R17 and H3R2 (the major sites previously mapped for CARM1 and PRMT6, respectively) are within tryptic peptides that are not suitable for the current quantification methods used in the Garcia laboratory (personal communication).

It is possible that interaction with different factors might impart different specificities to the enzymes or cause their recruitment to different regions. I show in **Figure 3.4B** that recombinant CARM1 methylates H3R42 less efficiently when in a nucleosome context compared to octamer. This can be explained by the fact that the DNA might partially block the enzyme from targeting this site. It is very likely that efficient R42 methylation *in vivo* requires the activity of nucleosome-remodelling enzymes. In support of this hypothesis, it has been shown that CARM1 co-purifies with several components of the ATP-dependent SWI-SNF chromatin remodelling complex, and that this interaction enhances its methyltransferase activity (Xu et al., 2004). Future experiments aimed at purifying specific interactors for both enzymes will help gain a better understanding of this aspect.

5.3 H3R42me2a as a direct modulator of transcription

In Chapter 3, I asked whether methylation of H3R42 had an effect on *in vitro* transcription. With the use of a designer histone strategy combined with *in vitro*

transcription assays, I showed that H3R42me2a makes chromatin templates intrinsically better substrates for transcription (**Figure 3.10**). This result was obtained through productive collaborations with the Muir and Roeder laboratories.

I speculate that the observed increase in transcription is due to the weakening of the interaction between H3R42 and DNA when the residue is methylated. I am currently testing this hypothesis by assembling unmodified or designer (H3R42me2a) mononucleosomes and incubating aliquots at increasing salt concentrations. After PAGE and ethidium bromide staining I should be able to quantify the degree of DNA unwrapping from the nucleosomes (free DNA migrates faster than DNA complexed with histones), and compare it between the two kinds of input nucleosomes. Although a rigorous proof is still lacking, several previously reported observations support this hypothesis: 1) the DNA entry/exit region is important in controlling the unwrapping of DNA from nucleosomes (North et al., 2012); 2) mutation of residue 42 to alanine makes nucleosomes more mobile (Somers and Owen-Hughes, 2009); 3) mutation of residue 42 to alanine in *S. cerevisiae* results in a hyper-transcription phenotype (Hyland et al., 2011).

This speculation is also in agreement with the finding that H3R42A mutant chromatin is a better substrate for transcription than H3R42K, and that both mutants are better substrates than wild type (**Figure 3.5**). Mutation to alanine, in fact, abolishes the positive charge at this position and eliminates interaction potential with DNA; lysine, while still retaining the charge, is a worse DNA-

interactor than arginine (Luscombe et al., 2001). This is particularly interesting from an evolutionary standpoint: *S. cerevisiae* is one of the few organisms that has a lysine at position 42 and this might be explained by the fact that only ~1.5% of human DNA is coding, relative to 50% for *S. cerevisiae*, and that the baseline state of yeast chromatin is less compact and repressive (Alberts, 2008; Lohr and Hereford, 1979). By having a lysine instead of an arginine at position 42, *S. cerevisiae* makes its chromatin potentially more permissive to transcription.

5.4 H3R42me2a as "protection" from deacetylation

Although the findings discussed in the previous sections argue for a *cis* effect of H3R42me2a, I did not want to rule out the possibility *a priori* that this modification might have effector-mediated consequences. Binding of effector proteins in this region of H3 is, in fact, possible: binding of the chromoshadow domain of HP1α extends between residues 37 and 56 of H3 (Richart et al., 2012), a region that also includes R42. This may look surprising given that this region should be sterically occluded by the presence of DNA (**Figure 1.8A**). It has been shown that the DNA at the entry/exit point can unwrap spontaneously from the nucleosome, and that, in physiological conditions, nucleosomes are in equilibrium between wrapped and partially unwrapped states (Li and Widom, 2004). This also explains how recombinant CARM1 can methylate R42 in a nucleosome context (**Figure 3.4**).

In Chapter 4, through unbiased peptide pull-down experiments, I demonstrate that the N-CoR complex binds to histone H3 in a region centered on R42, and that the dimethylation of H3R42 prevents this binding (**Figure 4.5** and **4.6**). The binding observed is direct through the WD40 repeat domains in the subunits TBL1/TBLR1 (**Figure 4.7**). This finding is very interesting since no function has been assigned yet to those domains, although it has been hypothesized that they might mediate interactions with nucleosomes (Oberoi et al., 2011). No tridimensional structure of the TBL-WD40 domains is available, so it is hard to predict which residues could be involved in the observed binding. I will attempt to design mutants based on conservation or structure prediction algorithms to find ones that negate the binding.

Using *in vitro* deacetylase assays, I also showed that binding of the N-CoR complex to H3 stimulates the intrinsic histone deacetylase activity of the complex (**Figure 4.10**), although the mechanism underlying this stimulatory effect remains unclear. It is possible that the catalytic subunit HDAC3 itself “senses” the lack of methylation on R42 and that this stimulates its enzymatic activity. I am planning to test this hypothesis by using recombinant HDAC3, instead of the purified NCoR complex, in the same *in vitro* deacetylase assays. Another more likely possibility is that binding of TBL1/R1 to H3 induces a conformational change in the complex that renders it more active. This could be tested by using histone binding-deficient TBL mutants in the same HDAC assays.

The overall observation of H3R42me2a protecting from histone deacetylation, fits well with the demonstration that H3R42me2a stimulates transcription *in vitro*.

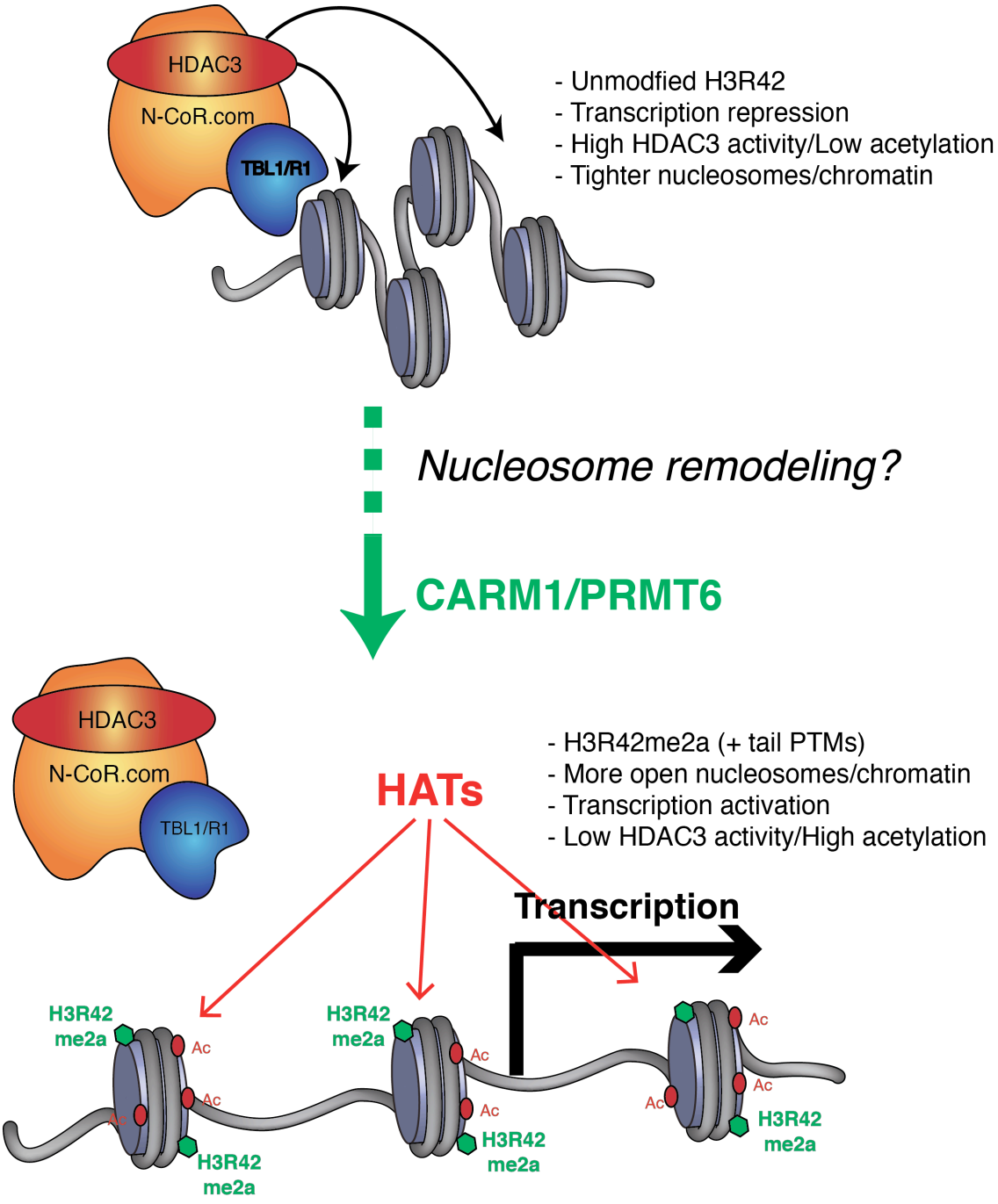

Figure 5.1: Model for H3R42me2a function

H3R42me2a stimulates transcription by making chromatin intrinsically more open and by protecting histones from deacetylation

Interestingly, a recent report suggests that the two previously known sites of methylation on the H3 N-tail catalyzed by CARM1 (H3R17me2a and R26me2a), also prevent histone deacetylation by blocking the binding to chromatin of co-repressor complexes NuRD and TIF1 (Wu et al., 2012). Taken together, these observations suggest a general role for CARM1 activity as a protective mechanism against deacetylation.

5.5 Summary and perspective

While several groups have shown the direct effects of acetylation of specific lysines on the lateral surface of the nucleosomes (Manohar et al., 2009; Neumann et al., 2009; Shimko et al., 2011; Simon et al., 2011; Tropberger et al., 2013), the experiments presented in this thesis are the first, to my knowledge, to examine the effects of methylation events within the nucleosome lateral surface. I identified H3R42 as a novel methylation site in mammalian cells in keeping with a conserved function in evolution and with a role in stimulating transcription. With a combination of mass spectrometry and *in vitro* enzymatic reactions, I demonstrated that R42 can be dimethylated and that CARM1 and PRMT6 are the relevant methyltransferases. I show a dual-effect role for this mark: 1) to facilitate a structural alteration in the chromatin, making it easier to transcribe in our transcription assays; and 2) to “protect” the chromatin template from N-CoR-mediated histone deacetylation.

The model that arises from these findings is shown in **Figure 5.1**. In the initial state, a hypothetical target gene is maintained repressed by the HDAC activity of

N-CoR (and potentially other deacetylase complexes). Local CARM1/PRMT6 activity results in decompaction of chromatin due to H3R42 methylation. Because of the inefficiency of R42 methylation by recombinant CARM1 on nucleosomes compared to free octamers (**Figure 3.4B**), it is possible that nucleosome remodeling activities might be necessary to help expose the target residue. H3R42me2a in turn prevents histone deacetylation by N-CoR, and as a result histone acetylation increases, further increasing chromatin decompaction and transcriptional activation. I propose that H3R42me2a might be deposited at specific genomic locations to modulate the expression of target genes and to prevent their silencing brought about by histone deacetylation.

Several other arginines on the DNA path in the nucleosome have been found to be methylated in large-scale proteomic studies (Cosgrove et al., 2004; Tan et al., 2011). In **Figure 1.7** I highlighted where these arginines are located on the *X .laevis* nucleosome structure. H3R52 and H3R53 are at the DNA entry/exit point and it can be hypothesized that methylation on these residues might have very similar effects to methylation of H3R42. Interestingly, R52A or R52K mutants are lethal in *S. cerevisiae,* suggesting a critical role for this residue in chromatin structure (Hyland et al., 2005). H3R63, H4R35, H2AR42, H2AR77 and H2BR83 are also on the lateral surface of the nucleosome, but outside of the DNA entry/ exit point: H3R63 and H4R35 make hydrogen bonds with phosphate groups in the DNA major grove, while H2AR42, H2AR77 and H2BR83 penetrate the minor grove to form hydrogen bonds with DNA bases (Luger et al., 1997). Given the buried nature of these residues, it is very unlikely that reader proteins can

interpret their modified state. Also, methylation must occur either in the absence of DNA (pre-deposition) or mechanisms must exist to temporarily expose the nucleosome lateral surface to modifying enzymes. I predict that methylation on these residues affects directly the stability and intrinsic properties of nucleosomes and chromatin, resulting in effects to DNA-templated processes that include, but are not limited to, transcription.

With the work presented in this thesis I demonstrated that methylation can directly alter the properties of chromatin, and I envision that by extending these studies to other strategically placed methylations, we will be able to understand how histone:DNA interactions are dynamically modulated and lead to changes in downstream chromatin structure and function.

Materials and Methods

Antibodies and Plasmids

Anti-CARM1, anti-PRMT6, anti-NCOR1, anti-TBL1 and anti-WDR5 antibodies were purchased from Bethyl Laboratory. Anti-H3 antibody was obtained from Millipore (Billerica, MA). Anti-pan(Kac) was purchased from PTM Biolabs. Anti-H3(R17me2a) and anti-mono and dimethyl arginine (ab412) were purchased from Abcam.

The plasmids encoding the Flag-HA-tagged PRMTs were kindly provided by Dr. Ernesto Guccione (IMCB, Singapore). For bacterial expression, the ORFs for CARM1 and PRMT6 were cloned into plasmid pGEX-6p1 (GE Life Sciences, Piscataway, NY). The TBL1 and TBLR1 constructs were as described in (Yoon et al., 2003) and were obtained from Dr. Jiemin Wong.

Dharmacon ON-TARGET*plus* SmartPool siRNAs against CARM1 and PRMT6 were purchased from Thermo Scientific.

Cell Lines and Regents

HEK293 cells and HeLa cells were from ATCC. CARM1-/- and +/+ MEFs were obtained from Mark Bedford's Laboratory. Cells were maintained in DMEM (Invitrogen, Grand Island, NY) supplemented with 10% FBS (PAA, Westborough, MA). *Trans*IT®-LT1 Transfection Reagent (Mirus Bio, Madison, WI) was used for

plasmid transfections. DharmaFECT Transfection Reagents (Thermo Scientific) were used for siRNA transfections.

Nuclear Extract Preparation

Nuclear extracts were prepared according to the Dignam and Roeder method (Dignam et al., 1983). Briefly, cells were swelled in hypotonic buffer (10mM Hepes pH 7.9, 10mM KCl, and 1.5mM $MgCl_2$) and then lysed by mechanical disruption in low salt buffer (20mM Hepes pH 7.9, 25% glycerol, 1.5mM $MgCl_2$, 20mM KCl). Soluble nuclear were then extracted by dropwise addition of high salt buffer (20mM Hepes pH 7.9, 25% glycerol, 1.5mM $MgCl_2$, 1.2M KCl) to a final KCl concentration of ~320mM KCl, leaving behind the chromatin pellet.

Acid Extraction of Histones and Enrichment

Histones were purified by acid extraction as previously described (Shechter et al., 2007). Briefly, nuclei were purified by resuspending cells in hypotonic lysis buffer (10 mM Tris–Cl pH 8.0, 1 mM KCl, 1.5 mM MgCl2 and 1 mM DTT). Nuclei were resuspended in nuclei in 0.4 N H_2SO_4 and the soluble proteins were precipitated by adding 33% TCA (Sigma).

For the initial enrichment strategy, we first obtained a chromatin pellet from HeLa cells following the classic Dignam and Roeder nuclear extract preparation. The final pellet was then acid extracted and the resulting extract was resuspended in PBS supplemented with 0.1% NP-40 and incubated for 4 hours with anti methyl-arginine antibodies (ab412). After incubation with Protein A/G

agarose beads, the bound proteins were eluted in 100 mM Glycine pH 2.5 and analyzed by MS.

Liquid Chromatography Mass Spectrometry and Sample Preparation

MS analysis was performed by Gary LeRoy in Benjamin Garcia's laboratory, then at Princeton University. Histones were propionyl derivatized with propionic anhydride, trypsinized and prepared for MS as described in (Plazas-Mayorca et al., 2009) with minor adjustments. 2-Propanol was substituted for Methanol during the derivatization reaction. Histone peptides were separated by reverse phase nanospray liquid chromatography on C18 resin with an Agilent 1200 series HPLC. Mass spectrometry was performed on a LTQ-Orbitrap mass spectrometer (ThermoFisher Scientific).

Mass Spectrometry Data Analysis

All MS/MS spectra were processed with the Bioworks 2.0 program using the Sequest algorithm. The MS/MS database searching parameters included a precursor tolerance of 0.1 Da, and fragment tolerance of 0.5 Da. Computer searches were performed using the trypsin protease enzyme parameters (with up to 3 missed cleavages) against a database with the human Histone sequences. A static modification of 56 Da for N-terminal propionylation and dynamic lysine and arginine modifications of 14 Da (methylation), 28 Da (dimethylation or formylation), 42 Da (trimethylation or acetylation), 56 Da (propionylation), and

serine/threonine phosphorylation (80 Da) were used in the computer searches. Lastly, all data from modified peptides were manually inspected with the Bioworks 2.0 program.

Quantification of H3R42me2

Quantification of the propionylated/triptic histone H3 peptides (a.a. 41-49) Pr-YRPGTVALR (+/- R42me2) was accomplished by measuring the area under the XIC peaks corresponding to the +2 charged precursor ions to Pr-YRPGTVALR (544.815 m/z) and Pr-YRme2PGTVALR (558.831 m/z). Relative quantification was accomplished by comparing such XIC peak data from the Pr-YRme2PGTVALR ion to the Pr-YRPGTVALR ion.

Enzymatic Assays on Peptides

Cells were transfected with plasmids expressing Flag-HA-tagged human PRMTs. 48 hours after transfection, cells were washed with ice-cold PBS and lysed with 1 ml of IP buffer (50 mM Hepes (pH 7.8), 250 mM NaCl, 0.5% Nonidet P-40) with protease inhibitor cocktail. Insoluble materials were removed by centrifugation. Whole cell lysates were incubated for 2 hours at 4°C with 5 ul of EZview Red Anti-HA beads (Sigma). After extensive washes, the beads were incubated with 1 ug of histone H3 peptides for 2 h at 30°C in HMT buffer (PBS, 1 mM DTT) with 2 ul 3H-Adomet (1 uCi, Perkin-Elmer). Tritiated labeled proteins were run on SDS-PAGE, stained with Coomassie R-250 dye, soaked in Amplify

solution (GE Healthcare) for 30 min, vacuum-dried onto filter paper, and exposed to x-ray film; exposures ranged from overnight to 1 week at -80 °C.

Recombinant GST-CARM1 and GST-PRMT6 were purified from *E. coli* using standard methods. Cells were disrupted by high pressure on an Emulsiflex (Avestin) in PBS supplemented with 500 mM NaCl, 1 mM DTT and protease inhibitor cocktail tablets (Sigma), and the cleared lysates were incubated with Glutathione-Sepharose 4B resin (GE Healthcare). After extensive washes bound proteins were eluted with 20 mM reduced glutathione. 1 ug of each enzyme was incubated with 1 ug of histone H3 peptides for 1 h at 30°C in HMT buffer with 2 ul 3H-Adomet. The reaction mix was spotted on P81 filter paper and air-dried. After washing five times with 100 ml of sodium carbonate buffer (0.1 M, pH 8.5) and a final wash with acetone, the filter papers were air-dried and put into scintillation vials containing 2.5 ml of scintillation liquid. Counts per minute (cpm) were measured via a scintillation counter (Beckman).

Recombinant JAK2 was purchased from Active Motif. As per manufacturer's instructions, 0.1 ug of active kinase was incubated with 1 ug peptide substrate in reaction buffer (60 mM HEPES-NaOH, pH 7.5, 3 mM $MgCl_2$, 3 mM $MnCl_2$, 3 µM Na-orthovanadate, 1.2 mM DTT, 2.5 µg/50 µl PEG20.000) and 1 uCi of gamma-32P ATP (Perkin-Elmer) for 30 minutes at 37°C. The reaction mix was spotted on P81 filter paper and air-dried. After washing five times with 100 ml of 1% phosphoric acid and a final wash with acetone, the filter papers were air-dried and put into scintillation vials containing 2.5 ml of scintillation liquid. Counts per minute (cpm) were measured via a scintillation counter (Beckman).

The peptides used in these assays (H3(1-20), H3(34-52), H3(34-52)R42me1 and H3(34-52)R42me2a) were synthesized by the Rockefeller University Proteomics Resource Center (New York, NY).

In vitro citrullination assay

Purified PAD4 (a gift from Dr. Sonja Staedler) was incubated with substrates in Assay Buffer (100 mM Tris-HCl, pH 7.4, containing 5 mM DTT and 2 mM $CaCl_2$) for 30 min at room temperature. The reactions were stopped by the addition of 5 × SDS-PAGE sample loading buffer and analyzed by Western blot after SDS-PAGE. Citrulline was detected using an anti-citrulline (modified) detection kit (Upstate, Millipore).

Peptide synthesis

Peptides were synthesized by Sam Pollock in Tom Muir's laboratory at Princeton University.

Amino-acid derivatives, chlorotrityl resin and coupling reagents were purchased from Novabiochem.

Peptide 1: The sequence corresponding to residues 1-28 of human H3.2 was synthesized on a mercaptopriopionamide-Arg-PAM resin, which affords a peptide α-thioester upon cleavage. Chain assembly employed manual solid-phase peptide synthesis with a t-butyloxycarbonyl (Boc) Nα protection strategy and using 2-(1H-benzotriazole-1-yl)-1,1,3,3-tetramethyluronium hexafluorophosphate (HBTU) for amino-acid activation. The peptide was cleaved from the resin on a

500mg peptide-resin scale by stirring in 10mL anhydrous HF (Sigma) at 0° C for 1hr with p-Cresol (Sigma) as a scavenger before work-up in cold ether, dissolution in 50% solvent B, and lyophilization. Cleaved product was purified by RP-HPLC, yielding approximately 35mg peptide 1 which was characterized by electrospray mass spectrometry; measured mass = 3239.8 Da, predicted = 3239.8 Da.

Peptide 2: The sequence corresponding to residues 29-46 of human H3 containing a Ala29-Cys mutation and was synthesized on 2-chlorotritylhydrazine resin (~0.4mmol/g), which was derived as described previously (42). The peptide itself was synthesized using manual solid-phase peptide synthesis with a fluorenylmethyloxycarbonyl (Fmoc) Nα protection strategy and using HBTU for amino-acid activation (Sigma). The peptide was cleaved from the resin on a 500mg peptide-resin scale by shaking in 10mL 95:2.5:2.5 TFA:H2O:TIPS (triisopropylsilane) at room temperature for 1.5hr before rotary evaporation of the TFA and work-up in cold ether, dissolution in 50% solvent B, and lyophilization. Cleaved product was purified by RP-HPLC, yielding approximately 30mg peptide 2 which was characterized by electrospray mass spectrometry; measured mass = 1966.1, predicted = 1966.1 Da.

Preparation of H3(47-135)A47C,C110A

A template pET3 plasmid containing hH3.2 was amplified by PCR to afford a fragment containing residues 47-135 with a Ala47-to Cys mutation. This was inserted into a pET30a(-) vector plasmid containing N-terminal poly-His and

SUMO elements and verified by DNA sequencing. E. coli BL21(DE3) cells (Invitrogen) transformed with the above His-SUMO-H3(47-135, A47C) construct were grown in Luria-Bertani (LB) medium at 37 °C until mid-log phase, and protein expression was induced by the addition of 0.6 mM IPTG and allowed to continue at 37°C for 4 hr. After harvesting the cells by centrifugation at 3,000g for 20 min, the cell pellet was resuspended in lysis buffer (50 mM Tris, 200 mM NaCl, 1 mM EDTA, pH 7.5) and frozen at -80 °C. Thawed cells were lysed by sonication and passage through a French press and the soluble material was removed by centrifugation at 30,000g for 30 min. The inclusion bodies, containing the desired fusion protein, were re-dissolved in lysis buffer + 6M guanidinium chloride (GuHCl) for 3hr and the solution was centrifugated as before and the supernatant incubated for 1.5hr at 4 °C with Ni-NTA resin (Qiagen) pre-equilibrated in lysis buffer + GuHCl. The resin was washed with 10 column volumes (CV) of D500 (6M GuHCl, 50mM Tris, 500mM NaCl, 3mM β-mercaptoethanol, pH 8.0) and 10CV D1000 (D500 with 1M NaCl) followed by 5CV urea buffer (6M urea, 50mM Tris, 150mM NaCl, pH 7.9). Elution was carried out with 7x1mL elution buffer (urea buffer + 500mM imidazole). Fractions were analyzed by SDS-PAGE and combined before immediately undertaking cleavage of the His-SUMO tag. Proteolytic cleavage of the His-SUMO-H3 construct proceeded under the following conditions: the construct was diluted in cleavage buffer to afford a final concentration of 2M urea, 166mM imidazole, (2mM DTT, 150mM L-Arginine, 10mM L-Cysteine, 50mM Tris, 150mM NaCl, pH 8) and 1U Ulp1 SUMO protease per 100ug cleavable material . The final concentration of fusion protein was

~0.25 mg/mL. The solution was left overnight with stirring. The imidazole remaining in solution was removed using 3000MWCO spin concentrators, the uncleaved material was removed by successive depletion on Ni-beads. The resulting eluent was purified using preparative-HPLC. The identity of the purified protein 3 was confirmed by mass spectrometry; measured mass = 10403.3, predicted = 10403.1 Da. This protocol afforded ~0.5 mg of purified protein per L of intial bacterial culture.

Ligation and desulphurization

Ligations were carried out by Sam Pollock in Tom Muir's laboratory at Princeton University.

Ligation of thioester peptides 1 (1 mM) and 2 (2.5 mM) to form polypeptide 4 was carried out in ligation buffer (6M GuHCl, 0.2M phosphate pH 7.0, 50mM MPAA, 20mM TCEP) under argon at room temperature. The reaction was complete after 3hrs and the product purified by semi-preparative HPLC and characterized by ESI-MS (measured mass = 4944.9, predicted = 4944.8 Da). The hydrazine moeity in 4 was converted into a thioester as described (40). Briefly, polypeptide 4 was added at 2.5mM to sparged 6M GuHCl, 0.2M phosphate at pH 3.0, and cooled to -10deg C before adding 10mM $NaNO_2$, letting sit 25min, and thioesterifying by addition of 150mM MPAA, 1mM polypeptide 3 and base up to pH 7.0. Following the addition of 30mM TCEP after 1hr, and a complete reaction time of 6hr, full length histone protein 5 was purified by semi-preparative HPLC and characterized by ESI-MS (measured mass =

15316.7, predicted = 15316.9 Da). The final product 6 in which the cysteines at the ligation junctions were converted back to the native alanines was obtained through radical desulfurization according to established protocols (34). Briefly, protein 5 (0.3 mM) was dissolved in desulfurization buffer (6M GuHCl, 0.2M phosphate, 250mM TCEP, pH 7.0) and the reaction initiated through the addition of reduced glutathione (final concentration 30mM) and VA-061 (final concentration 16mM). The desulfurization solution was flushed with argon, wrapped in parafilm, and placed at 37° C overnight. Semisynthetic protein 6 was then purified out of the solution by semi-preparative HPLC purification. Fractions were analyzed by ESI-MS and lyophilized, yielding approximately 1mg of final product (measured mass = 15252.7, predicted = 15252.8 Da).

Histone purification and octamer formation

Wild-type, recombinant human histones were purified as described previously (Luger et al., 1999a; Ruthenburg et al., 2011). Mutant histones were generated by Quikchange mutagenesis (Stratagene). Briefly, His-histone constructs were transformed into BL21(DE3)PlysS cells (Invitrogen) and expressed as inclusion bodies. After 4 hours of IPTG induction at a final concentration of 1mM, the cells were harvested and mechanically lysed. The crude inclusion bodies were harvested and solubilised in buffer D500 (6.0M Guanidine•HCl, 500 mM NaCl, 50 mM Tris•HCl pH 8, 10 mM 2-mercaptoethanol). The clarified denatured histones were incubated with Ni-NTA resin (Qiagen). After extensive washing histone protein was eluted and concentrated.

Histone octamers were prepared essentially as previously described (Luger et al., 1999b; Ruthenburg et al., 2011). Briefly, stoichiometric quantities of each core histone were dissolved from lyophilized pellets in unfolding buffer (50mM Tris•HCl pH 8, 6 M Guanidine•HCl, 10mM 2-mercaptoethanol, 1mM EDTA), and dialyzed overnight against several buffer changes of refolding buffer (20 mM Tris•HCl pH 7.8, 2M NaCl, 1mM EDTA, 5 mM DTT). 1/50 mass equivalents of TEV and PreScission proteases were added after this overnight dialysis and permitted to cleave tagged histones for at least six hours. The resultant crude octamer was then applied directly to an analytical Superdex 200 10/300 GL (GE Healthcare) resolved in refolding buffer. Peak fractions of octamer were pooled and concentrated in Amicon Ultra 10K N.M.C.O. centrifugal concentrators (Millipore).

Nucleosome assembly

DNA fragments corresponding to the 601 positioning sequence were prepared by EcoRV digestion of 32x153bp tandem repeats cloned into pUC19 (from Alex Ruthenburg). The 601 fragments were purified by plasmid backbone purification in 500 mM NaCl with 7.5% polyethylene glycol (PEG-6000) on ice for several hours. The soluble DNA fragments were further purified with several rounds of Phenol/Chloroform extraction and finally ethanol precipitated.

Gradient dyalisis was used to assemble mononucleosomes from octamers and 601 fragments. Equimolar amounts of purified octamers and DNA were mixed in refolding buffer. Starting in 1 volume of refolding buffer, a peristaltic

pump was used to add no salt buffer (10mM Tris pH 7.5, 1 mM EDTA) dropwise over 30 hours to a final volume of 10 volumes. Completed assemblies were cleared by centrifugation and visualized on a native 5% polyacrilamaide gel, stained with ethidium bromide.

Chromatin Transcription Assays

Transcription assays were performed by Dr. Xiangdong Lu in the laboratory of Robert Roeder at the Rockefeller University. Chromatin templates were assembled as described previously (An and Roeder, 2004; Ito et al., 1999). Transcription assays using activator p53 (20 ng) and coactivator p300 (10 ng) were conducted essentially as described previously (An et al., 2004; An and Roeder, 2004).

Peptide Pull-Down Assays

Biotinylated H3(34-52) peptides (or control peptides) were bound to High Capacity Streptavidin Agarose resin (Thermo) and incubated for 4 hours at 4°C with either nuclear extract or purified proteins. After extensive washes with PPD wash buffer (50mM Tris pH 7.5, 300 mM NaCl, 0.1% NP-40), bound proteins were eluted with 100mM glycine pH 2.5 and run on SDS-PAGE gels. Proteins were visualized by silver staining or western blot.

Recombinant GST-TBL1(228-600) and GST-TBLR1(165-550) were purified from *E. coli* Rosetta2. Cells were disrupted by high pressure on an Emulsiflex (Avestin) in PBS supplemented with 500 mM NaCl, 1 mM DTT and protease

inhibitor cocktail tablets (Sigma). Cleared lysates were incubated with Glutathione-Sepharose 4B resin (GE Healthcare). After extensive washes bound proteins were eluted with 20 mM reduced glutathione. Around 100 µg of protein was used in each pull-down. *In vitro* transcription/translation of the same domains was carried out using TNT Coupled Reticulocyte Lysate (Promega). 1 µg of template DNA was incubated for 90 minutes at 30°C with 25 µl of TNT Rabbit Reticulocyte Lysate supplemented with amino acid mix and 20 µCi [35S]methionine. At the end of the reaction, equal volumes were added to pull-down tubes.

HDAC Assays

Reagents were from Fluorescent HDAC Assay kit (Active Motif). 0.5 µg of affinity purified N-CoR complex were incubated with HDAC Substrate in HDAC Assay Buffer and increasing concentrations of histone peptides for 1 hour at 37°C in black 96-well plates. The reactions were stopped by adding HDAC Assay Developing Solution. After a 15 minutes incubation at room temperature, fluorescence was measured with a fluorescent plate reader Synergy H4 (Biotek) with excitation wavelength at 360 nm and emission wavelength at 460 nm.

References

Alberts, B. (2008). Molecular biology of the cell, 5th edn (New York: Garland Science).

Allfrey, V.G., Faulkner, R., and Mirsky, A.E. (1964). Acetylation and Methylation of Histones and Their Possible Role in the Regulation of Rna Synthesis. Proc Natl Acad Sci U S A *51*, 786-794.

Allis, C.D., Jenuwein, T., and Reinberg, D. (2007). Epigenetics (Cold Spring Harbor, N.Y.: Cold Spring Harbor Laboratory Press).

Allis, C.D., and Muir, T.W. (2011). Spreading chromatin into chemical biology. Chembiochem *12*, 264-279.

Altaf, M., Utley, R.T., Lacoste, N., Tan, S., Briggs, S.D., and Cote, J. (2007). Interplay of chromatin modifiers on a short basic patch of histone H4 tail defines the boundary of telomeric heterochromatin. Mol Cell *28*, 1002-1014.

An, W., Kim, J., and Roeder, R.G. (2004). Ordered cooperative functions of PRMT1, p300, and CARM1 in transcriptional activation by p53. Cell *117*, 735-748.

An, W., and Roeder, R.G. (2004). Reconstitution and transcriptional analysis of chromatin in vitro. Methods Enzymol *377*, 460-474.

Andrews, A.J., Chen, X., Zevin, A., Stargell, L.A., and Luger, K. (2010). The histone chaperone Nap1 promotes nucleosome assembly by eliminating nonnucleosomal histone DNA interactions. Mol Cell *37*, 834-842.

Arents, G., Burlingame, R.W., Wang, B.C., Love, W.E., and Moudrianakis, E.N. (1991). The nucleosomal core histone octamer at 3.1 A resolution: a tripartite protein assembly and a left-handed superhelix. Proc Natl Acad Sci U S A *88*, 10148-10152.

Arents, G., and Moudrianakis, E.N. (1993). Topography of the histone octamer surface: repeating structural motifs utilized in the docking of nucleosomal DNA. Proc Natl Acad Sci U S A *90*, 10489-10493.

Baldwin, G.S., and Carnegie, P.R. (1971). Specific enzymic methylation of an arginine in the experimental allergic encephalomyelitis protein from human myelin. Science 171, 579-581.

Bannister, A.J., Zegerman, P., Partridge, J.F., Miska, E.A., Thomas, J.O., Allshire, R.C., and Kouzarides, T. (2001). Selective recognition of methylated lysine 9 on histone H3 by the HP1 chromo domain. Nature 410, 120-124.

Bedford, M.T., and Clarke, S.G. (2009). Protein arginine methylation in mammals: who, what, and why. Mol Cell *33*, 1-13.

Bernstein, B.E., Meissner, A., and Lander, E.S. (2007). The mammalian epigenome. Cell *128*, 669-681.

Bonaldi, T., Regula, J.T., and Imhof, A. (2004). The use of mass spectrometry for the analysis of histone modifications. Methods Enzymol *377*, 111-130.

Brownell, J.E., Zhou, J., Ranalli, T., Kobayashi, R., Edmondson, D.G., Roth, S.Y., and Allis, C.D. (1996). Tetrahymena histone acetyltransferase A: a homolog to yeast Gcn5p linking histone acetylation to gene activation. Cell *84*, 843-851.

Burton, D.R., Butler, M.J., Hyde, J.E., Phillips, D., Skidmore, C.J., and Walker, I.O. (1978). The interaction of core histones with DNA: equilibrium binding studies. Nucleic Acids Res *5*, 3643-3663.

Chang, B., Chen, Y., Zhao, Y., and Bruick, R.K. (2007). JMJD6 is a histone arginine demethylase. Science *318*, 444-447.

Chatterjee, C., and Muir, T.W. (2010). Chemical approaches for studying histone modifications. J Biol Chem *285*, 11045-11050.

Chen, C.C., Carson, J.J., Feser, J., Tamburini, B., Zabaronick, S., Linger, J., and Tyler, J.K. (2008). Acetylated lysine 56 on histone H3 drives chromatin assembly after repair and signals for the completion of repair. Cell *134*, 231-243.

Chen, D., Ma, H., Hong, H., Koh, S.S., Huang, S.M., Schurter, B.T., Aswad, D.W., and Stallcup, M.R. (1999). Regulation of transcription by a protein methyltransferase. Science *284*, 2174-2177.

Cheng, D., Vemulapalli, V., and Bedford, M.T. (2012). Methods applied to the study of protein arginine methylation. Methods Enzymol *512*, 71-92.

Cosgrove, M.S., Boeke, J.D., and Wolberger, C. (2004). Regulated nucleosome mobility and the histone code. Nat Struct Mol Biol *11*, 1037-1043.

Couture, J.F., Collazo, E., and Trievel, R.C. (2006). Molecular recognition of histone H3 by the WD40 protein WDR5. Nat Struct Mol Biol *13*, 698-703.

Cuthbert, G.L., Daujat, S., Snowden, A.W., Erdjument-Bromage, H., Hagiwara, T., Yamada, M., Schneider, R., Gregory, P.D., Tempst, P., Bannister, A.J*., et al.* (2004). Histone deimination antagonizes arginine methylation. Cell *118*, 545-553.

Dawson, M.A., Bannister, A.J., Gottgens, B., Foster, S.D., Bartke, T., Green, A.R., and Kouzarides, T. (2009). JAK2 phosphorylates histone H3Y41 and excludes HP1alpha from chromatin. Nature *461*, 819-822.

Denis, H., Deplus, R., Putmans, P., Yamada, M., Metivier, R., and Fuks, F. (2009). Functional connection between deimination and deacetylation of histones. Mol Cell Biol *29*, 4982-4993.

Dignam, J.D., Lebovitz, R.M., and Roeder, R.G. (1983). Accurate transcription initiation by RNA polymerase II in a soluble extract from isolated mammalian nuclei. Nucleic Acids Res *11*, 1475-1489.

Fang, G.-M., Li, Y.-M., Shen, F., Huang, Y.-C., Li, J.-B., Lin, Y., Cui, H.-K., and Liu, L. (2011). Protein Chemical Synthesis by Ligation of Peptide Hydrazides. Angewandte Chemie International Edition *50*, 7645-7649.

Fierz, B., Chatterjee, C., McGinty, R.K., Bar-Dagan, M., Raleigh, D.P., and Muir, T.W. (2011). Histone H2B ubiquitylation disrupts local and higher-order chromatin compaction. Nat Chem Biol *7*, 113-119.

Fischle, W., Tseng, B.S., Dormann, H.L., Ueberheide, B.M., Garcia, B.A., Shabanowitz, J., Hunt, D.F., Funabiki, H., and Allis, C.D. (2005). Regulation of HP1-chromatin binding by histone H3 methylation and phosphorylation. Nature *438*, 1116-1122.

Fischle, W., Wang, Y., and Allis, C.D. (2003). Binary switches and modification cassettes in histone biology and beyond. Nature *425*, 475-479.

Flemming, W. (1882). Zellsubstanz, Kern und Zelltheilung (Leipzig, Germany: F.C.W Vogel).

Frankel, A., Yadav, N., Lee, J., Branscombe, T.L., Clarke, S., and Bedford, M.T. (2002). The novel human protein arginine N-methyltransferase PRMT6 is a nuclear enzyme displaying unique substrate specificity. J Biol Chem 277, 3537-3543.

Fry, C.J., Norris, A., Cosgrove, M., Boeke, J.D., and Peterson, C.L. (2006). The LRS and SIN domains: two structurally equivalent but functionally distinct nucleosomal surfaces required for transcriptional silencing. Mol Cell Biol *26*, 9045-9059.

Garcia, B.A., Mollah, S., Ueberheide, B.M., Busby, S.A., Muratore, T.L., Shabanowitz, J., and Hunt, D.F. (2007a). Chemical derivatization of histones for facilitated analysis by mass spectrometry. Nat Protoc *2*, 933-938.

Garcia, B.A., Shabanowitz, J., and Hunt, D.F. (2007b). Characterization of histones and their post-translational modifications by mass spectrometry. Curr Opin Chem Biol *11*, 66-73.

Guccione, E., Bassi, C., Casadio, F., Martinato, F., Cesaroni, M., Schuchlautz, H., Lüscher, B., and Amati, B. (2007). Methylation of histone H3R2 by PRMT6 and H3K4 by an MLL complex are mutually exclusive. Nature *449*, 933-937.

Guccione, E., Martinato, F., Finocchiaro, G., Luzi, L., Tizzoni, L., Dall' Olio, V., Zardo, G., Nervi, C., Bernard, L., and Amati, B. (2006). Myc-binding-site recognition in the human genome is determined by chromatin context. Nat Cell Biol *8*, 764-770.

Hall, M.A., Shundrovsky, A., Bai, L., Fulbright, R.M., Lis, J.T., and Wang, M.D. (2009). High-resolution dynamic mapping of histone-DNA interactions in a nucleosome. Nat Struct Mol Biol *16*, 124-129.

Hansen, J.C. (2002). Conformational dynamics of the chromatin fiber in solution: determinants, mechanisms, and functions. Annu Rev Biophys Biomol Struct *31*, 361-392.

Harrison, M.J., Tang, Y.H., and Dowhan, D.H. (2010). Protein arginine methyltransferase 6 regulates multiple aspects of gene expression. Nucleic Acids Res *38*, 2201-2216.

Hirota, T., Lipp, J.J., Toh, B.H., and Peters, J.M. (2005). Histone H3 serine 10 phosphorylation by Aurora B causes HP1 dissociation from heterochromatin. Nature *438*, 1176-1180.

Hyland, E.M., Cosgrove, M.S., Molina, H., Wang, D., Pandey, A., Cottee, R.J., and Boeke, J.D. (2005). Insights into the role of histone H3 and histone H4 core modifiable residues in Saccharomyces cerevisiae. Mol Cell Biol *25*, 10060-10070.

Hyland, E.M., Molina, H., Poorey, K., Jie, C., Xie, Z., Dai, J., Qian, J., Bekiranov, S., Auble, D.T., Pandey, A.*, et al.* (2011). An evolutionarily 'young' lysine residue in histone H3 attenuates transcriptional output in Saccharomyces cerevisiae. Genes Dev *25*, 1306-1319.

Hyllus, D., Stein, C., Schnabel, K., Schiltz, E., Imhof, A., Dou, Y., Hsieh, J., and Bauer, U.M. (2007). PRMT6-mediated methylation of R2 in histone H3 antagonizes H3 K4 trimethylation. Genes Dev *21*, 3369-3380.

Iberg, A.N., Espejo, A., Cheng, D., Kim, D., Michaud-Levesque, J., Richard, S., and Bedford, M.T. (2007). Arginine methylation of the histone H3 tail impedes effector binding. J Biol Chem.

Ichimura, S., Mita, K., and Zama, M. (1982). Essential role of arginine residues in the folding of deoxyribonucleic acid into nucleosome cores. Biochemistry *21*, 5329-5334.

Ito, T., Levenstein, M.E., Fyodorov, D.V., Kutach, A.K., Kobayashi, R., and Kadonaga, J.T. (1999). ACF consists of two subunits, Acf1 and ISWI, that function cooperatively in the ATP-dependent catalysis of chromatin assembly. Genes Dev *13*, 1529-1539.

Ito, T., Yadav, N., Lee, J., Furumatsu, T., Yamashita, S., Yoshida, K., Taniguchi, N., Hashimoto, M., Tsuchiya, M., Ozaki, T.*, et al.* (2009). Arginine methyltransferase CARM1/PRMT4 regulates endochondral ossification. BMC Dev Biol *9*, 47.

Jenuwein, T., and Allis, C.D. (2001). Translating the histone code. Science *293*, 1074-1080.

Kim, J., Lee, J., Yadav, N., Wu, Q., Carter, C., Richard, S., Richie, E., and Bedford, M.T. (2004). Loss of CARM1 results in hypomethylation of thymocyte cyclic AMP-regulated phosphoprotein and deregulated early T cell development. J Biol Chem *279*, 25339-25344.

Kirmizis, A., Santos-Rosa, H., Penkett, C.J., Singer, M.A., Vermeulen, M., Mann, M., Bähler, J., Green, R.D., and Kouzarides, T. (2007). Arginine methylation at histone H3R2 controls deposition of H3K4 trimethylation. Nature *449*, 928-932.

Koh, S.S., Chen, D., Lee, Y.H., and Stallcup, M.R. (2001). Synergistic enhancement of nuclear receptor function by p160 coactivators and two coactivators with protein methyltransferase activities. J Biol Chem *276*, 1089-1098.

Kornberg, R.D. (1974). Chromatin structure: a repeating unit of histones and DNA. Science 184, 868-871.

Kornberg, R.D., and Thomas, J.O. (1974). Chromatin structure; oligomers of the histones. Science 184, 865-868.

Kossel, A. (1911). Ueber die chemische Beschaffenheit des Zelkerns. Munchen. Med. Wochenschrift *58*, 65-69.

Kouskouti, A., and Talianidis, I. (2005). Histone modifications defining active genes persist after transcriptional and mitotic inactivation. EMBO J *24*, 347-357.

Kouzarides, T. (2007). Chromatin modifications and their function. Cell *128*, 693-705.

Krause, C.D., Yang, Z.H., Kim, Y.S., Lee, J.H., Cook, J.R., and Pestka, S. (2007). Protein arginine methyltransferases: evolution and assessment of their pharmacological and therapeutic potential. Pharmacol Ther *113*, 50-87.

Kruger, W., Peterson, C.L., Sil, A., Coburn, C., Arents, G., Moudrianakis, E.N., and Herskowitz, I. (1995). Amino acid substitutions in the structured domains of histones H3 and H4 partially relieve the requirement of the yeast SWI/SNF complex for transcription. Genes Dev 9, 2770-2779.

Kurumizaka, H., and Wolffe, A.P. (1997). Sin mutations of histone H3: influence on nucleosome core structure and function. Mol Cell Biol 17, 6953-6969.

Lachner, M., O'Carroll, D., Rea, S., Mechtler, K., and Jenuwein, T. (2001). Methylation of histone H3 lysine 9 creates a binding site for HP1 proteins. Nature *410*, 116-120.

Lakowski, T.M., and Frankel, A. (2008). A kinetic study of human protein arginine N-methyltransferase 6 reveals a distributive mechanism. J Biol Chem *283*, 10015-10025.

Larsen, B.D., and Holm, A. (1994). Incomplete Fmoc deprotection in solid-phase synthesis of peptides. Int J Pept Protein Res *43*, 1-9.

Lee, Y.H., Ma, H., Tan, T.Z., Ng, S.S., Soong, R., Mori, S., Fu, X.Y., Zernicka-Goetz, M., and Wu, Q. (2012). Protein arginine methyltransferase 6 regulates embryonic stem cell identity. Stem Cells Dev *21*, 2613-2622.

Lee, Y.H., and Stallcup, M.R. (2009). Minireview: protein arginine methylation of nonhistone proteins in transcriptional regulation. Mol Endocrinol *23*, 425-433.

Li, G., and Widom, J. (2004). Nucleosomes facilitate their own invasion. Nat Struct Mol Biol *11*, 763-769.

Liu, K., Guo, Y., Liu, H., Bian, C., Lam, R., Liu, Y., Mackenzie, F., Rojas, L.A., Reinberg, D., Bedford, M.T.*, et al.* (2012). Crystal structure of TDRD3 and methyl-arginine binding characterization of TDRD3, SMN and SPF30. PLoS ONE *7*, e30375.

Lohr, D., and Hereford, L. (1979). Yeast chromatin is uniformly digested by DNase-I. Proc Natl Acad Sci U S A *76*, 4285-4288.

Lorch, Y., LaPointe, J.W., and Kornberg, R.D. (1987). Nucleosomes inhibit the initiation of transcription but allow chain elongation with the displacement of histones. Cell 49, 203-210.

Lowary, P.T., and Widom, J. (1998). New DNA sequence rules for high affinity binding to histone octamer and sequence-directed nucleosome positioning. J Mol Biol *276*, 19-42.

Luger, K., Mader, A.W., Richmond, R.K., Sargent, D.F., and Richmond, T.J. (1997). Crystal structure of the nucleosome core particle at 2.8 A resolution. Nature *389*, 251-260.

Luger, K., Rechsteiner, T.J., and Richmond, T.J. (1999a). Expression and purification of recombinant histones and nucleosome reconstitution. Methods Mol Biol *119*, 1-16.

Luger, K., Rechsteiner, T.J., and Richmond, T.J. (1999b). Preparation of nucleosome core particle from recombinant histones. Methods Enzymol *304*, 3-19.

Luscombe, N.M., Laskowski, R.A., and Thornton, J.M. (2001). Amino acid-base interactions: a three-dimensional analysis of protein-DNA interactions at an atomic level. Nucleic Acids Res *29*, 2860-2874.

Malik, H.S., and Henikoff, S. (2003). Phylogenomics of the nucleosome. Nat Struct Biol *10*, 882-891.

Manohar, M., Mooney, A.M., North, J.A., Nakkula, R.J., Picking, J.W., Edon, A., Fishel, R., Poirier, M.G., and Ottesen, J.J. (2009). Acetylation of histone H3 at the nucleosome dyad alters DNA-histone binding. J Biol Chem *284*, 23312-23321.

Margueron, R., Justin, N., Ohno, K., Sharpe, M.L., Son, J., Drury, W.J., 3rd, Voigt, P., Martin, S.R., Taylor, W.R., De Marco, V.*, et al.* (2009). Role of the polycomb protein EED in the propagation of repressive histone marks. Nature *461*, 762-767.

Martin, D.G., Baetz, K., Shi, X., Walter, K.L., MacDonald, V.E., Wlodarski, M.J., Gozani, O., Hieter, P., and Howe, L. (2006). The Yng1p plant homeodomain finger is a methyl-histone binding module that recognizes lysine 4-methylated histone H3. Mol Cell Biol *26*, 7871-7879.

Maurer-Stroh, S., Dickens, N.J., Hughes-Davies, L., Kouzarides, T., Eisenhaber, F., and Ponting, C.P. (2003). The Tudor domain 'Royal Family': Tudor, plant Agenet, Chromo, PWWP and MBT domains. Trends Biochem Sci *28*, 69-74.

Migliori, V., Mapelli, M., and Guccione, E. (2012a). On WD40 proteins: propelling our knowledge of transcriptional control? Epigenetics *7*, 815-822.

Migliori, V., Muller, J., Phalke, S., Low, D., Bezzi, M., Mok, W.C., Sahu, S.K., Gunaratne, J., Capasso, P., Bassi, C.*, et al.* (2012b). Symmetric dimethylation of H3R2 is a newly identified histone mark that supports euchromatin maintenance. Nat Struct Mol Biol *19*, 136-144.

Murray, K. (1964). The Occurrence of Epsilon-N-Methyl Lysine in Histones. Biochemistry *3*, 10-15.

Neault, M., Mallette, F.A., Vogel, G., Michaud-Levesque, J., and Richard, S. (2012). Ablation of PRMT6 reveals a role as a negative transcriptional regulator of the p53 tumor suppressor. Nucleic Acids Res *40*, 9513-9521.

Neumann, H., Hancock, S.M., Buning, R., Routh, A., Chapman, L., Somers, J., Owen-Hughes, T., van Noort, J., Rhodes, D., and Chin, J.W. (2009). A method for genetically installing site-specific acetylation in recombinant histones defines the effects of H3 K56 acetylation. Mol Cell *36*, 153-163.

Ng, H.H., Feng, Q., Wang, H., Erdjument-Bromage, H., Tempst, P., Zhang, Y., and Struhl, K. (2002). Lysine methylation within the globular domain of histone H3 by Dot1 is important for telomeric silencing and Sir protein association. Genes Dev *16*, 1518-1527.

Nishioka, K., and Reinberg, D. (2003). Methods and tips for the purification of human histone methyltransferases. Methods *31*, 49-58.

North, J.A., Shimko, J.C., Javaid, S., Mooney, A.M., Shoffner, M.A., Rose, S.D., Bundschuh, R., Fishel, R., Ottesen, J.J., and Poirier, M.G. (2012). Regulation of the nucleosome unwrapping rate controls DNA accessibility. Nucleic Acids Res *40*, 10215-10227.

O'Brien, K.B., Alberich-Jorda, M., Yadav, N., Kocher, O., Diruscio, A., Ebralidze, A., Levantini, E., Sng, N.J., Bhasin, M., Caron, T.*, et al.* (2010). CARM1 is required for proper control of proliferation and differentiation of pulmonary epithelial cells. Development *137*, 2147-2156.

Oberoi, J., Fairall, L., Watson, P.J., Yang, J.C., Czimmerer, Z., Kampmann, T., Goult, B.T., Greenwood, J.A., Gooch, J.T., Kallenberger, B.C.*, et al.* (2011). Structural basis for the assembly of the SMRT/NCoR core transcriptional repression machinery. Nat Struct Mol Biol *18*, 177-184.

Ong, S.E., Mittler, G., and Mann, M. (2004). Identifying and quantifying in vivo methylation sites by heavy methyl SILAC. Nat Methods *1*, 119-126.

Perissi, V., Jepsen, K., Glass, C.K., and Rosenfeld, M.G. (2010). Deconstructing repression: evolving models of co-repressor action. Nat Rev Genet *11*, 109-123.

Phalke, S., Mzoughi, S., Bezzi, M., Jennifer, N., Mok, W.C., Low, D.H., Thike, A.A., Kuznetsov, V.A., Tan, P.H., Voorhoeve, P.M.*, et al.* (2012). p53-Independent regulation of p21Waf1/Cip1 expression and senescence by PRMT6. Nucleic Acids Res *40*, 9534-9542.

Plazas-Mayorca, M.D., Zee, B.M., Young, N.L., Fingerman, I.M., LeRoy, G., Briggs, S.D., and Garcia, B.A. (2009). One-pot shotgun quantitative mass spectrometry characterization of histones. J Proteome Res *8*, 5367-5374.

Rea, S., Eisenhaber, F., O'Carroll, D., Strahl, B.D., Sun, Z.W., Schmid, M., Opravil, S., Mechtler, K., Ponting, C.P., Allis, C.D.*, et al.* (2000). Regulation of chromatin structure by site-specific histone H3 methyltransferases. Nature *406*, 593-599.

Richart, A.N., Brunner, C.I., Stott, K., Murzina, N.V., and Thomas, J.O. (2012). Characterization of chromoshadow domain-mediated binding of heterochromatin protein 1alpha (HP1alpha) to histone H3. J Biol Chem *287*, 18730-18737.

Robinson, P.J., An, W., Routh, A., Martino, F., Chapman, L., Roeder, R.G., and Rhodes, D. (2008). 30 nm chromatin fibre decompaction requires both H4-K16 acetylation and linker histone eviction. J Mol Biol 381, 816-825.

Ruthenburg, A.J., Li, H., Milne, T.A., Dewell, S., McGinty, R.K., Yuen, M., Ueberheide, B., Dou, Y., Muir, T.W., Patel, D.J.*, et al.* (2011). Recognition of a mononucleosomal histone modification pattern by BPTF via multivalent interactions. Cell *145*, 692-706.

Sakabe, K., and Hart, G.W. (2010). O-GlcNAc transferase regulates mitotic chromatin dynamics. J Biol Chem 285, 34460-34468.

Schurter, B.T., Koh, S.S., Chen, D., Bunick, G.J., Harp, J.M., Hanson, B.L., Henschen-Edman, A., Mackay, D.R., Stallcup, M.R., and Aswad, D.W. (2001). Methylation of histone H3 by coactivator-associated arginine methyltransferase 1. Biochemistry *40*, 5747-5756.

Shechter, D., Dormann, H.L., Allis, C.D., and Hake, S.B. (2007). Extraction, purification and analysis of histones. Nature protocols *2*, 1445-1457.

Shi, X., Hong, T., Walter, K.L., Ewalt, M., Michishita, E., Hung, T., Carney, D., Peña, P., Lan, F., Kaadige, M.R.*, et al.* (2006). ING2 PHD domain links histone H3 lysine 4 methylation to active gene repression. Nature *442*, 96-99.

Shimko, J.C., North, J.A., Bruns, A.N., Poirier, M.G., and Ottesen, J.J. (2011). Preparation of fully synthetic histone H3 reveals that acetyl-lysine 56 facilitates protein binding within nucleosomes. J Mol Biol *408*, 187-204.

Shogren-Knaak, M., Ishii, H., Sun, J.M., Pazin, M.J., Davie, J.R., and Peterson, C.L. (2006). Histone H4-K16 acetylation controls chromatin structure and protein interactions. Science *311*, 844-847.

Shogren-Knaak, M.A., and Peterson, C.L. (2004). Creating designer histones by native chemical ligation. Methods Enzymol *375*, 62-76.

Simon, M., North, J.A., Shimko, J.C., Forties, R.A., Ferdinand, M.B., Manohar, M., Zhang, M., Fishel, R., Ottesen, J.J., and Poirier, M.G. (2011). Histone fold modifications control nucleosome unwrapping and disassembly. Proc Natl Acad Sci U S A *108*, 12711-12716.

Somers, J., and Owen-Hughes, T. (2009). Mutations to the histone H3 alpha N region selectively alter the outcome of ATP-dependent nucleosome-remodelling reactions. Nucleic Acids Res *37*, 2504-2513.

Stavropoulos, G., Gatos, D., Magafa, V., and Barlos, K. (1996). Preparation of polymer-bound trityl-hydrazines and their application in the solid phase synthesis of partially protected peptide hydrazides. Letters in Peptide Science *2*, 315-318.

Stein, C., Riedl, S., Ruthnick, D., Notzold, R.R., and Bauer, U.M. (2012). The arginine methyltransferase PRMT6 regulates cell proliferation and senescence through transcriptional repression of tumor suppressor genes. Nucleic Acids Res *40*, 9522-9533.

Strahl, B.D., and Allis, C.D. (2000). The language of covalent histone modifications. Nature *403*, 41-45.

Strahl, B.D., Briggs, S.D., Brame, C.J., Caldwell, J.A., Koh, S.S., Ma, H., Cook, R.G., Shabanowitz, J., Hunt, D.F., Stallcup, M.R.*, et al.* (2001). Methylation of histone H4 at arginine 3 occurs in vivo and is mediated by the nuclear receptor coactivator PRMT1. Curr Biol *11*, 996-1000.

Tan, M., Luo, H., Lee, S., Jin, F., Yang, J.S., Montellier, E., Buchou, T., Cheng, Z., Rousseaux, S., Rajagopal, N.*, et al.* (2011). Identification of 67 histone marks and histone lysine crotonylation as a new type of histone modification. Cell *146*, 1016-1028.

Taunton, J., Hassig, C.A., and Schreiber, S.L. (1996). A mammalian histone deacetylase related to the yeast transcriptional regulator Rpd3p. Science *272*, 408-411.

Taverna, S.D., Ilin, S., Rogers, R.S., Tanny, J.C., Lavender, H., Li, H., Baker, L., Boyle, J., Blair, L.P., Chait, B.T.*, et al.* (2006). Yng1 PHD finger binding to H3 trimethylated at K4 promotes NuA3 HAT activity at K14 of H3 and transcription at a subset of targeted ORFs. Mol Cell *24*, 785-796.

Taverna, S.D., Li, H., Ruthenburg, A.J., Allis, C.D., and Patel, D.J. (2007). How chromatin-binding modules interpret histone modifications: lessons from professional pocket pickers. Nat Struct Mol Biol *14*, 1025-1040.

Tee, W.W., Pardo, M., Theunissen, T.W., Yu, L., Choudhary, J.S., Hajkova, P., and Surani, M.A. (2010). Prmt5 is essential for early mouse development and acts in the cytoplasm to maintain ES cell pluripotency. Genes Dev *24*, 2772-2777.

Tropberger, P., Pott, S., Keller, C., Kamieniarz-Gdula, K., Caron, M., Richter, F., Li, G., Mittler, G., Liu, E.T., Buhler, M.*, et al.* (2013). Regulation of Transcription through Acetylation of H3K122 on the Lateral Surface of the Histone Octamer. Cell *152*, 859-872.

Tse, C., Sera, T., Wolffe, A.P., and Hansen, J.C. (1998). Disruption of higher-order folding by core histone acetylation dramatically enhances transcription of nucleosomal arrays by RNA polymerase III. Mol Cell Biol *18*, 4629-4638.

Turner, B.M. (2000). Histone acetylation and an epigenetic code. Bioessays 22, 836-845.

Van Holde, K.E. (1989). Chromatin (New York: Springer-Verlag).

van Leeuwen, F., Gafken, P.R., and Gottschling, D.E. (2002). Dot1p modulates silencing in yeast by methylation of the nucleosome core. Cell *109*, 745-756.

Vermeulen, M., Mulder, K.W., Denissov, S., Pijnappel, W.W., van Schaik, F.M., Varier, R.A., Baltissen, M.P., Stunnenberg, H.G., Mann, M., and Timmers, H.T. (2007). Selective anchoring of TFIID to nucleosomes by trimethylation of histone H3 lysine 4. Cell *131*, 58-69.

Waldmann, T., Izzo, A., Kamieniarz, K., Richter, F., Vogler, C., Sarg, B., Lindner, H., Young, N.L., Mittler, G., Garcia, B.A.*, et al.* (2011). Methylation of H2AR29 is a novel repressive PRMT6 target. Epigenetics Chromatin *4*, 11.

Wan, Q., and Danishefsky, S.J. (2007). Free-radical-based, specific desulfurization of cysteine: a powerful advance in the synthesis of polypeptides and glycopolypeptides. Angew Chem Int Ed Engl *46*, 9248-9252.

Wang, Y., Wysocka, J., Sayegh, J., Lee, Y.H., Perlin, J.R., Leonelli, L., Sonbuchner, L.S., McDonald, C.H., Cook, R.G., Dou, Y.*, et al.* (2004). Human PAD4 regulates histone arginine methylation levels via demethylimination. Science *306*, 279-283.

Watson, P.J., Fairall, L., and Schwabe, J.W. (2012). Nuclear hormone receptor co-repressors: structure and function. Mol Cell Endocrinol *348*, 440-449.

Webby, C.J., Wolf, A., Gromak, N., Dreger, M., Kramer, H., Kessler, B., Nielsen, M.L., Schmitz, C., Butler, D.S., Yates, J.R., 3rd*, et al.* (2009). Jmjd6 catalyses

lysyl-hydroxylation of U2AF65, a protein associated with RNA splicing. Science *325*, 90-93.

Wechser, M.A., Kladde, M.P., Alfieri, J.A., and Peterson, C.L. (1997). Effects of Sin- versions of histone H4 on yeast chromatin structure and function. EMBO J 16, 2086-2095.

Weil, P.A., Luse, D.S., Segall, J., and Roeder, R.G. (1979). Selective and accurate initiation of transcription at the Ad2 major late promotor in a soluble system dependent on purified RNA polymerase II and DNA. Cell *18*, 469-484.

Williams, S.K., Truong, D., and Tyler, J.K. (2008). Acetylation in the globular core of histone H3 on lysine-56 promotes chromatin disassembly during transcriptional activation. Proc Natl Acad Sci U S A *105*, 9000-9005.

Workman, J.L., and Roeder, R.G. (1987). Binding of transcription factor TFIID to the major late promoter during in vitro nucleosome assembly potentiates subsequent initiation by RNA polymerase II. Cell 51, 613-622.

Wu, J., Cui, N., Wang, R., Li, J., and Wong, J. (2012). A role for CARM1-mediated histone H3 arginine methylation in protecting histone acetylation by releasing corepressors from chromatin. PLoS ONE *7*, e34692.

Wysocka, J. (2006). Identifying novel proteins recognizing histone modifications using peptide pull-down assay. Methods *40*, 339-343.

Wysocka, J., Swigut, T., Milne, T.A., Dou, Y., Zhang, X., Burlingame, A.L., Roeder, R.G., Brivanlou, A.H., and Allis, C.D. (2005). WDR5 associates with histone H3 methylated at K4 and is essential for H3 K4 methylation and vertebrate development. Cell *121*, 859-872.

Wysocka, J., Swigut, T., Xiao, H., Milne, T.A., Kwon, S.Y., Landry, J., Kauer, M., Tackett, A.J., Chait, B.T., Badenhorst, P.*, et al.* (2006). A PHD finger of NURF couples histone H3 lysine 4 trimethylation with chromatin remodelling. Nature *442*, 86-90.

Xu, F., Zhang, K., and Grunstein, M. (2005). Acetylation in histone H3 globular domain regulates gene expression in yeast. Cell *121*, 375-385.

Xu, W., Cho, H., Kadam, S., Banayo, E.M., Anderson, S., Yates, J.R., 3rd, Emerson, B.M., and Evans, R.M. (2004). A methylation-mediator complex in hormone signaling. Genes Dev *18*, 144-156.

Yadav, N., Cheng, D., Richard, S., Morel, M., Iyer, V.R., Aldaz, C.M., and Bedford, M.T. (2008). CARM1 promotes adipocyte differentiation by coactivating PPARgamma. EMBO Rep *9*, 193-198.

Yadav, N., Lee, J., Kim, J., Shen, J., Hu, M.C., Aldaz, C.M., and Bedford, M.T. (2003). Specific protein methylation defects and gene expression perturbations in coactivator-associated arginine methyltransferase 1-deficient mice. Proc Natl Acad Sci U S A *100*, 6464-6468.

Yang, Y., Lu, Y., Espejo, A., Wu, J., Xu, W., Liang, S., and Bedford, M.T. TDRD3 is an effector molecule for arginine-methylated histone marks. Mol Cell *40*, 1016-1023.

Yang, Y., Lu, Y., Espejo, A., Wu, J., Xu, W., Liang, S., and Bedford, M.T. (2010). TDRD3 is an effector molecule for arginine-methylated histone marks. Mol Cell *40*, 1016-1023.

Ye, J., Ai, X., Eugeni, E.E., Zhang, L., Carpenter, L.R., Jelinek, M.A., Freitas, M.A., and Parthun, M.R. (2005). Histone H4 lysine 91 acetylation a core domain modification associated with chromatin assembly. Mol Cell *18*, 123-130.

Yoon, H.G., Chan, D.W., Huang, Z.Q., Li, J., Fondell, J.D., Qin, J., and Wong, J. (2003). Purification and functional characterization of the human N-CoR complex: the roles of HDAC3, TBL1 and TBLR1. EMBO J *22*, 1336-1346.

Zhang, L., Eugeni, E.E., Parthun, M.R., and Freitas, M.A. (2003). Identification of novel histone post-translational modifications by peptide mass fingerprinting. Chromosoma *112*, 77-86.